The Dynamics of Coarse Sediment Transfer in an Upland Bedrock River

ALISTAIR IAN CRAY

The Dynamics of Coarse Sediment Transfer in an Upland Bedrock River

Alistair I. Cray

January 2010

A thesis submitted in accordance with the
requirements for the degree of
Master of Science

Department of Geography
Durham University

Declaration

I confirm that no part of the material presented in this thesis has previously been submitted by me or any other person for a degree in this or any other university. In all cases, where it is relevant, material form the work of others has been acknowledged.

Alistair I. Cray

Department of Geography,
Durham University.
January 2010.

Abstract

Bedrock channels in UK upland environments have received relatively little attention despite their importance within upland river systems and their influence on controlling the conveyance of sediment downstream. This thesis aims to quantify and model the transfer of coarse sediment through Trout Beck, an upland bedrock reach in the North Pennines, UK. The transport of coarse sediment has been quantified through field monitoring of the sediment characteristics, repeat magnetic tracer surveys and *in situ* bed load impact sensors. This was carried out in conjunction with surveys of channel morphology, using terrestrial laser scanning and repeat dGPS surveys and continuous flow monitoring. This has enabled sediment transport dynamics to be related to the hydraulic conditions throughout the reach.

Differences between channel types have been conceptualised using the continuum of the 'fluvial trinities'. This model demonstrates that the interaction of sediment and channel morphology is partly disconnected in bedrock channels. Conversely, in partially alluvial and alluvial channels there are important feedbacks between sediment stored locally in the channel, channel form and sediment transport. It has been shown that bedrock, partially alluvial and alluvial sections of the river channel have a considerable and varied influence on conveyance of sediment through these types of reaches.

Sediment storage defines the partially alluvial and alluvial sections of the channel, with very little sediment storage in bedrock reaches, except in hydraulically sheltered sites. More efficient sediment transfer through bedrock channels is the result of the local hydraulics. The low resistance to flow and stable channel boundaries cause little sediment storage and a downstream conveyance of the full grain-size distribution during periods when flow is competent and sediment is supplied from external sources.

The detailed morphological survey has provided the necessary boundary conditions, along with the flow data, to apply a one-dimensional hydraulic model (HEC-RAS) of the bedrock channel. The modelling results have quantified the hydraulic regime of the channel. Furthermore, using local shear stress as a proxy for sediment transport, sediment transport potential for the dominant grain-size distribution of the reach (16-256 mm) has been assessed for different locations in the channel. There are significant differences in the critical threshold of shear stress for sediment transport down reach. Sediment which is transported through the bedrock reach will be deposited and stored, in the partially alluvial and alluvial sections of the reach, at the same flow conditions. As the flow magnitude increases above the critical threshold, the sediment transport potential increases throughout the whole channel until the conditions in the whole reach have the potential to transport sediment. The sediment transport potential in the bedrock sections of the channel is always greater than in the partially alluvial and alluvial sections of the channel.

By combining the field and modelling approaches an improved understanding of the flow thresholds and spatial variations in sediment transport, in an upland bedrock channel, has been achieved.

Acknowledgments

Firstly, I would like to thank my supervisors: Rich Hardy and Jeff Warburton. Their support has been invaluable in motivating me to complete this research. Rich's guidance throughout the year has focused the model development in this thesis; whilst Jeff's unwavering enthusiasm for field work is infectious. Between them, Rich and Jeff have made it possible for me to investigate an aspect of British upland river systems, which has previously had little coverage, and to develop skills which I will use for the rest of my life. For this I will be forever grateful.

Secondly, I would like to acknowledge the support team within the Department of Geography at Durham. Most particularly Eddie Million and Mervyn Brown, who were always willing to sort field work equipment and offer some perspective during the long winter of failed field work. The experience of Ed and Merv, along with the other support staff, is important in the development of any project as they are able to offer insight into the techniques and equipment with works best and technical knowledge to put ideas into practice.

Next, I would like to thank family. My parents have always made any opportunity I have had a reality, and supported me in all my decisions. This thesis could not have been completed without their support and words of encouragement.

Finally, I would like to acknowledge my friends both in Durham and further a field. Here in Durham my friends have offered an outlet during times of frustrations, offered congratulations when things were going well and provided the answers, however simple or complex, when problems have arisen. My friends from home and abroad, who I see less frequently, all in their own way, have offered support and advice when needed.

Contents

Figures

Tables

Equations

Notation

Greek Symbols

α	Dimensionless velocity distribution coefficient	(-)
ρ	Density of water	(kg m^{-3})
ρ_s	Density of sediment	(kg m^{-3})
τ	Shear stress	(N m^{-1})
τ_{cr}	Critical shear stress	(N m^{-1})
τ_{ci}	Dimensionless critical shear stress	(-)
ω	Stream Power per unit area	(W m^{-2})

Latin Symbols

A	Flow area	(m^2)
$C_{c,e}$	Dimensionless coefficient for contraction or expansion	(-)
D_i	Grain-size of interest	(mm)
d	Flow depth (stage)	(m)
g	Acceleration due to gravity	(m s^{-2})
h_f	Energy loss due to friction	(m)
$h_{L_{1-2}}$	Combined energy loss, between cross sections, due to friction and expansion or contraction of the channel	(m)
h_o	Energy loss due to expansion or contraction of the channel	(m)
k	Unit conversion constant of 1 for metric units	(-)
L	Distance between two cross sections	(m)
n	Manning's roughness coefficient	(-)
Q	Reach average discharge	(m^3 s^{-1})
q	Average discharge for the individual cross section	(m^3 sec^{-1})
R	Hydraulic radius	(m)
S	Water-surface gradient	(-)
S_f	Slope of the bed a individual cross section	(-)
S_{fr}	Slope through the channel due to friction	(-)
t	Time	(sec)
V	Reached average flow velocity (downstream)	(m s^{-1})
v	Average downstream flow velocity for individual cross section	(m sec^{-1})
$WSEL$	Water surface elevation at the cross section	(m)
w	Channel width	(m)
χ	Distance downstream of the cross section	(m)
y	Hydraulic depth, calculated by: dividing the flow area by width of the channel at the top of the water profile	(m)

Chapter 1:

Introduction and Background: The significance of bedrock channels in determining sediment transport in upland fluvial systems

1.1 **Scope of chapter**

In recent years studies of bedrock rivers have become increasingly common (Tinkler and Wohl, 1998). However, in the UK, bedrock channels have received little attention. This has left a gap in our process understanding of the role bedrock reaches play in governing sediment transport. The aim of this thesis is to describe the transport of sediment through a mixed bedrock and alluvial channel and to consider the impact of this on the sediment dynamics of the river system. This chapter provides a context for characterising river channel form by considering the interactions between channel morphology, flow and sediment transport. This consideration has lead to the development of a conceptual model, based on the 'fluvial trinity', which expands our understanding of alluvial channels to partially alluvial and bedrock channels (Ashworth and Ferguson, 1986; Best, 1986). In this chapter, the impact of different river reaches in defining the sediment balance of the whole river system, through their role in controlling sediment transport is examined. To conclude, this chapter defines the aims, objectives and research framework designed to improve our understanding of sediment transport through a mixed bedrock and alluvial river reach.

1.2 **Characterising river channels**

Bedrock channels are a specific type of channel within the overall river system (Montgomery and Buffington, 1997; Wohl and Merritt, 2001) and contrast with other channel types (e.g. alluvial which are defined as having a bed of sediment deposited by flowing water). Bedrock channels are cut into rock and have previously been defined as having a wetted perimeter of greater than fifty percent bedrock (Ferguson, 1981; Tinkler and Wohl, 1998). They appear along a river where resistant rock is present (Howard, 1987; Wohl and Merritt, 2001) and the river is sufficiently competent to incise through the surface rock layer or exploit weaknesses in the rock structure. Traditionally the view has been that the high sediment transport capacity of bedrock channels has been caused by the rigid nature of the channel boundary, resulting in little interaction, between the channel morphology, flow and sediment, and efficient downstream sediment transport (Montgomery and Buffington, 1997; Tinkler and Wohl, 1998; Whipple, 2004; Carling, 2006; Pelletier, 2008). However more recent observations suggest that the interaction between form and process in bedrock river channels operate differently to alluvial channels and must be considered in their own right (Richardson and Carling, 2006). In order to do this, the process understanding used to conceptualise sediment transport in alluvial channels needs to be modified for bedrock channels.

1.2.1 **Processes in alluvial rivers**

Sediment transport in alluvial rivers is controlled by a complex set of interactions between channel morphology, flow and the sediment available for entrainment and is schematically represented in the conceptual model of Ashworth and Ferguson (1986) (Figure 1.1). This model highlights the feedbacks between the channel morphology and sediment properties determined by flow (Hardy, 2006) and the in-channel distribution of erosion and deposition which determines the morphology (Lane and Richards, 1997). The magnitude and frequency of feedbacks in this system are determined by the discharge and the sediment calibre within the catchment (Reid and Dunne, 1996; Higgitt et al., 2001). A more general model has been proposed by Best (1986) which considers the 'fluvial trinity' of alluvial channels (Figure 1.2). This second model is a simplistic representation of the main interactions between channel morphology, flow

and sediment transport observed in the Ashworth-Ferguson model, and is the basis of the conceptual model developed here for both partially alluvial and bedrock channels.

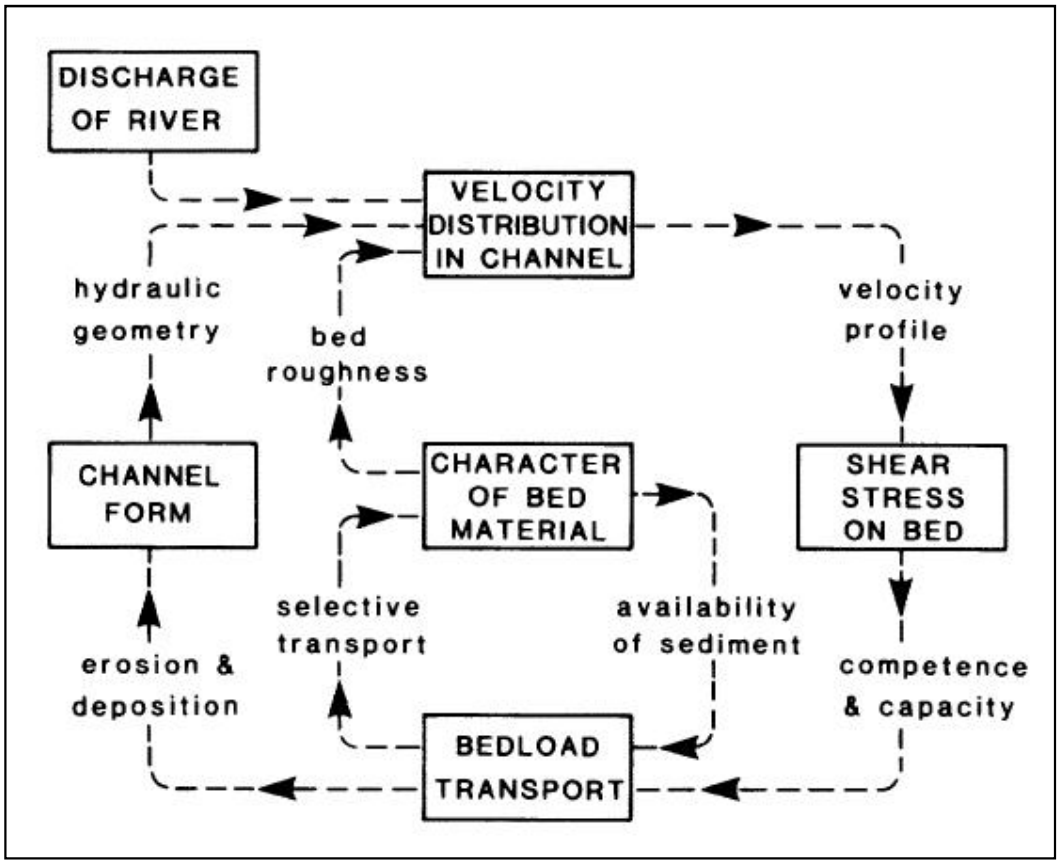

Figure 1.1 Interrelationships amongst form, flow and sediment in active gravel-bed rivers (Ashworth and Ferguson, 1986).

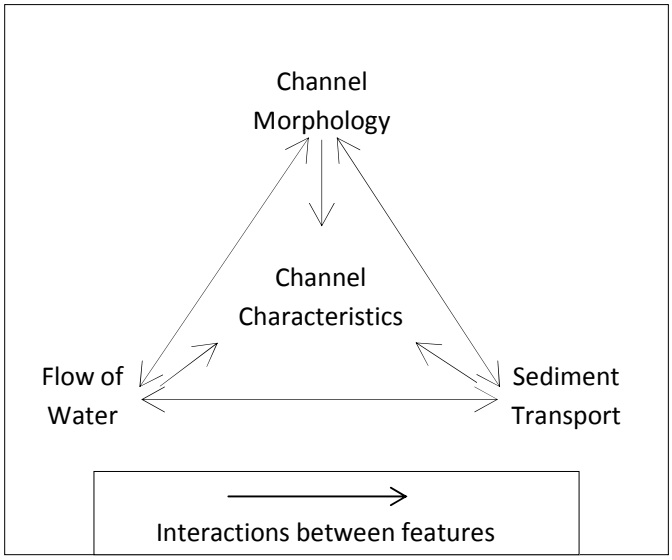

Figure 1.2 'Fluvial trintiy' used by Best (1986), to consider the interaction occurring at channel confluences in alluvial rivers.

1.2.2 **The interaction between channel morphology, flow and sediment transport in bedrock channels**

The morphology of bedrock channels is important in determining the nature of sediment transport and water conveyance. Bedrock reaches occur where stream power is greater than the critical threshold needed for sediment transport to occur and at present or in the past flows have been sufficient to incise the bedrock. This is largely controlled by the gradient of the river as bedrock channels are usually steeper than their alluvial counterparts (Hooke, 2003). However it is questionable whether this is the only controlling variable or whether the channel gradient is a product of increased erosion due concentration of the flow and less armouring of the bed by sediment. The general shape of a bedrock channel has been characterised as having a single inner channel which increases in width at discrete intervals due to the presence of steps in the channel walls (Wohl et al., 1994; Broadhurst and Heritage, 1998; Johnson and Whipple, 2007) (Figure 1.3). This rigid channel shape focuses flow: causing smoothing of channel boundaries, reducing hydraulic roughness and enabling greater stream power. The result is that this inner channel will have a higher sediment transport capacity than alluvial channels operating at similar discharges (Tinkler and Wohl, 1998). In bedrock channels there are however local areas of weaker flow which occur in the outer regions away from the inner channel, or where the bed is sheltered, which allow sediment settling (e.g. potholes, Johnson and Whipple, 2007). Therefore, traditionally accepted alluvial river concepts such as a channel morphology which may be characterized as straight, meandering or braided; incision rates which are directly proportional to stream power; and reach averaged sediment transport approximation, cannot always be directly applied to bedrock channels (Knighton, 1984; Wohl and Merritt, 2001).

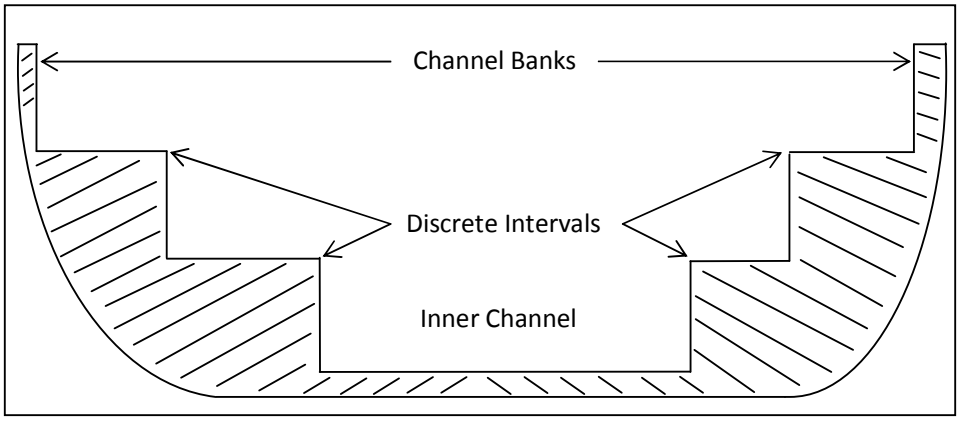

Figure 1.3 Conceptual diagram of bedrock channel with single inner channel and changes in channel width at morphologically controlled discrete intervals (Wohl et al., 1994; Broadhurst and Heritage, 1998; Johnson and Whipple, 2007).

The reach averaged flow velocity in bedrock channels is traditionally characterised as high due to the low hydraulic roughness. However recent studies of the flow dynamics of bedrock channels have shown that central highly turbulent regions and areas of slack flow (at the margins) can occur in conjunction and result in local variation (Richardson and Carling, 2006). The central portion of the flow is generally contained within an inner channel (Figure 1.3) and at low flows is the only active region of the channel. As discharge and flow depth increase the wetted area changes at discrete intervals (defined by the shape of the channel walls, Figure 1.3). In bedrock channels the interaction between the channel morphology and flow causes hydraulic jumps at definable flow depths resulting in changing flow patterns and fluctuating sediment transport

competence (Heritage et al., 2001; Jansen, 2006). These interactions result in localised dead zones in what are otherwise highly competent reaches for sediment transport (Young et al., 2001).

The mechanics of sediment transport are modelled through entrainment, transport and deposition processes (Chalov, 2004). These are normally defined as a product of channel morphology, flow and sediment characteristics, which describe the probability of sediment transport at the scale of enquiry. Empirically the conditions can be modelled at the reach scale using a stream power equation (Equation 1.1, Bagnold, 1977). However, the changeable flow in bedrock channels suggests that local shear stress may provide a better approximation, if used at a series of cross sections (Equation 1.2, Meyer-Peter and Müller, 1948).

$$\omega = \frac{\rho g Q S}{w} \text{ or } \omega = \tau V \quad \text{(Eq. 1.1)}$$

Where, ω is the stream power per unit bed area (W m^{-2}); ρ is the density of water (g m^{-3}); g is acceleration due to gravity (m s^{-2}); Q is the discharge ($m^3 s^{-1}$); w is the channel width (m); and V is the reach averaged flow velocity (m s^{-1}).

$$\tau = \rho g d S \quad \text{(Eq. 1.2)}$$

Where, ρ is the density of water (kg m^3), g is acceleration due to gravity (m s^{-2}), d is the flow depth (m) and S is the water-surface gradient (-).

Each of these equations take into account the form of the channel and the flow, but do not address the individual sediment characteristics at the point of entrainment (Coleman and Nikora, 2008). In alluvial rivers pivoting analysis and incipient motion of the sediment are used as proxies for predicting sediment transport (White, 1940; Bagnold, 1941; Garde and Ranga Raju, 1977). In bedrock channels however, little work has been done to investigate these assumptions, except that of Komar and Reimers (1978) who found that more spherical sediment particles require low flow velocities to keep them entrained. Coupled with the low levels of sediment in bedrock river channels, there has been little common consensus on the influence of channel sediment characteristics on sediment transport through bedrock channels. Currently it is thought that the controls in high gradient bedrock streams are a product of low surface friction and shallow depth of the alluvial layer and, transport and deposition are dictated by local morphology, flow and sediment properties (e.g. Wiberg and Smith, 1987; Carling and Tinkler, 1998; Carling et al., 2002).

1.2.3 **A revised conceptual model for bedrock channels**

The different interactions between channel morphology, flow and sediment transport in alluvial and bedrock channels have been discussed in the previous two sections. In all channel types there is an interaction between flow and morphology. However in bedrock channels the morphology is relatively stable over the time-scale of several years. The interactions between sediment transport and channel morphology only occur intermittently when sediment is present in the bedrock channel, through external supply or breakdown of the bedrock boundary. The high transport potential of bedrock channels also limits the potential storage of sediment and therefore restricts short-term interactions between alluvial channel elements the characteristics of sediment transport.

The partial decoupling, over short (minutes/hours) to medium (days/months) time-scales, between sediment dynamics and channel morphology in bedrock channels has influence on the interaction between channel form, flow and sediment transport downstream. Whilst in bedrock channels the morphology controls the hydraulics of the flow, low levels of sediment in the

channel (available for transport) control where sediment transport occurs (Turowski et al., 2008). At the transition between alluvial and bedrock channels, the situation is less clear. The transition is not defined by a discrete boundary and the river channel may fluctuate between alluvial and bedrock reaches over short distances, as a result of changing sediment supply and flow magnitude. As a result partially alluvial zones have an important role in defining the sediment transport through the whole reach. During periods of low flow or as a result of excess sediment supply, the sediment stored in partially alluvial zones may increase, waiting to be re-entrained during the next high flow event. This changing significance of channel morphology and sediment supply, in generating partially alluvial zones, bridges the divide between fully alluvial and fully bedrock river channels. This has led to the proposal of a new conceptual model for partially alluvial and bed rock channels (Figure 1.4b and c) that demonstrate the active linkages between channel morphology, flow and sediment transport, in river channels which have partially alluvial and bedrock characteristics. The differing form of these 'fluvial trinities' is developed later, in relation to the amount of sediment stored in the channel. This is used to characterise zones within the study reach which are alluvial, partially alluvial or bedrock (section 4.2.1). The role of different channel types defining the sediment balance of the river system is now considered.

1.3 **The reach-based sediment balance**

By combining the rate of sediment transport in every sub-reach of a river, it is possible to predict the response of the fluvial system to changes in their catchments over short and long time periods (Holliday et al., 2003; Hooke, 2003; Carling, 2006) and to study landscape evolution (Sklar and Dietrich, 2001, 2004). The rate of sediment transport through a river is quantified through a standard mass balance approach and then combining all the local sediment fluxes through all river reaches (Equation 1.3, Richards, 1982).

$$Output = Input \pm (Change\ in)\ Storage \quad \text{(Eq. 1.3)}$$

Each local sediment balance is controlled by the sediment transport potential through the reach as defined by the reach type and the interactions, between channel morphology, flow and sediment transport (Broadhurst and Heritage, 1998). The sequence of bedrock, partially alluvial and alluvial zones, therefore defines the flux of sediment downstream in response to changing catchment conditions (Montgomery and Buffington, 1997; Wohl and Merritt, 2001). This relies on understanding of the sediment transport processes that occur in different reach types (bedrock reaches being the focus of this thesis).

1.3.1 **The sediment balance of bedrock channels.**

Pelletier (2008) comments that in order for a bedrock reach to exist then the transport capacity within the reach must be greater than the sediment flux entering from upstream and the wider catchment. Under supply limited conditions it has been suggested that sediment supply within the catchment is more important than the hydraulic conditions in determining the volume of sediment output from the catchment (Carling, 1983). This has been considered in the context of bedrock channels as an 'exposure fraction' defined as the relationship between sediment supply per unit width and transport capacity (Sklar and Dietrich, 1998, 2004). If the 'exposure fraction' is high then the transport capacity exceeds the sediment supply and as a result the channel is free of sediment. As the 'exposure factor' reduces the sediment stored in the channel increases and the form of the channel will shift towards partially alluvial and alluvial. These situations have been considered by Hooke (2003) in the context of a connectivity hypothesis where a river reach fulfils one of three situations (Table 1.1).

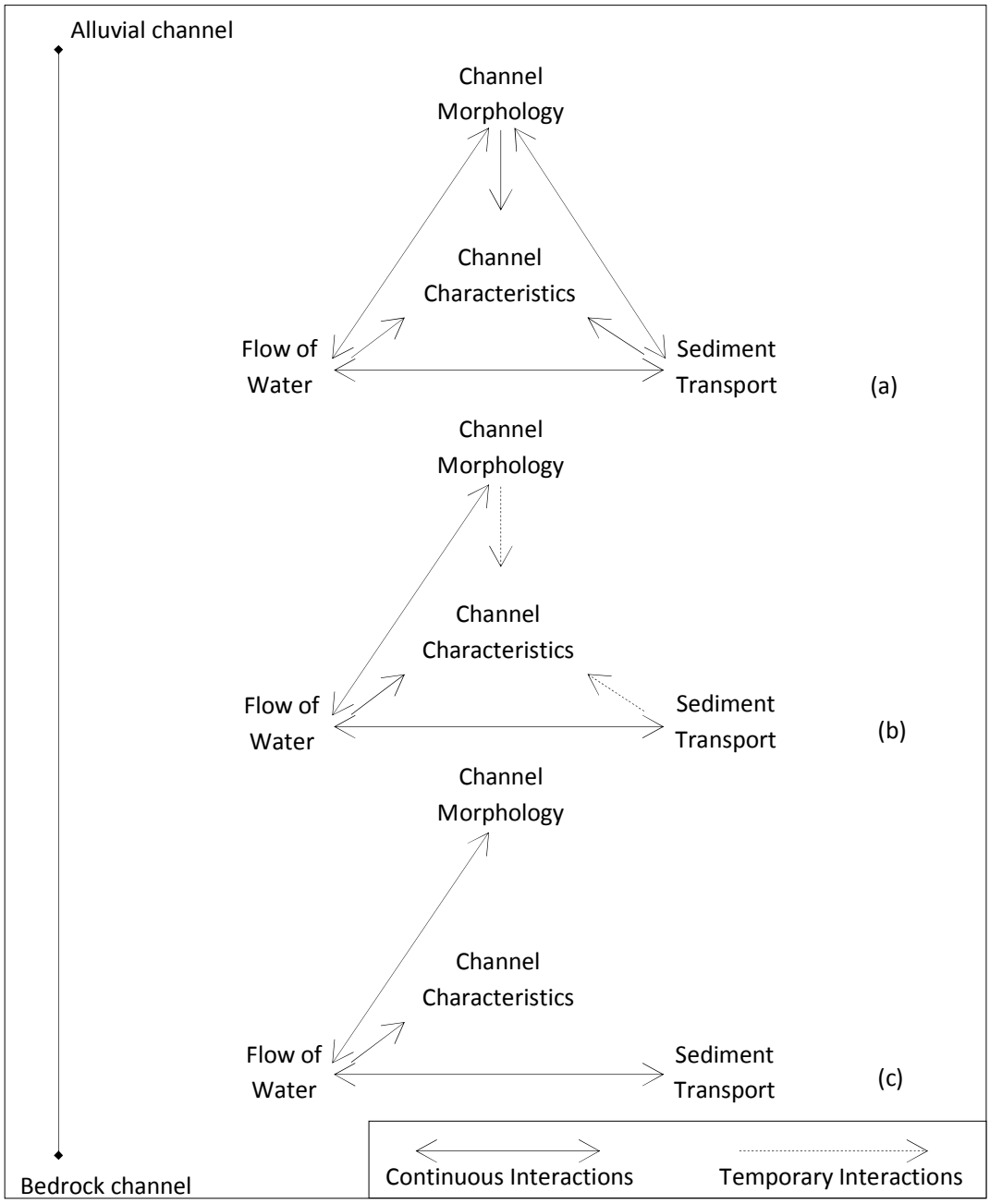

Figure 1.4 The conceptual model proposed for studying partially alluvial and bedrock channels. This has been developed from the original model of Best (1986, Figure 1.3a). The model has been subsequently developed for partially alluvial (b) and bedrock river channel forms (c).

Situation	Reach Properties
Situation 1	The reach is of low competence and coarse sediment cannot be transported through the reach.
Situation 2	The reach is highly competent and coarse material is flushed through the reach in high flows but because of the high power, the material is not deposited within the reach.
Situation 3	The reach is competent to transport coarse material but such material is not available due to lack of supply.

Table 1.1 Table showing the three flow – sediment situations which determine the connectivity of river reaches within the sediment cascade (Hooke, 2003).

Situation 1 can be recognised by increased aggradation of sediment at the upper end of the bedrock reach. This causes a feedback which reduces slope and decreases the velocity of flow (Figure 1.5, the 'lack of competence' reach). The second situation has been identified in many bedrock reaches (e.g. Montgomery and Buffington, 1997; Tinkler and Wohl, 1998; Carling, 2006; Pelletier, 2008), and arises due to the decreased bed roughness of bedrock channels and reduced near-bed flow resistance (Carling et al., 1992). This is defined by a reach exhibiting 'flush through' characteristics (Figure 1.5). Situation 3 is controlled by sediment supply rather than the two previous situations which are flow controlled. This means that the properties of the reach are defined by sediment conditions in the wider catchment rather than the hydraulic conditions within the reach. This condition is termed 'sediment exhaustion' as the flow moves all the sediment which is available in the reach (Figure 1.5). Overall bedrock channels interact with adjacent alluvial reaches and any external sediment supply, to transport sediment through the river channel, maintaining the sediment cascade. In order to understand the rate at which sediment is transported the interactions between channel form, flow and sediment transport must be investigated.

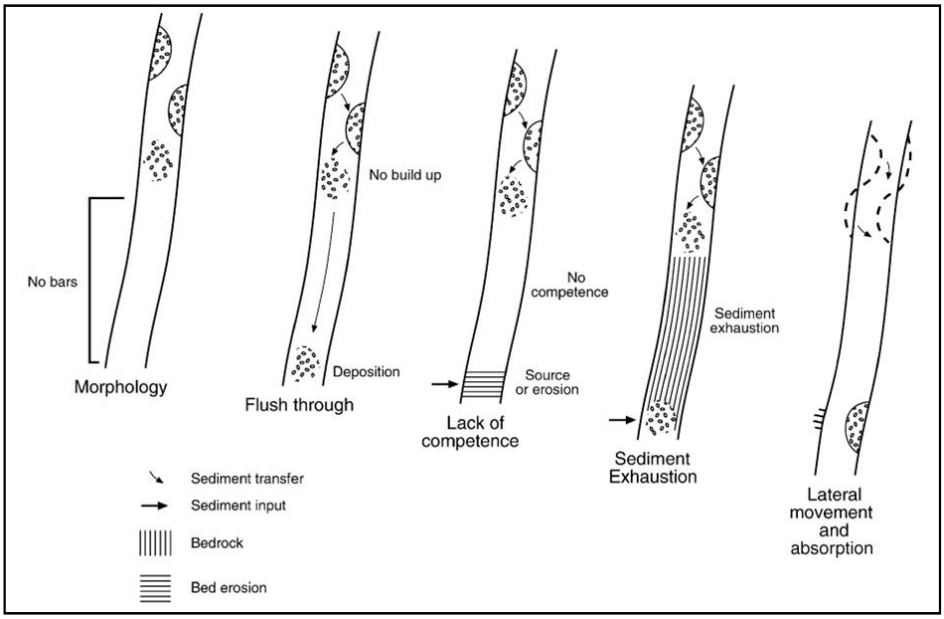

Figure 1.5 The range of possible conditions for reaches that lack coarse sediment stores (Hooke, 2003).

1.4 **Studies of UK bedrock channels**

Studies of river systems, river dynamics and the response to changing catchment conditions, have primarily focused on alluvial rivers in the UK. However bedrock channels play an important role in controlling the sediment balance of the river system (section 1.3) and defining the landscape evolution processes which are governed by incision rates (Chatanantavet and Parker, 2008). There is currently a gap in our understanding of sediment transport dynamics in bedrock river channels in the UK (Table 1.2). Existing work has examined the boulder entrainment in bedrock channels (Carling and Grodek, 1994; Carling, 1995; Carling and Tinkler, 1998; Carling et al., 2002) but there has been little other work into the overall impact of bedrock channels in controlling the rates of sediment transport. Two exceptions are Smith (2004) and Warburton and Smith (2005), which considered the interaction between bedrock channel form and the routing of sediment in an UK upland bedrock channel (Table 1.2).

Author	Year	Site	Research Content
Carling and Grodeck	1994	Sleightolme, County Durham	Estimation of peak discharge in an ungauged bedrock channel.
Carling	1995	Birk Beck, Cumbria	Sediment features considered alongside morphological controls.
Carling and Tinkler	1998	River Dee, Cumbria	Initial motion of boulders in bedrock channels.
Carling, Hoffman and Blatter	2002	River Dee and Birk Beck, Cumbria	Initial motion of boulders in bedrock channels.
Smith	2004	Trout Beck, Cumbria	Bedrock morphology and sediment dynamics.
Warburton and Smith	2005	Trout Beck, Cumbria	Re-sedimentation of excavated bedrock river reach.

Table 1.2 Studies of bedrock channels in the UK.

1.5 **Research structure**

This thesis aims to use the 'fluvial trinities' model (Figure 1.3), to assess the magnitude and frequency potential of a bedrock river channel to convey sediment downstream. By considering the influence of channel form and flow on sediment transport, in bedrock and partially alluvial zones of the river, conclusions will be drawn of when and where sediment transport is occurring.

1.5.1 **Objectives**

To address this general aim, the following five objectives will quantify and model the movement of sediment through the study reach:

1. *Identify the nature of sediment storage through the study reach*. The classification of the study reach as alluvial, partially alluvial and bedrock will be used to identify the conceptual model most appropriate to the channel. From this the physical conditions within the channel will be

better understood. To do this the continuum of fluvial trinities and channel characteristic definitions, will be used to determine the interactions between flow, sediment transport and channel morphology in different areas of the study reach (Figure 1.4).

2. *Monitor temporal nature of sediment transport.* By quantifying how much sediment and the type of mobile sediment over time, the influence of the flow on controlling sediment transport can be assessed. This will be done by considering when sediment transport is occurring in the reach. Two methods will be used to assess sediment transport. Firstly sediment tracers will be employed to monitor the movement of individual sediment clasts. Secondly *in situ* impact sensors will be used to capture the timing of sediment transport events in four locations in the channel.

3. *Monitor the spatial movement of sediment through the bedrock channel*. Capturing the spatial pattern of sediment movement will provide insight into where sediment is entrained and where it is deposited. This will address the role which different channel characteristics have in controlling sediment movement. The magnitude of sediment movement in different areas of the channel will be monitored using the *in situ* impact sensors.

4. *Modelling the temporal and spatial hydraulics of the study reach*. Modelling the in channel distribution of hydraulic properties for the study reach will couple the morphological and flow properties together to allow for considerations of how they interact to cause sediment transport. This will primarily be done using the HEC-RAS one dimensional model. This model considers the interaction between morphology and flow by solving the St. Venant equations at a series of cross sections downstream through the river reach. The hydraulic properties at each of these cross sections will then be used in the analysis of sediment transport through river channels.

5. *Defining the different rates of sediment transport through contrasting sections of the channel.* By considering the rate of sediment transport through bedrock, partially alluvial and alluvial stretches of the study reach, the sediment balance of a river with channel types of mixed characteristic will be conceptualised. This will draw together the empirical evidence of sediment transport with the modelled potential of sediment transport to determine the role bedrock channels play in routing sediment downstream.

1.5.2 **Research framework: addressing the research aims and objectives**

In order to assess the changing sediment dynamics through the study reach, a research framework has been developed (Figure 1.6). This framework consists of three main parts. Firstly the collection of field data provides empirical data of the natural river conditions. The field monitoring has been designed to capture each aspect of the 'fluvial trinity' and specifically to fulfil objectives 1-3, outline above. The channel morphology will be captured through high resolution surveying by differential GPS and terrestrial laser scanning. The reach scale flow regime gauged both locally and downstream will be monitored using pressure transducers and a compound weir. Local sediment movement will be assessed using in situ impact sensors and sediment tracers.

Secondly, using the HEC-RAS one dimensional model, a numerical modelling approach will be used to consider how the interactions between channel morphology and flow cause specific hydraulic conditions through the study reach. This will be considered in conjunction with the empirical equations governing sediment transport derived from the field data collected at the study site. Finally, by combining the two modelling approaches, the sediment dynamics through the study reach will be considered.

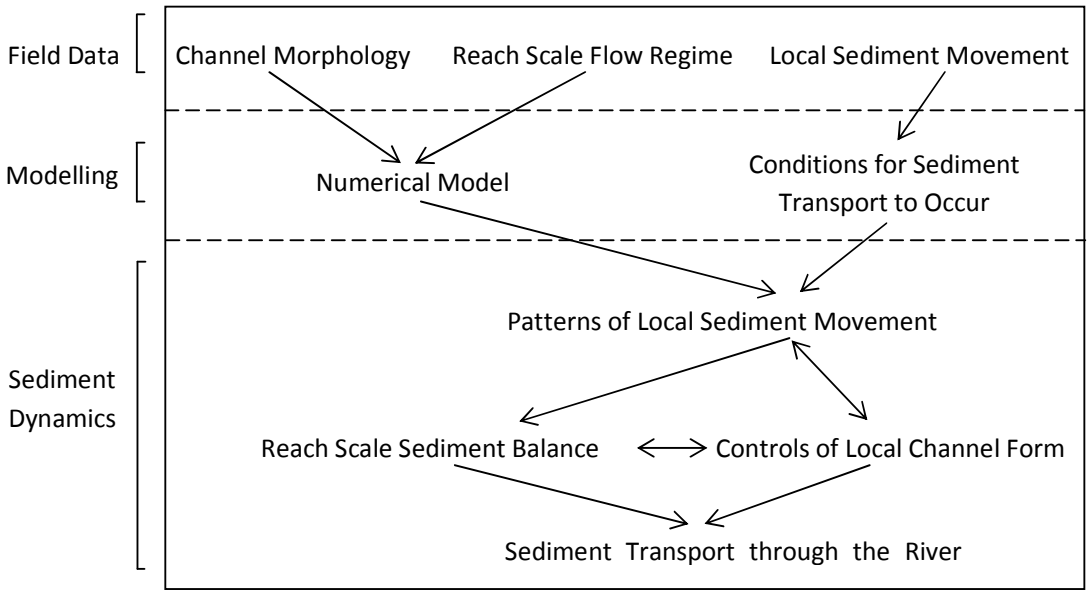

Figure 1.6 Research framework: incorporating field data collection and numerical modelling to investigate the local sediment dynamics of an upland bedrock river reach.

1.5.3 **Thesis Structure**

The thesis is structured into six chapters. Chapter 1 has provided an introduction and background into the role of bedrock channels in controlling the rate of sediment transport through the river system. This chapter explored the in-channel interactions which control the rate of sediment transport and the role bedrock channels within the sediment balance of the wider river system. However, as previous discussed we do not yet have a full understanding of the rate and patterns of sediment transport through bedrock channels. The aim of this thesis is to readdress the lack of process understanding.

Chapter 2 describes the study site at Trout Beck, Northern England. The chapter identifies the geological, hillslope and climatic conditions which define the flow regime and sediment supply to the river; and describes the River Tees system, in which Trout Beck is a tributary. By understanding the reach through catchment conditions, the impact headwater activities have on conditions downstream can be better understood.

Chapter 3 outlines the methodology developed and applied to integrate field monitoring and numerical modelling, in order to quantify the spatial and temporal patterns of sediment movement through bedrock and partially alluvial sections of the study reach. The field monitoring section defines the methods used to monitor each of the three elements in the 'fluvial trinity'. Meanwhile, the modelling section defines the theoretical basis of the HEC-RAS one dimensional flow model and describes the flood hydrograph used in calibration.

Chapters 4 and 5 respectively, present the results and analysis of field monitoring and the development and results produced from modelling. The field monitoring (Chapter 4) follows the structure of the 'fluvial trinity' by capturing the morphology of the river channel, the short- and long- term flow regime of Trout Beck and both the in-channel sediment characteristics and sediment transport, through bedrock and partially alluvial zones. The model development and results (Chapter 5) discusses the calibration of the HEC-RAS model for the bedrock channel, exploring the sensitivity of geomorphological and hydraulic parameters, as well as examining the

modelled spatial distribution of shear stress through the study reach, over the course of a modelled storm event.

Chapter 6 concludes the thesis. The research aims and objectives are discussed with reference to the results of field monitoring and the modelling. Finally, the general conclusions, relating to the role of bedrock channels in controlling the transfer of coarse sediment through an upland river system, are surmised.

Chapter 2:

Study Location: Trout Beck, Moor House and Upper Teesdale National Nature Reserve, North Pennines, UK

2.1 **Introduction**

The bedrock river channel studied as part of this project is a reach of Trout Beck, a tributary of the River Tees in North England. This chapter describes the characteristics of the River Tees and the Trout Beck, river catchments and the properties of the bedrock river channel, in which sediment transport has been monitored.

2.2 **The River Tees catchment**

The River Tees originates at Cross Fell in the North Pennines. It flows 157 km to Redcar and the North Sea and has a catchment area of 1906 km^2 (Woodhouse, 1991). The headwater region of the River Tees is dominated by a British upland climate. Climate, landscape and human activities have an important influence on the nature of the discharge regime and sediment movement through the river (Hudson-Edwards et al., 1997; Baker et al., 2004). As a result the headwater region of the river is important in determining the quantity and quality of water received downstream (Burt, 1992). This importance is heightened due to the efficient hydrologic connectivity of this river network. This connectivity has been suggested as the cause of downstream pollution by sediment-born contaminants derived from mining sites in upland areas (Hudson-Edwards et al., 1997). As a result, several studies have examined the nature of the discharge regime and sediment transport through the River Tees in order to assess the impact downstream of headwater activities (e.g. Augustin et al., 2008).

2.3 **Trout Beck catchment**

Trout Beck is situated within the Moor House and Upper Teesdale National Nature Reserve (NNR) (Sykes and Lane, 1996; Cundill et al., 2007). The Trout Beck catchment is defined by the summits of Hard Hill (678m), Great Dun Fell (848m) and Knock Fell (794m) (Figure 2.1). The catchment covers an area of 11.5 km^2, the majority of which is covered by blanket peat. Peat is important in defining the hillslope surface runoff regime in the catchment and discharge regime of Trout Beck (Worrall et al. 2006 a and b). The discharge regime of Trout Beck has been classified as flashy, with a mean lag time, between peak precipitation and peak discharge, of only 2.8 hours (Evans et al., 1999). This is a result of the high connectivity between hillslope and river channel, determined by efficient flow through the surface peat layer and a high drainage density of 3.57 km km^{-2} (Conway and Millar, 1960; Burt et al., 1998; Evans et al., 1999).

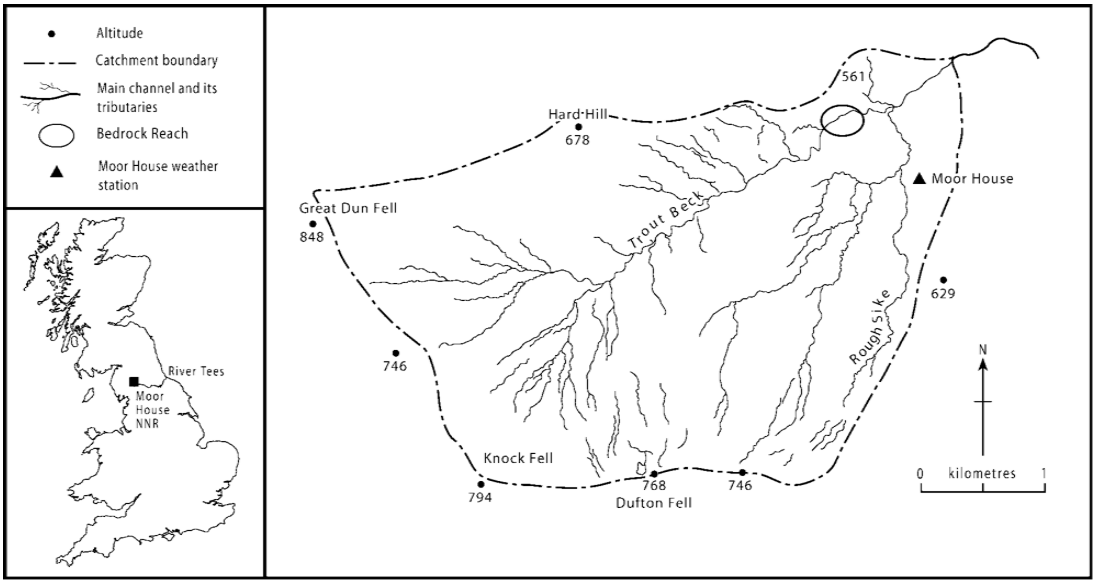

Figure 2.1 Location map of the Trout Beck catchment.

2.3.1 **Geology of the Trout Beck catchment**

The geology of the Trout Beck catchment is described by Johnson and Dunham (1963). The bedrock comprises of Limestone, Sandstone and Mudstone (Figure 2.2) of Upper Carboniferous (c.300 mya) and Lower Carboniferous (c.350 mya) age (Table 2.1). The inter-bedded nature of the Limestone bedrock with other geological types, occurs throughout the catchment, with Limestone dominating several river reaches (Figure 2.2).

The surface geology of Moor House is a mixture of areas dominated by superficial deposits and areas where active erosion has exposed the bedrock. These deposits (Table 2.1) are mainly post-glacial and glacial sediment. They are dominated by blanket peat, alluvium and till (Figure 2.3). Along the course of Trout Beck, sections of the river flow through the blanket peat (which covers 90% of the catchment, Evans et al. (1999)); through mixed bottom land soil complexes (dominated by till, alluvium and peaty alluvium, Figure 2.3); and solid bedrock. Analysis of the river channel type in the region by Smith (2004) found that 82% of Trout Beck is alluvial, 13% is mixed bedrock-alluvial and 5% is solely bedrock. The bedrock reach investigated in this project is an example of where superficial surface cover has been eroded and incision into the limestone bedrock has occurred (Johnson and Dunham, 1963). The down-cutting of Trout Beck, to form a bedrock gorge, is repeated at similar elevations and geological settings in other sub-catchments of the Tees river system (e.g. Netherhearth Sike: Johnson and Dunham (1963)).

Superficial Deposits:		
Recent and Post-Glacial	c.10 kya	Blanket peat, basin peat, alluvium and alluvial fans
Glacial and Periglacial	c.2.6 mya	Solifluxion deposits, sandy and stony clays, boulder clay
Solid Formations:		
Upper Carboniferious	c.300 mya	Upper limestone group – sandstones, grits and shales with coal seams and limestone bands
Lower Carboniferious	c.350 mya	Middle limestone group – a rhythmic sequence of limestone, shales, sandstones and coal seams
		Lower limestone group – massive limestone overlain by thin bands of shale, sandstone and limestone
		Basement series, upper division – sandstone and shale with thin limestones
		Basement series, lower division – massive conglomerates with interbedded sandstone
Ordovician	c.450 mya	Skiddaw slate series – slates, flag tuffs and lavas

Table 2.1 Surface and subsurface geological features of Moor House and Upper Teesdale NNR, (Johnson and Dunham, 1963).

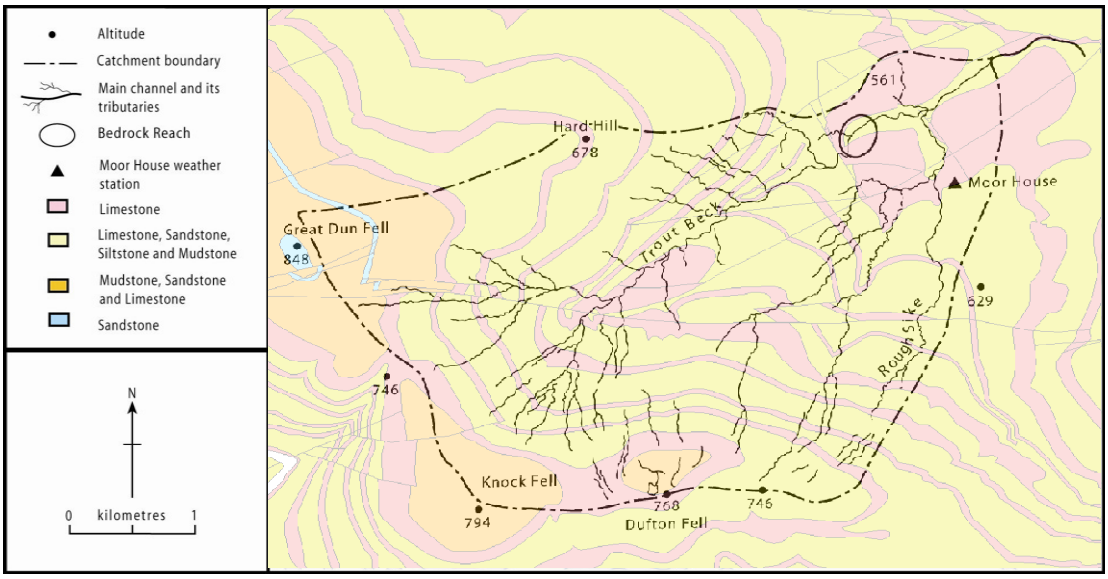

Figure 2.2 Geology of the Trout Beck catchment (Ordnance Survey, 2009).

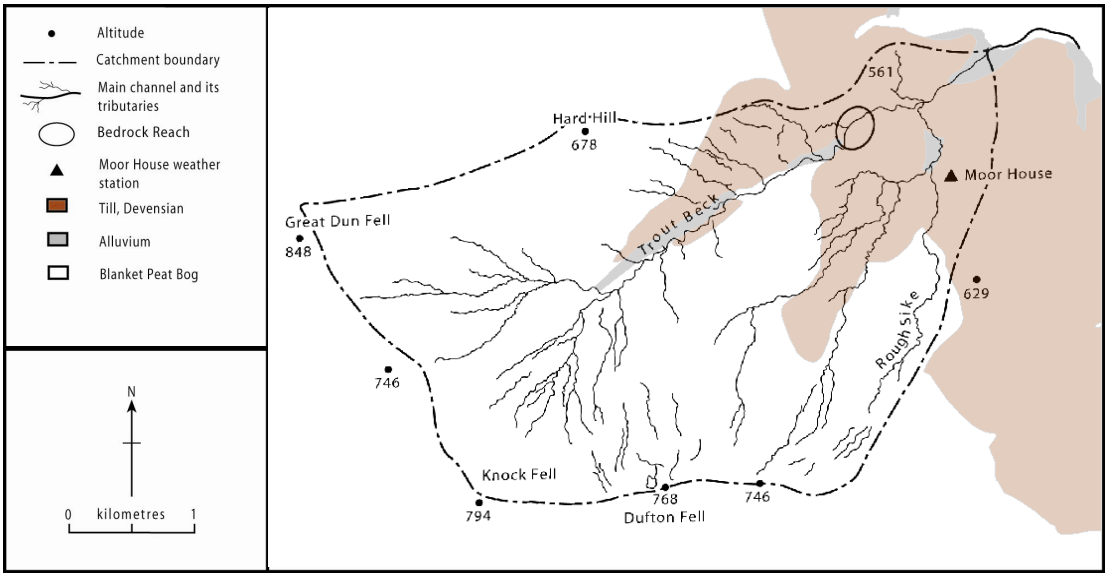

Figure 2.3 Surface cover of the Trout Beck catchment (Ordnance Survey, 2009).

2.3.2 **Surface features in the Trout Beck catchment**

The surface cover of the Trout Beck catchment is a combination of naturally occurring soils and vegetation, modified by human activity. Johnson and Dunham (1963) divided the main soil types into organic, gleys, podzol and brown earths. Peat formations, the main organic soil type, are most prevalent. Widespread peat development occurred due to the decline of indigenous woodland c.3,800 years ago and deterioration of climatic conditions in the area (Pounder, 1989). In the Trout Beck catchment the peat soils are very effective at conveying storm runoff, but produce little baseflow. This together with the concave shape of the hillslopes, with the river channel at the centre, aids the rapid transfer of runoff to the channel (Burt et al., 1998).

Although the near surface features in the Trout Beck catchment are important in defining the discharge timing of the river, there are also other factors in determining the overall river characteristics. Landuse in Moor House and Upper Teesdale NNR has been continuously changing.

Intense mining practices during the 19th century have influenced the hillslope drainage patterns and hillslope sediment supply to rivers (Macklin and Rose, 1986). At Moor House, the metal mining has led to a change in the general pattern of alluviation and in places has produced partial valley infilling, which is now being actively eroded by the cotemporary river system (Macklin, 1997; Warburton, 1998). A shift towards environmental conservation, since the decline in mining at the turn of the 19th and 20th Centuries has led to re-vegetation of hillslopes and a stabilising of hillslope sediment, with sheep grazing and moorland management for game-bird shooting being the only major present-day landuses.

2.3.3 **Climatic conditions in the Trout Beck catchment**

Moor House holds the longest record for climate monitoring of any upland site in the UK (Holden and Adamson, 2002). The recording has been in operation since 1931 at its current location (550m above sea level). Monitoring of temperature, pressure, humidity, rainfall, wind and cloud cover at Moor House has allowed long-term averages of the weather conditions to be calculated. The local climate has been classified as 'ocean subarctic' (Manley, 1941; Clark et al., 2005; Cundill et al., 2007). Statistical values calculated from the record until the year 2000 showed the average temperate to be 5.3°C and average precipitation of 1,982 millimetres per year (Holden and Adamson, 2001). The mean number of frost days per year is 105 and the mean number of days with snow lying is 55 per year (Archer and Stewart, 1995; Holden, 2001). These latter factors indicate that winter precipitation is often 'locked' in the catchment and thus not transferred immediately to the river channel. Comparison of these values to those of the UK average and a similar station at Malham Tarn, show that precipitation and frost days at Moor House are significantly higher in both categories (Table 2.2). This is because Moor House is in the middle of the UK at a high elevation: thus exposing the station to westerly weather systems and decreasing temperatures at higher altitude.

Location	Elevation (m)	Number of Frost Days per year	Total Precipitation per year (mm)	Source
Moor House	550	105	1982	(Holden and Adamson, 2001)
Malham Tarn	381	79	1518	(Met Office, 2009)
UK average	-	56	1126	(Met Office, 2009)

Table 2.2 Average number of frost days and annual precipitation for Moor House, Malham Tarn and the UK average.

2.3.4 **The Trout Beck bedrock channel reach**

The reach of Trout Beck under investigation is 423 metres long (Upstream OS-Grid NY749330, downstream NY752332). The bedrock reach was chosen due to the isolation of the single bedrock reach within an otherwise alluvial river system. The result is that sediment transport through the river system must interact with the bedrock reach and thus the bedrock reach is a controlling variable over the rate of sediment transport through the reach. The downstream end of this reach is situated 1.06 km upstream from the confluence of Trout Beck and the River Tees (Figure 2.1). The contributing catchment area above the bedrock reach is 7.13 km^2 and contributing area at the bottom by the end of the reach is 7.29 km^2. The 0.16 km^2 of catchment surrounding the bedrock reach has no major tributaries hence flow has been modelled

as constant through the reach. Lateral inputs of sediment to the reach are also minimal. The only significant evidence of hillslope-channel sediment coupling is a 24 m^2 bank failure 100 metres upstream from the end of the reach (Figure 2.4). However this appears to be re-vegetating indicating that the failure has been stable over the short-term and thus is not actively supplying sediment to the channel. As a result sediment transport through the study reach is determined by upstream supply and the competence of the channel to maintain transport through the reach.

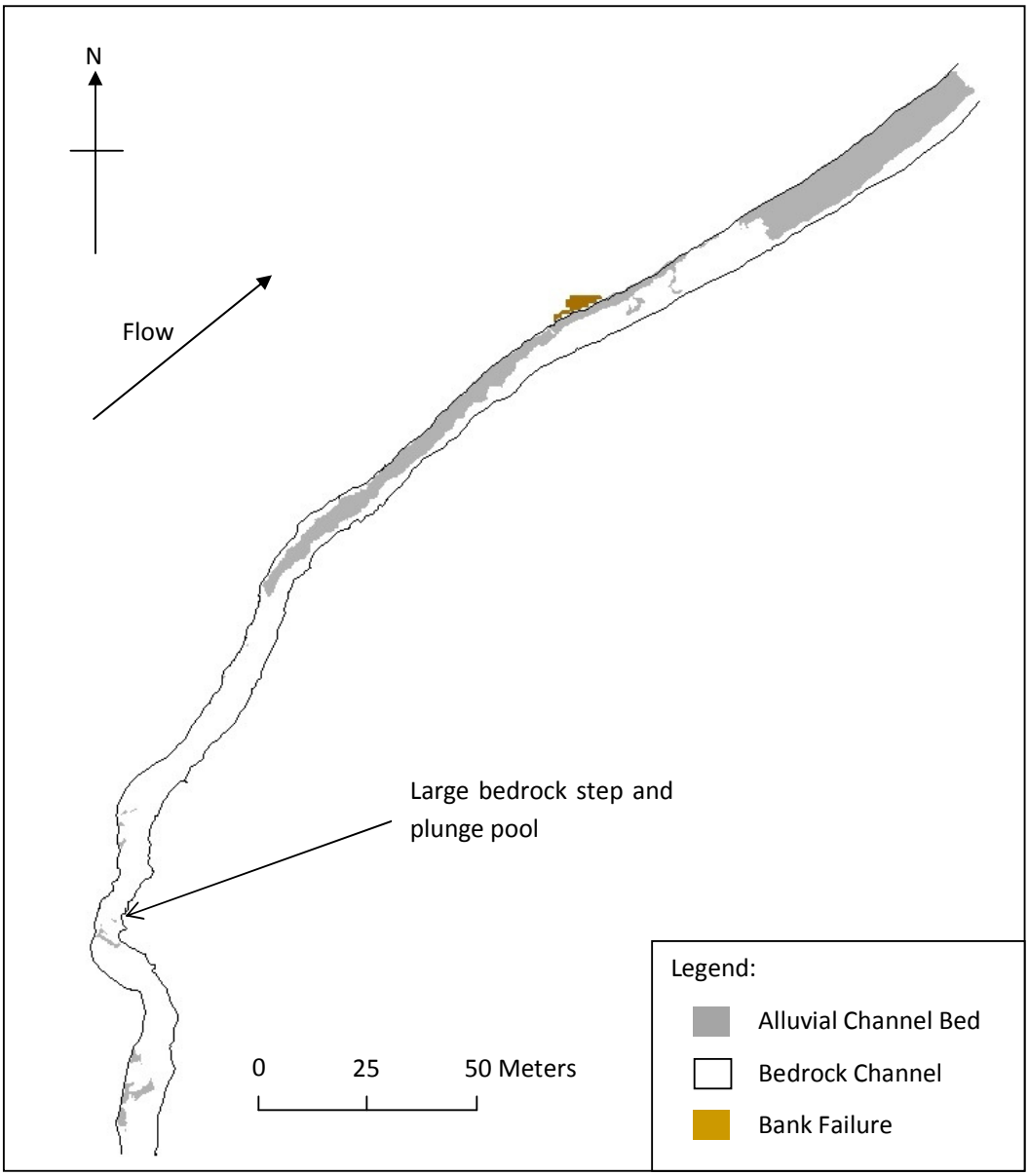

Figure 2.4 Map of Trout Beck study reach showing the bedrock channel and extent of alluvial cover.

Trout Beck is a predominately alluvial river. However the reach studied here shows a distinct downstream pattern fluctuating between alluvial, bedrock, partially alluvial and finally alluvial (Figure 2.4). Smith (2004) found that the stretches of bedrock which occurred in Trout Beck were in conjunctions with the steeper channel gradients, associated with erosional landforms. At the local scale of the study reach this was also found to be true with bedrock boundaries dominating the 80 metres of channel downstream of the large step at 70 metres along

the long profile (Figure 2.5). Downstream from the large step the river has incised deeply to form a bedrock gorge (Figure 2.6). This narrow section of the channel was found by Smith (2004) to be almost completely free of sediment, except for small pockets of sediment in sheltered regions of the channel. Further downstream the channel turns to partially alluvial and then fully alluvial (Tinkler and Wohl, 1998; Smith, 2004) (Figure 2.7). This pattern of sediment storage, the result of fluctuating sediment transport conditions through the study reach, is the focus of this thesis.

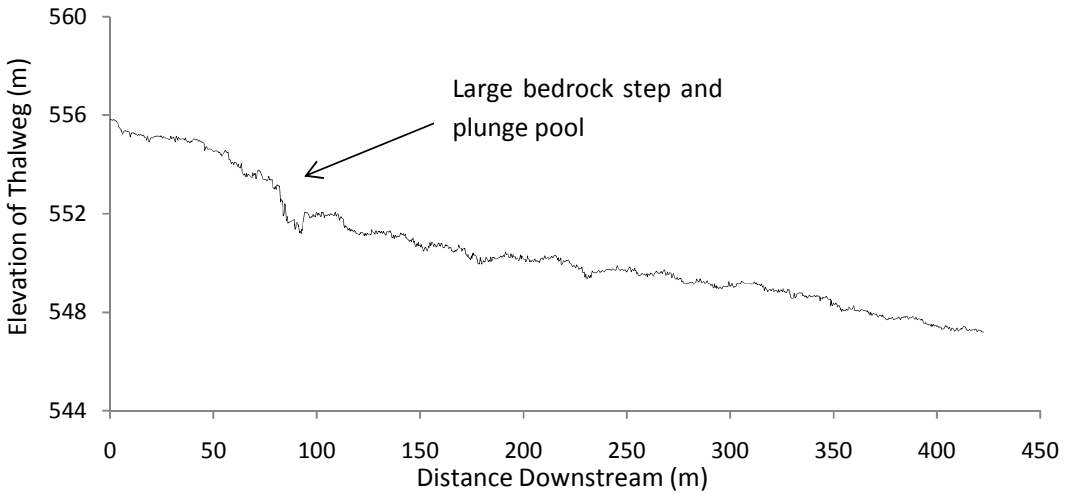

Figure 2.5 Long profile of Trout Beck study reach. The average gradient of the river channel is 0.05, however there is significant variation in the local slope on the bed (for example at the tracer seeding site the slope is 0.0039).

Figure 2.6 Picture showing the upstream end of Trout Beck bedrock gorge, taken from the tracer seeding site, and showing the stage recording site, discussed in chapter 3.

Figure 2.7 Picture showing the alluvial channel in foreground and partially alluvial channel in the background: downstream of the bedrock gorge.

2.4 **Summary**

Geology, soil, vegetation cover and long term changes in landuse are factors which influence runoff and sediment supply at the local scale (Conway and Millar, 1960; Gustard, 1996; Evans et al., 1999). Resistant limestone outcrops are particularly evident along local river courses, where the flashy nature of the flow drives active sediment transport. Although the Trout Beck catchment is dominated by a blanket peat cover, vegetation in recent decades has begun to lock sediment on the eroded hillslopes, stabilising old mining waste and bare peat areas. The Trout Beck study reach shows a range of sub-reach conditions from bedrock to alluvial dominated sections which span the full range of possible process-form linkages identified in Figure 1.3.

Chapter 3:

Methodology: Integrated field monitoring and numerical modelling

3.1 **Introduction**

In Chapter 1, the conceptual model (Figure 1.4), structured around the 'fluvial trinity', was developed and it is this framework that is used in the collection of field data (Figure 1.6) and the development of a numerical model for the bedrock reach. The channel morphology, flow regime and sediment transport characteristics of the study reach have been quantified through field work between October 2008 and August 2009. Channel morphology of the study reach is measured using high resolution surveys (section 3.1.1). The flow regime of Trout Beck is monitored both locally in the study reach, over short time periods, and over longer time periods downstream at an EA compound weir gauging site (section 3.1.2). Sediment characteristics and sediment transport through the study reach have been quantified and classified (sections 3.1.3 – 3.1.5). Finally the HEC-RAS one dimensional model is introduce to identify how the field data is used in calibration of an existing model.

3.1.1 **Channel morphology**

Traditionally channel morphology has been characterised by monitoring rivers in one dimension through time (Lane et al., 1994). In order to do this, cross sections have been surveyed and spatially located relative to each other. The accuracy of the survey is determined by the resolution of the equipment used. Two methods of measuring the morphology of the study reach have been employed here. Firstly river cross sections and position of monitoring stations were recorded using a differential Global Positioning System (dGPS) and secondly the whole study reach was surveyed using a terrestrial laser scanner.

A Leica 1200 dGPS system was used to survey the channel banks, the channel thalweg and 21 channel cross sections at breaks of slope through the reach. The GPS was used in two modes for surveying the channel. Channel banks and the thalweg were surveyed using the continuous streaming feature, whilst the specific locations of particular features were recorded using single point marker mode. In this way, the river channel morphology was quantified and spatially located in the British National Grid coordinate system. DGPS was used to survey individual cross sections due to the minimal errors it produces. The errors recorded from the system, for continuous and single point measurements, show greater error for the single point measures (Table 3.1). This is due to the automated sampling rate for continuous measurements being faster than the rate of data acquisition in single point mode.

Continuous	X (m)	Y (m)	Z (m)	Single point	X (m)	Y (m)	Z (m)
max	0.077	0.075	0.170	max	0.159	0.112	0.326
min	0.003	0.003	0.007	min	0.004	0.003	0.009
average	0.008	0.007	0.018	average	0.012	0.009	0.028

Table 3.1 Summary of the dGPS errors recorded, using both the continuous streaming and single point modes.

The Trimble GS 3D terrestrial laser scanner has been used to measure the spatial characteristics of the channel morphology. The design of the surveying scans was developed to mitigate error propagation against the sources of error identified by Lichti et al. (2005). Firstly, the error incurred from the hardware is reduced by the high frequency scan resolution used (Lichti et al., 2005). The scans were set to take a point every 0.1 m^2 at a distance of 200 m. The scanner uses a green laser, pulsing at 532 nano-metres and at 200 m the scan has, a single point positional

accuracy of 12 millimetres and a distance accuracy 7 millimetres from the scanner (Trimble Navigation Limited, 2007). The error induced from differences in surface irregularities (geometry and reflectivity) were mitigated against by using, the workflow model developed by Lemmon and Biddiscobme (2005), to take multiple scans of the river channel from different locations (Lichti et al., 2005). These scans were integrated to build a three dimensional surface model of the channel. Each scan incorporated between three and five targets, which were stationary such that each target was scanned from at least three locations. The scanner and target locations were manually marked using dGPS, for use later in spatially locating the separate scans. By scanning each target, and subsequently the river channel, from multiple locations the effect of channel geometry and different surface reflectivity were reduced. Also the scans were carried out during low flow periods such that only a minimal area of the channel was covered by water.

The digital elevation models developed from the channel surveying has been identified as a particularly useful methodology for monitoring bedrock river channels, as there is less volumetric change than in a gravel-bed rivers over the timescale which sediment movement occurs (Pickup and Rieger, 1979). However, the form and processes representation derived from a DEM of solely bedrock channels are typically more accurate than those calculated for shifting bedrock/alluvial channels (Thompson and Croke, 2008) and time constraints dictated that only a single survey was carried at the study site.

3.1.2 **River discharge and stage**

River discharge and stage have been monitored *in situ* by continuous methods, in order to characterise the flow regime of the river. The long term discharge has been monitored at the Environment Agency (EA) gauging station (Figure 3.1). The gauging station is situated at Trout Beck Bridge, 450m upstream of the Trout Beck – River Tees confluence and 550m downstream of the study reach. The gauging station consists of a compound crump weir established in 1971 (Demir, 2000). This longer term record of discharge recorded every 15 minutes, has been collected from 1992 until March 2009. Since the 24th of February 2009 the local stage in the bedrock study reach has also been monitored. Local stage has been recorded using a pressure transducer and Campbell CR500 data logger every 15 minutes at the same time intervals as downstream discharge (Figure 3.2). By combining the two flow data sets a local stage – downstream discharge relationship has been produced (Figure 4.5). This is used to predict the flow at the upstream station, in the study reach, during unmonitored periods (section 4.3).

Figure 3.1 EA compound weir gauging station on Trout Beck, downstream of the study reach.

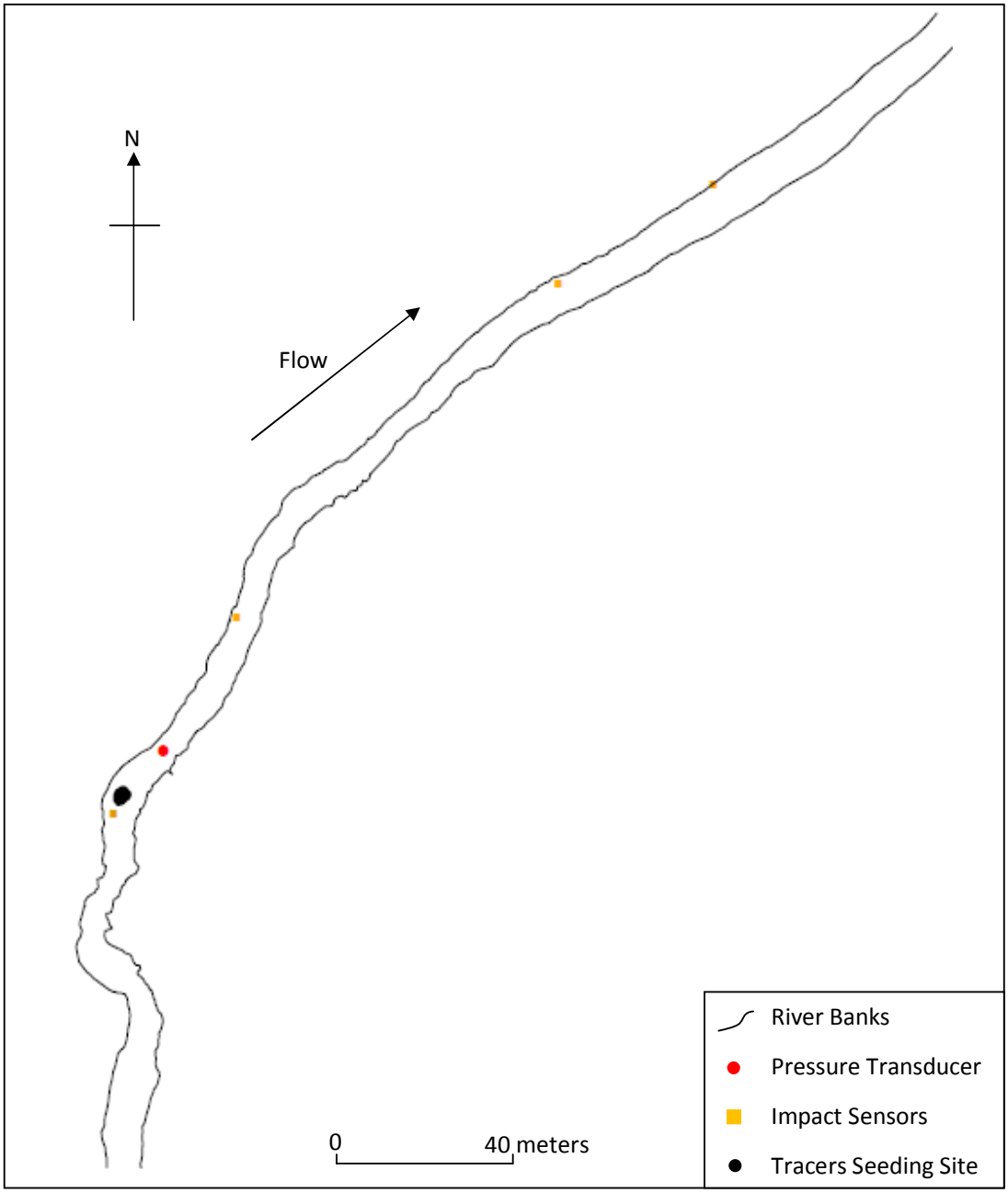

Figure 3.2 The location of the pressure transducer, impact sensors and tracer seeding site in the study reach.

3.1.3 **Channel sediment grain size**

Bedrock channels are relativity free of sediment. However the sediment which is present must be quantified in order to determine the homogeneity of the bed, which is important in predicting the potential for sediment transport (Ferguson, 1994). The general size characteristics of sediment in the river channel are described by the grain-size distribution. This involves measuring the size of a sample of sediment to determine the range and distribution of grain-sizes present in the river channel. When measuring the grain-size the sampling technique must be unbiased and the method of measurement clearly specified (Rice and Church, 1996; Green, 2003). In this study, sediment size was measured by two methods. Firstly manual Wolman sampling was

undertaken at five sites in the channel and used to characterise the grain-size distribution of the coarse sediment, using a bulk sampling method. Then, to extend the spatial coverage of the sampling, the grain-size distributions at 41 sites (including the five measured by Wolman method), were measured in an automated manner applying digital photogrammetry (Figure 3.3). The sampling sites were distributed through the 423 m study reach, covering all areas of sediment storage, on the 15th of October 2008 (Figure 3.3). The sampling was undertaken laterally across the channel, as well as down the long profile, to account for spatial difference in the grain-size distributions through the study reach (Nelson et al., 2009). The automated methodology used to measure the 41 sampling sites involved taking digital photographs of the sediment and the measuring the grain size distributions using Sedimetrics: a digital gravelometer software package (Version 1.0, Sedimetrics ® Digital Gravelometer, 2006).

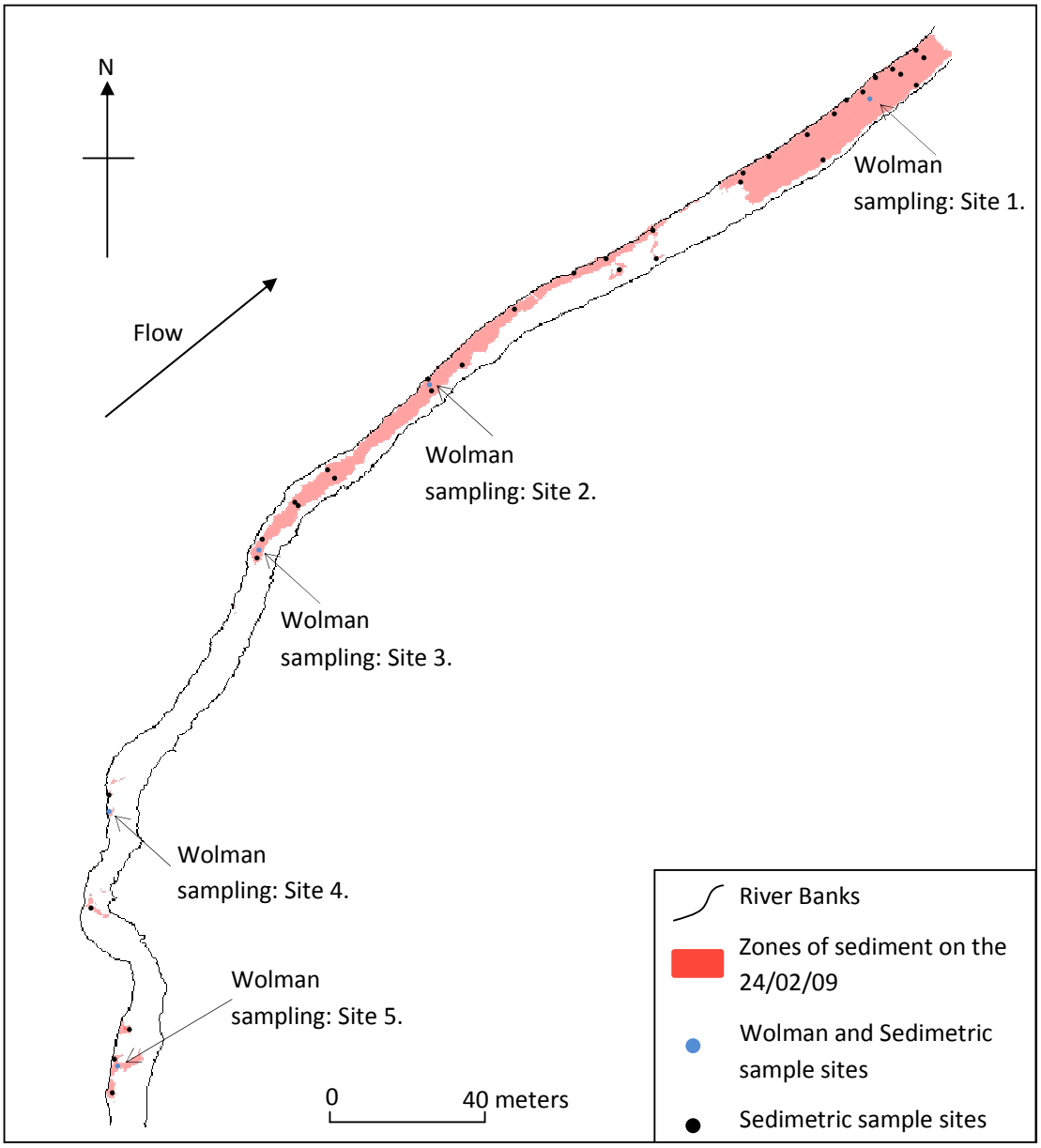

Figure 3.3 The spatial locations where particle size was sampled in the study reach. Blue dots represent locations of Wolman samples, black dots represent locations where digital photogrammetry was applied.

The Wolman method of measuring the grain-size distribution at sample sites, involved taking a random sample of 100 clasts at each site (Wolman, 1954; Fripp and Diplas, 1993). The grain-sizes of the 100 clasts were measured at half phi intervals using Wolman plates (sizes: 16, 21, 32, 45, 64, 90.5, 128, 181 and 256 mm). With the exception of Site 2 (Figure 3.4) there appears to be a decrease in the proportion of fine 16mm and 21mm particles in a downstream direction. Based on these samples the variability in the grain-size is generally low suggesting that the size distribution is relatively homogenous through the study reach. However Wolman samples were only taken at five sites and so more extensive sampling was undertaken using an automated method.

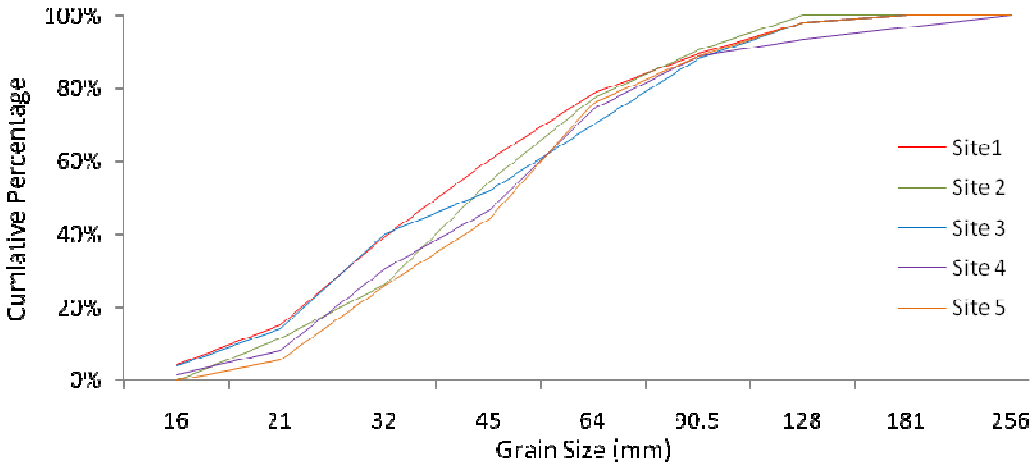

Figure 3.4 Grain-size distribution from Wolman methods (n = 5 samples).

The second method of measuring the grain-size of sediment in the study reach was through the use of digital images. Recent advances in resolution of digital images and software packages available for measuring image characteristics have provided an efficient and accurate alternative to the direct field intensive method of manually measuring grain-size. Digital images of a $1m^2$ area of the bed were captured using an 'Olympus FE220, X785' digital camera, providing a ground resolution of 0.33 millimetres by 0.43 millimetres. The samples were taken at 41 sites in the river channel, including the five sites sampled by the Wolman method. The images where imported into Sedimetrics. The use of this automated method removed the operator error in selecting grains from the bed and greatly increased the number and spatial coverage of sites sampled (Marcus et al., 1995). The comparison between the grain-size distributions measured by the Wolman and Sedimetrics methods are shown in Figure 3.5. The grain-size distributions, measured by Sedimetrics, have a greater proportion of finer sediment than those measured by Wolman sampling. This pattern occurs at all five sites. This arises for two main reasons. Firstly, it has been noted that there may be some un-avoidable bias in the selection of the coarsest sediment through Wolman sampling (Wolman, 1954) and secondly, the Sedimetrics software tends to over estimate finer grain-sizes as a result of the automated processing. Sedmetrics uses a processing technique to measure the grain-size distribution of the images, which identifies the grains in the image, separates touching grains and measure the grains (Sedimetrics ® Digital Gravelometer, 2006). However the identification of grains uses a greyscale image and thresholds this to create a binary image of individual grains. Grains with highly variant texture will subsequently be incorrectly subdivided into many smaller fractions. Overall, whilst the precision of the Sedimetrics technique is good, a bias to finer sizes may be introduced (Figure 3.6). The spatial variations in the grain-size distributions are discussed further in section 4.5.1.

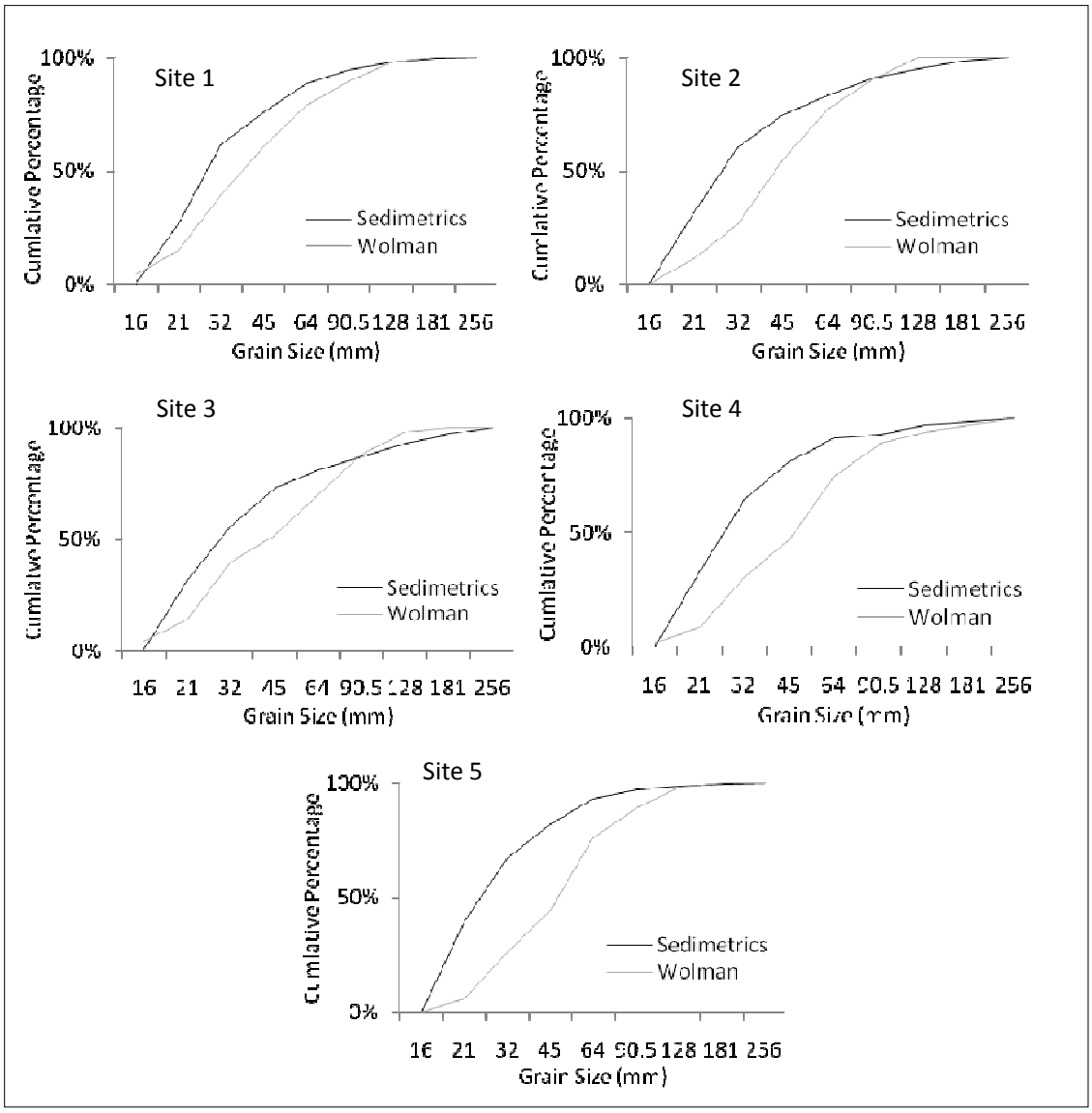

Figure 3.5 Comparison of grain-size distributions for the five sites in the study reach, where both Wolman and Sedimetrics measurements were made.

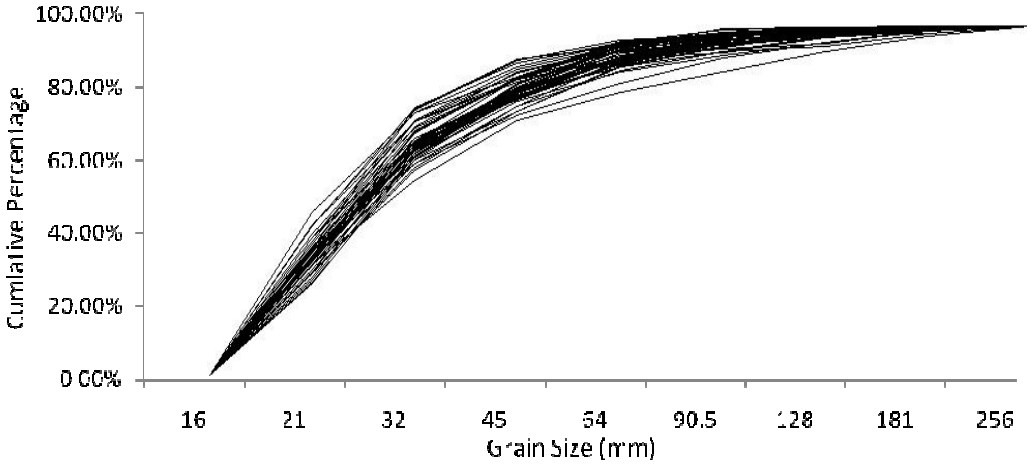

Figure 3.6 Grain size distributions measured using Sedimetrics (n = 41 samples, including the five samples measured by Wolman method).

3.1.4 **Monitoring bedload transport using sediment tracers**

A magnetic tracer experiment was setup in order to monitor the dynamic nature of sediment transport through the study reach. The experiment was based on the methodology of Demir (2000), Warburton and Demir (2000) and Ferguson et al. (2002). The method uses 800 naturally sourced coarse sediment tracers, between 32 and 256 millimetres intermediate axis ('b-axis'). The selection of the tracer sizes was determined from the analysis of the grain-size distributions measured in the field (Section 3.2.3). Results indicate that the grain-size distributions through the study reach do not vary significantly (Figure 3.6) and as a result the average grain-size distribution from the five Wolman sampling sites has been used to determine the distribution of tracer sizes (Figure 3.7). The tracer distribution (Figure 3.7), is biased to the larger size classes because sediment with 'b-axis' of less than 45mm was often too small to drill, for magnet insertion.

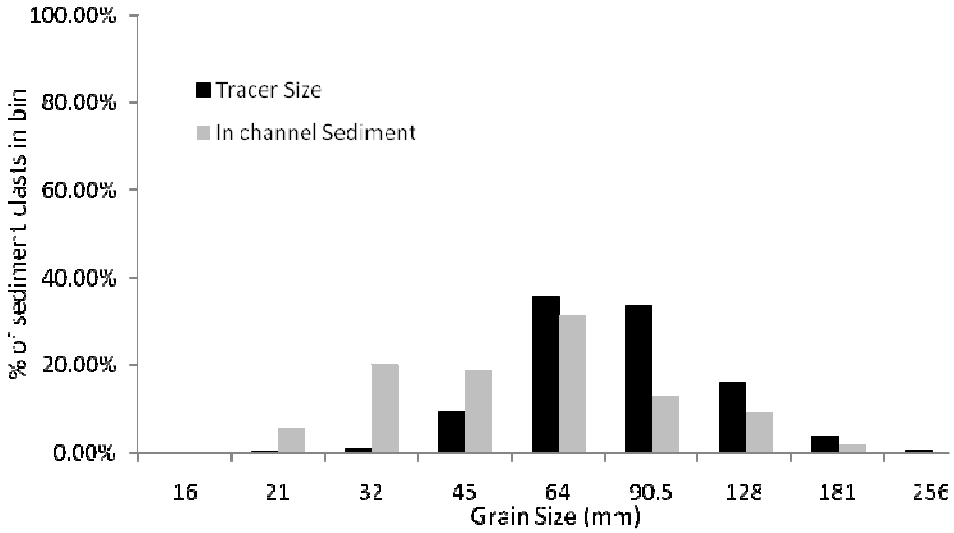

Figure 3.7 The distribution of percentage of sample in each bin range.

Each tracer was drilled and inserted with a 'RDAL Alcomax' rod ferromagnetic magnet. The size of the magnets varied with the size of the tracer, but all were between 10 and 20 millimetres in length and 3 and 6 millimetres in diameter. This lower limit of magnet size dictated the minimum dimensions of the tracers used (see above). Silicone gel was used to secure the magnet in the hole. Finally to make the tracers visible in the channel, pink masonry paint was applied to each clast. The inclusion of magnets allowed the tracers to be found even when buried or when the paint had been abraded (Schick et al., 1988). Finally the 'a', 'b', 'c' axes and mass, of each tracer was measured and they were numbered sequentially from 1 – 800. The numbers were used later in the field for primary identification, but where abrasion had occurred the tracer measurements were used to identify the individual tracers.

Seeding of the tracers into the river channel was undertaken on the 26th of February 2009. The location chosen for the initial placement of the tracers was a low gradient section of channel, located 20 m downstream of a 1.2 m high step and plunge pool (Figure 2.5 and Figure 3.2). As a result the predicted long residence time, for sediment in the plunge pool, the seeding site was chosen down stream of this to allow for tracer transport within the timescale of the field monitoring. This site is downstream of impact sensor number 1, and above a series of steps in the channel bed (Figure 3.2 and Figure 3.8). The placement of the tracers was carried out in a manner which represented the other sediment patches in the river channel (Figure 3.8). Larger tracers

were used to stop the smaller clasts moving when they were initially placed on the bed, but overall the tracers were evenly distributed on the bed.

Figure 3.8 Sediment Tracers in initial position 26th February 2009.

Trout Beck was visited on a regular basis (every 1 to 2 weeks), particularly following large flow events, in order to monitor the movement of the tracers. Tracers were located by sight or using a magnet detector. Once found the identity of the tracer was recorded through the procedure outlined above and finally the position of the tracers was fixed using dGPS. In all seven repeat surveys were used to characterise the downstream movement and timing of the sediment and this could be correlated with the flow in the bedrock reach.

3.1.5 **Monitoring bedload transport using *in situ* impact sensors**

Bedload impact sensors were installed on the bed of the channel at four locations (Figure 3.2). The locations covered the full extent of the bedrock reach and have been used to continuously monitor the relative intensity of sediment movement. Each impact sensor was installed at locations in the channel where: there was a focusing of flow, and therefore sediment transport, by the morphology of the channel; the bedrock was exposed to allow proper installation; and that were safely accessible. The sensors used were a modified version of a Tinytag data logger reported by Richardson et al. (2003) and which have been used in other investigations into the timing and magnitude of bedload transport (e.g. Reid et al., 2007; Raven et al., 2009). The sensor comprised of a metal impact plate, 150 x 130 x 6 mm in size, with a watertight case attached underneath to hold the sensor and data logger. The metal plate of the impact sensor, is fitted flush with the bed and is secured with masonry bolts (Figure 3.9). The internal components of the sensor consist of: an accelerometer; sensitivity dial; PC connector port; 3.7V battery; activity LED; and battery status LED. The design of the internal sensor also

incorporates a Tinytag data logger which records the number of impacts on the metal plate at 15 minute intervals and had been calibrated, in the factory, to detect impacts form clasts with a diameter of 20 approximately millimetres or larger. Field calibration was a continuous process, undertaken throughout analysis of impact rates with discharge. The logger was unable to distinguish between the sizes of particle causing the impact and is purely a binary count of impacts. The influence of impact saturation and sensor covering by the sediment layer, will be discussed furthering chapter 4. The data is then downloaded at periods of low flow when access to the bed is possible. Results can then be compared with the flow record measured in the study reach (section 4.6.3).

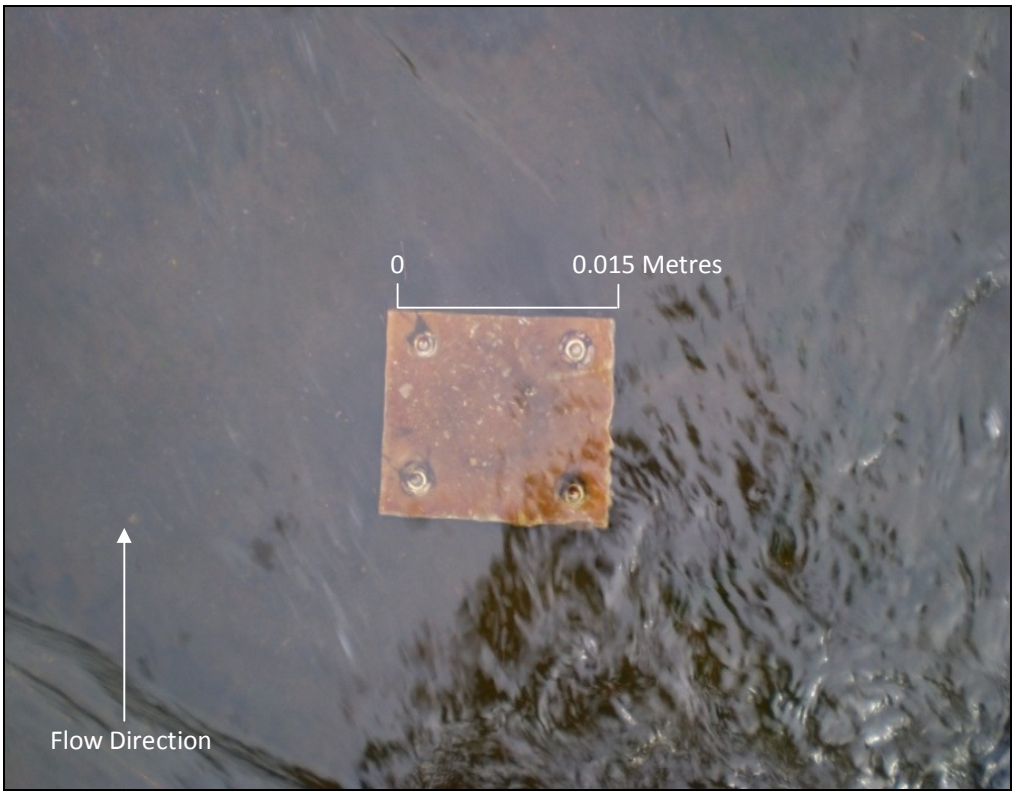

Figure 3.9 Impact sensor 1, *in situ* on the bed of the bedrock channel.

3.2 **One dimensional modelling of the study reach**

One dimensional modelling is used in this study to assess the interaction between channel morphology and flow. The morphology of the study reach and flow of the river have been quantified in the field (sections 3.2.1 and 3.2.2) and are subsequently used to define the boundary conditions of the numerical model. The numerical model used is the Hydrologic Engineering Centre's River Analysis System (HEC-RAS). The HEC-RAS model was designed to assess four components of a river system by solving a set of equations at a series of cross sections perpendicular to the channel flow (Haestad et al., 2003). These four components are: steady-state flow, unsteady flow simulations, movable boundary computations and water quality analysis. Of these components steady-state and unsteady flow simulations are used in this study to calibrate the HEC-RAS model for the study reach, and to calculate the spatial distribution of shear stress at cross sections through the channel.

3.2.1 **Theoretical basis of steady-state modelling in HEC-RAS**

When beginning a new study the initial use of the HEC-RAS model is usually done using steady-state simulations to consider a uniform flow at a set of cross sections perpendicular to the flow path. The model uses a constant discharge at each cross section in the river reach to simulate the flow conditions independently from time. In order to run to completion, the steady-state simulation must conserve the mass of water at each of the cross sections in the reach. To test this, the HEC-RAS model solves the continuity equation at each of the cross sections (Eq. 3.1, Haestad et al., 2003, p.571).

$$\frac{\Delta A}{\Delta t} + \frac{\Delta(vA)}{\Delta x} = q$$

(Eq. 3.1)

Where, A is the flow area (m^2); Δt is the change in time which is set to zero for steady flow (sec); v is the average velocity of the flow at the cross section (m s^{-1}); x is the distance downstream of the cross section (m); and q is the discharge at the cross section (m^3 s^{-1}).

In the continuity equation, the flow area at each cross section is calculated from the water surface elevation and where the water surface intersects the channel boundaries. Thus, as part of the standard step method of solving the continuity equation at each cross section HEC-RAS calculates the water surface profile at each cross section. In order to do this the water surface profile between each cross section and the penultimate one are also calculated. The water surface profile is calculated as the product of the difference in flow properties between the two cross sections and energy loss due to friction and channel contraction or expansion. Empirically this is shown in equation 3.6, which is developed from equations 3.2 to 3.6 (Haestad et al., 2003, pp. 56-58).

$$WSEL_2 + \frac{\alpha_2 v_2^2}{2g} = WSEL_1 + \frac{\alpha_1 v_1^2}{2g} + h_{L_{1-2}}$$

(Eq. 3.2)

Where, $WSEL_{1\&2}$ are the water surface elevations at the upstream and downstream cross sections (m); $\alpha_{1\&2}$ are the dimensionless velocity distribution coefficients; $v_{1\&2}$ are the average velocities for each of the cross sections (m s^{-1}); g is acceleration due to gravity (m s^{-2}); and $h_{L_{1-2}}$ is the combined energy loss due to friction and the expansion or contraction of the channel (m).

$$h_{L_{1-2}} = h_f - h_o$$

(Eq. 3.3)

Where, h_f is the energy loss due to friction between the two cross sections (m); and h_o is the energy loss due the expansion or contraction of the channel between the two cross sections (m).

$$h_f = LS_f$$

(Eq. 3.4)

Where, L is the distance between the two cross sections (m); and S_f is the bed slope at the cross section (-).

$$h_o = C_{c,e}\left|\frac{\alpha_2 v_2^2}{2g} - \frac{\alpha_1 v_1^2}{2g}\right|$$

(Eq. 3.5)

Where, $C_{c,e}$ is the dimensionless coefficient for contraction or expansion of the channel between two adjacent cross sections.

$$WSEL_2 - WSEL_1 = \left(\frac{\alpha_1 v_1^2}{2g} - \frac{\alpha_2 v_2^2}{2g}\right) + LS_f + C_{c,e}\left|\left(\frac{\alpha_2 v_2^2}{2g} - \frac{\alpha_1 v_1^2}{2g}\right)\right|$$

(Eq. 3.6)

The flow, the distance between the cross sections and the slope of the channel, are all measured in the field and are therefore accurately defined within the HEC-RAS model. The contraction and expansion coefficients, however, are not well defined, as they broadly represent the influence of channel contraction and expansion on the energy loss of the flow in the river (Hunt and Brunner, 1995). In bedrock channels fluvial incision has cut into the bedrock, resulting in smooth boundaries which are ridged (at the time-scale of years) and confine the flow the inner channel which changes width at discrete intervals (section 1.2.2). As a result it is suggested here that the energy loss due to changing channel shape is more significant than the losses due to friction. The sensitivity of the contraction and expansion coefficient and the geomorphological conditions they represent, are therefore discussed as part of the model calibration in section 5.3.1.

3.2.2 Introducing the time factor into the HEC-RAS model: unsteady flow simulations

In reality the discharge of a river is not steady over time and thus unsteady flow analysis is more representative of the natural conditions. The HEC-RAS model of unsteady flow combines the conservation of mass with the conservation of momentum. To do this the St. Venant equations are solved in an iterative manner through time and space. The St. Venant equations, derived at the beginning of the 19th Century, are a combination of mass and momentum equations. The equation set must be solved at each of the cross sections in the reach under investigation. The continuity equation (Eq. 3.1) is used to calculate the discharge of water at each cross section, whilst the momentum equation introduces the time component allowing fluctuations in flow levels (Eq. 3.7, Haestad et al., 2003, p.572). The momentum equation is the product of: the changing flow velocity, over time and space; the changing flow width to area ratio through the reach; and, the energy loss between subsequent cross sections. This energy loss component is the difference between channel slope and energy loss due to friction (Eq. 3.7). The slope of the river channel is defined as a result of the competence of flow to degrade the channel boundaries, although it is approximated by the flow velocity, Manning's roughness and hydraulic radius (Eq. 3.8 and (Eq. 3.9). Whilst flow velocity and the hydraulic radius at each cross section are defined by the flow and boundary conditions, the roughness of the channel is a subcomponent of the channels topography and as a result is collapsed to a single parameter value (as discussed in section 5.3.2).

$$\frac{\Delta v}{\Delta t} + v\frac{\Delta v}{\Delta x} + g\frac{\Delta y}{\Delta x} - g(S_f - S_{fr}) = 0$$

(Eq. 3.7)

Where, y is the hydraulic depth, calculated by dividing the flow area by width of the channel at the top of the water profile (m); S_{fr} is the slope through the channel due to friction (m m^{-1}).

$$v = \frac{k}{n} R^{\frac{2}{3}} S_f^{\frac{1}{2}}$$

(Eq. 3.8)

Where, Q is the discharge of flow at the cross section (m^3 s^{-1}); k is a unit conversion constant of 1 for metric units; n is the Manning's roughness coefficient; and R is the hydraulic radius of the cross section (m).

$$S_f = \sqrt{\frac{v\,n}{R^{\frac{2}{3}}k}}$$

(Eq. 3.9)

3.2.3 **Developing the HEC-RAS model for the Trout Beck study reach**

The geometric boundaries for the model of Trout Beck were set using 21 cross sections, taken at breaks in slope along the channel thalweg to capture the differences in channel form through the reach (Figure 5.2). Each cross section consisted of between eighteen and thirty manually surveyed points and varied in length between 11.5 and 20 metres. The input flow boundary condition was selected at the upstream cross section, using a hydrograph taken from 7th and 8th of March 2009 (Time base = 34.75 hours, discharge interval = 15 minute values, Figure 3.10). This particular hydrograph was selected as it represents a single peaked storm event, which occurred during the period when stage and discharge were both monitored. The event was observed to cause sediment transport, particularly through the tracer experiment (section 4.5.1). The downstream flow boundary condition was set using the normal depth value, the depth in a prismatic channel where the flow is uniform (Haestad et al., 2003). However because the natural channel cross sections are not prismatic, the true value of the normal depth could not be calculated. Sensitivity analysis was performed to determine the normal depth value which provided the greatest stability in the model. In a similar fashion sensitivity analysis was also performed on the contraction and expansion coefficients and the Manning's roughness coefficient in order to find the optimal parameter set for model stability and which represents the real world conditions (section 5.3). Once the HEC-RAS model of the study reach was verified and validated it was used to assess the spatial distribution of the in-channel shear stress through the study reach. This was part of the general aim to identify the interactions between morphology and flow that influence sediment transport.

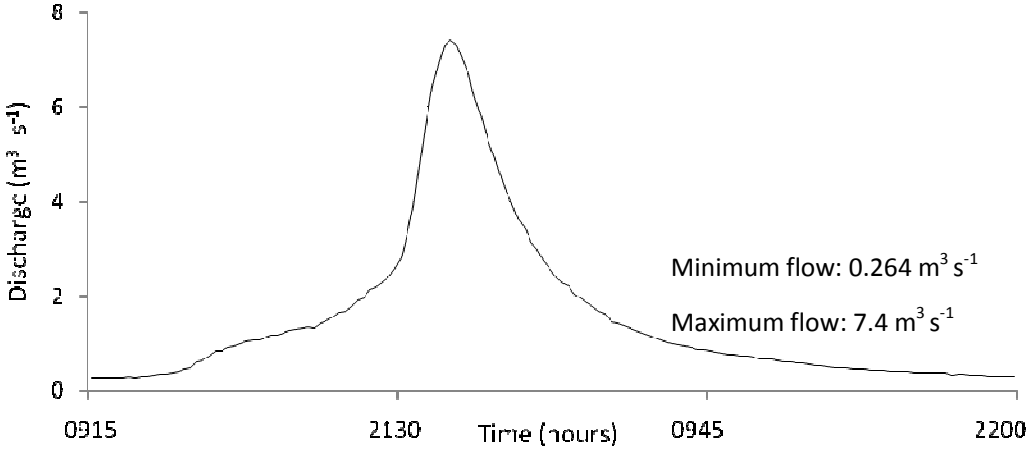

Figure 3.10 Hydrograph used as upstream flow input boundary condition.

Chapter 4:

Field Results and Analysis

4.1 **Channel morphology**

The river channel survey undertaken at Trout Beck was designed to capture the complete form of the study reach and specific channel features including: river banks; channel thalweg; and the cross sections used for defining the channel boundaries in the HEC-RAS model. By combining data from dGPS surveying and terrestrial laser scanning the overall form of the study reach has been modelled in a DEM. The dGPS was also used to quantify the shape of individual cross sections in the reach (taken at breaks in the channel slope).

4.1.1 **The general form of the study reach**

The general form of the study reach has been assessed using a digital elevation model (DEM) and field observations (Figure 4.1). The DEM combines spatial data from dGPS points, with terrestrial laser scans of the river reach. In zones were water blocked the view of the laser scanner, dGPS surveying was used to characterise the shape of the bed (e.g. the thalweg). Using the laser scanner the 400 m study reach was captured at a resolution of 0.1 m^2, through 16 scans. The scans were then combined, together with dGPS field survey data. When initially combining the surveys and scans, multiple measurements for the location were interpolated on the a 0.5 m^2 grid using a triangular-based method, calculating the elevation of each grid-cell, identified by an x and y coordinate (The Maths Works, 2007). The processing of the raw data to a grid of 0.5 m^2, reduced the elevation readings to 64911 grid squares. Due to the focusing of the data collection, to the active channel, gird cells beyond 5 m of the channel were excluded from further analysis. As a result of the processing and interpolation there is an average residual elevation error of 0.26 m, calculated by comparing five known heights in the field with the heights in the DEM.

Sections of the channel with high levels of sedimentation are clearly evident in the DEM. These zones are identifiable by their high surface roughness, which is an artefact of the scatter in scan returns and the increased variation in elevation due to sediment. These mainly occur in two sections: 175 – 275 m downstream; and 300 – 400 m downstream (Figure 4.1). Interspersed between these sections are smoother, bedrock dominated sections of the channel, between: 100 - 175 m; and 275 - 300 m (Figure 4.1). However, between 0 and 40 metres is a stretch of the channel which has a smooth central region and is rough at the margins (Figure 4.1). Together with field observations and estimates of percentage of sediment cover, a general channel classification can be devised for these five regions (Figure 4.1). An anomaly in this basic classification is the section of channel between 40 – 100 metres, where the heavily jointed and pot-holed nature of the channel bedrock produces a roughness effect which is not caused by in channel sediment. This section of the channel is also classified as bedrock.

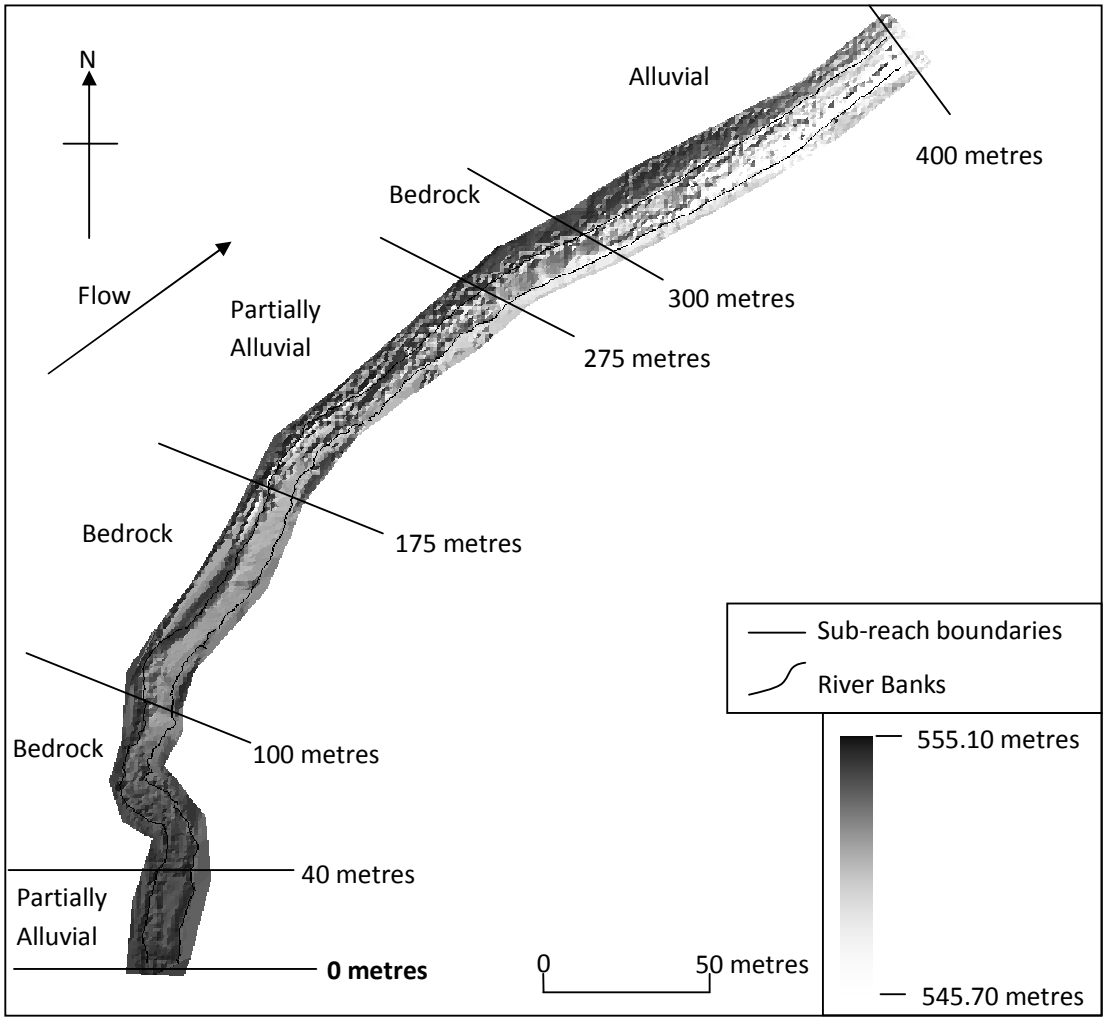

Figure 4.1 Digital elevation model of the study reach (Trout Beck) collated using survey and scan data taken during low flow conditions November and December 2009.

4.1.2 **Survey of channel cross sections at breaks of slope**

The mapping of individual channel cross sections has been used to examine the form of the river channel and to define the channel boundaries in the HEC-RAS model (Figure 4.2). The locations of cross sections, in the field were at specific breaks in the slope of the channel thalweg (Figure 5.1 and Figure 5.2). Cross section length was determined by surveying 3 m to each side of the active channel. The cross sections vary in width from 11.5 to 20.3 m, tending to increase in length downstream. There is a marked 'constriction' in channel width in the mid-section of the study reach corresponding with the gorge like section of the bedrock channel. Cross sections 1 – 4, situated in the alluvial zone of the reach, have low channel banks, flat channel bottoms and flat channel bottoms (Figure 4.2). Cross sections 5 – 11, are situated in the partially alluvial zone, but become more deeply incised into the bedrock in an upstream direction (Figure 4.2). Within this zone downstream cross sections have low channel banks and flat channel bottoms whilst upstream cross sections have higher banks, narrow active channels and laterally sloping channel bottoms as a result of sedimentation to one side of the channel. Furthest upstream, cross sections 12 – 21 are deeply cut into bedrock and as a result: the channel boundaries are ridged (due to structures in the lithology); the active channel is narrow; and the channel bottoms are flat.

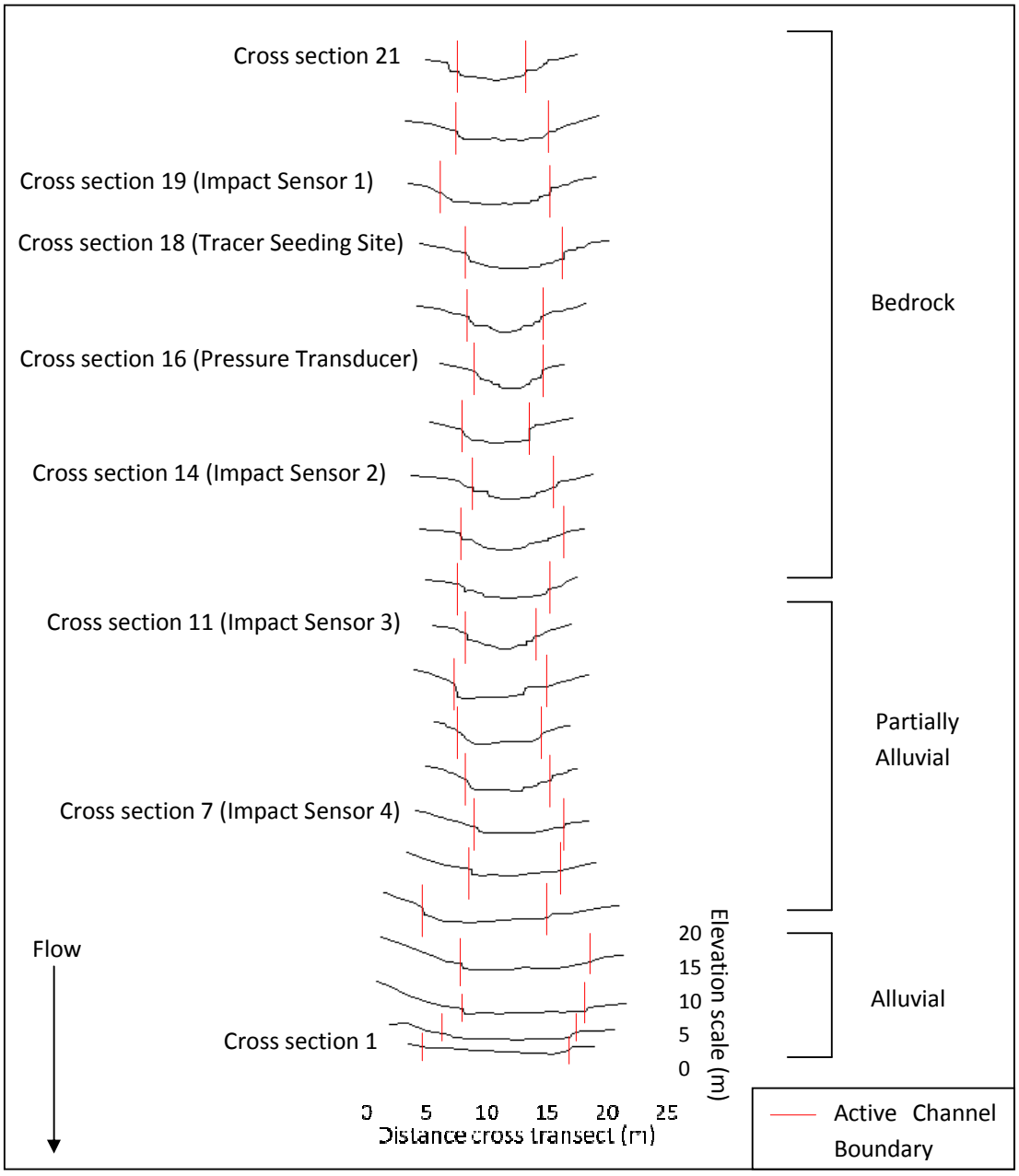

Figure 4.2 Sequence of 21 channel cross sections surveyed in the study reach, on the 26th of June 2009, and used to calibrate the HEC-RAS model. Cross section 21 is situation 93 m downstream from the start of the study reach (Figure 4.1). These are spatially located in Figure 5.1.

4.2 **Flow monitoring**

The flow of Trout Beck has been monitored downstream of the study reach, at Trout Beck bridge, since 1992. This record has been supplemented by local flow measurements collected during this study, resulting in a continuous record of local stage measured at the proximal end of the study reach (Figure 4.4). Local stage records and downstream discharge measurements have been correlated to produce an empirical relationship between the two sites. This relationship has then been used to infer the exceedence frequency of local stage in the bedrock reach, for the period from 1992 to March 2009.

4.2.1 **Trout Beck discharge measured at the downstream EA gauging station.**

The summary statistics for the flow period between the 1st of January 1992 and 8th of March 2009 are shown in Table 4.1. In addition a flow duration curve has been constructed (Figure 4.3). This record, of discharge in the catchment, shows that flows of more than 1.5 $m^3 s^{-1}$ have an exccedence of less than 10%. These flows are several magnitudes above base flow (0.01 – 0.056 $m^3 s^{-1}$, defined as flows with an exceedence of 80%) they only represent 3% of the peak flow magnitude on record. In terms of sediment transport the exceedence period of threshold conditions for bedload entrainment are considered in section 4.5.2 and the influence of the largest events in 2009 are discussed in section 5.3.

Statistical Characteristic	Discharge	Stage
Maximum	44.70 $m^3 s^{-1}$	1.25 m
Minimum	0.01 $m^3 s^{-1}$	0.06 m
Mode	0.03 $m^3 s^{-1}$	0.11 m
Mean	0.63 $m^3 s^{-1}$	0.14 m
Q_1	8.38 $m^3 s^{-1}$	0.72 m
Q_{99}	0.01 $m^3 s^{-1}$	0.12 m

Table 4.1 Summary discharge statistics for the flow at Trout Beck (1992 to 2009).

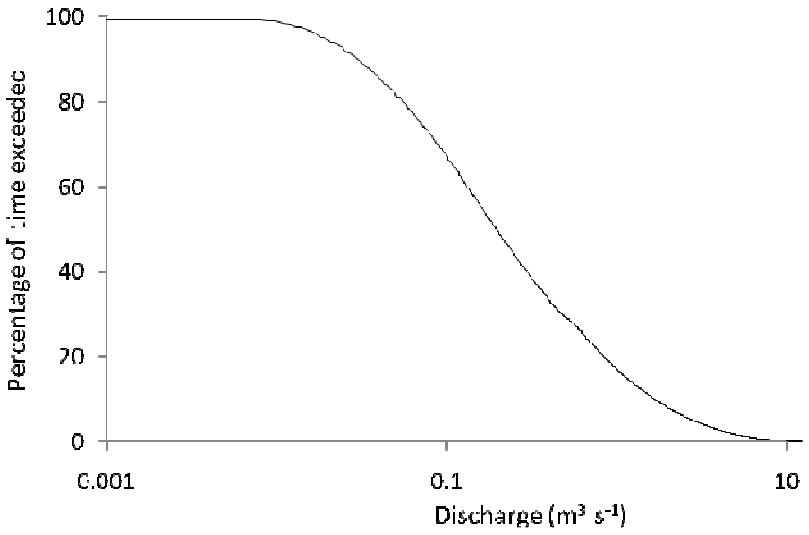

Figure 4.3 Flow duration curve for river discharge monitored at the Trout Beck bridge compound weir. Method after Young et al. (2001).

4.2.2 **Stage monitoring in the study reach**

In addition to long term monitoring of discharge, at the EA gauging station, local stage in the study reach was measured between the 24th of February and the 18th of July 2009 (Figure 4.4). The recorded was abruptly ended on the 18th of July as the monitoring station was damaged and the pressure transducer dislodged. The trend in base flow over the monitoring period is a decline from 0.13 m on the 20th of March to 0.08 m on the 29th of June 2009. This pattern in 2009 is representative of the trend observed in the longer term discharge. The stage series also shows the rapid rise and fall of individual storm events, as well as periods of more sustained flow. This

pattern is clearly shown in two examples: the flow period beginning on the 23rd of April and lasting until the 11th of May, incorporates a series of individual storm events; whilst the event on the 6th of June has a single peak and then returns to base flow. The sustained periods of flow above base level are common place; peaks in flow which are greater than 0.6 m are less frequent. The four largest peaks occur on the 7th of March (0.88 m), 26th of March (0.81 m), 6th of May (0.97 m) and 17th of July (1.23 m). The 17th of July peak corresponds to intense rainfall and wide spread flooding across the North of England. This is illustrated by the shape of the stage hydrograph (Figure 4.4). The peak rises from 0.16 ms at 18:00 h on the 16th of July to 1.25 m at 18:30 h on 17th of July. Following the flow peak the stage return to 0.15 at 09:00 h on the 18th of July. This large event is discussed further, in connection with sediment transport, in section 4.4.3.

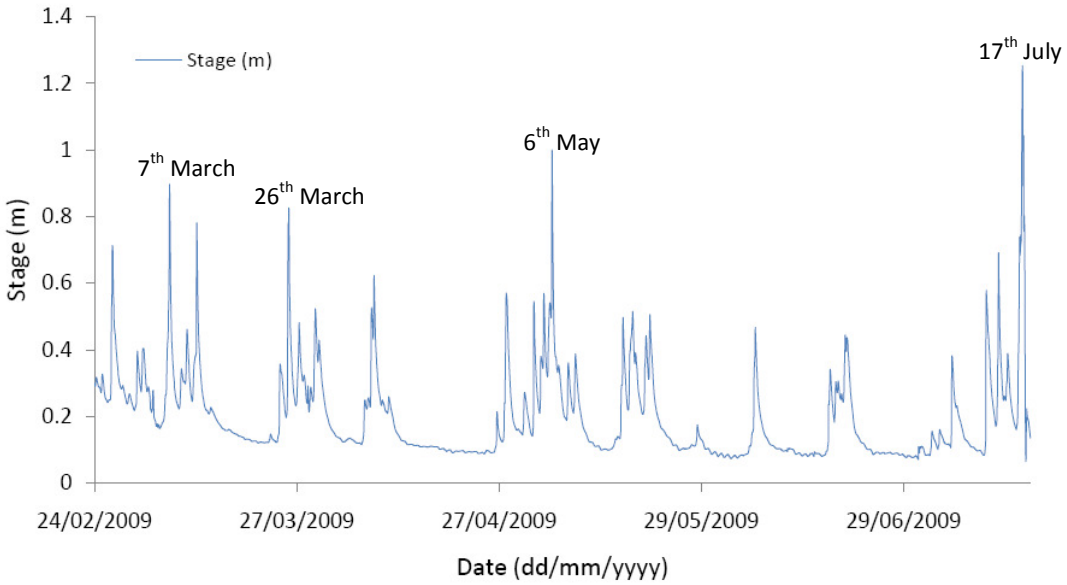

Figure 4.4 Flow series (stage record) for the Trout Beck study reach, February the 24th 2009 and July the 17th 2009. Stage recordings finish on the 18th of July 2009 as the pressure transducer was dislodged.

4.2.3 **Local stage-downstream discharge relationship**

A relationship relating the local stage measured in the study reach to the downstream discharge record has been developed from the discharge and stage data collected in field. Initially a single equation was developed, however at higher discharges this under predicted the stage values. As a result a compound relationship was developed using two equations (Figure 4.5, Eq. 4.1 and Eq. 4.2), which better predicts the stage-discharge relationship for either high or low flows (Herschy, 1999). This curve has a maximum residual of ±0.9m between the observed and predicted stage (Figure 4.6). The 90% confidence level, as suggested by Sivapragasam and Muttil (2005), has been identified by the boundary within which 90% of the monitored data is captured (Figure 4.5). This relationship is used to validate the HEC-RAS model in Chapter 5.

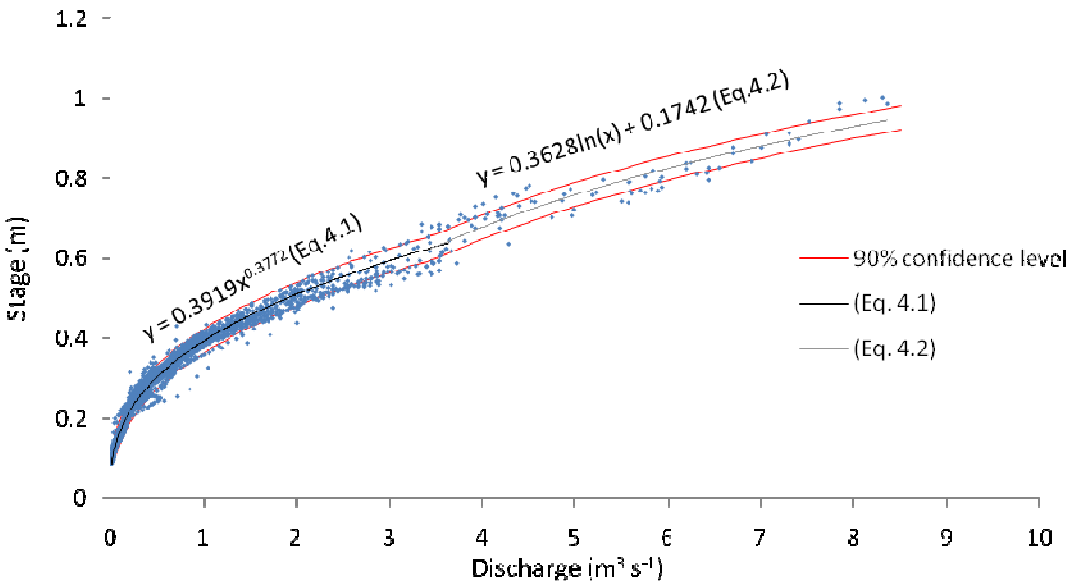

Figure 4.5 Stage (local) – discharge (downstream) relationship with 90% confidence level. The change in rating equation occurs at 3.49 $m^3 s^{-1}$.

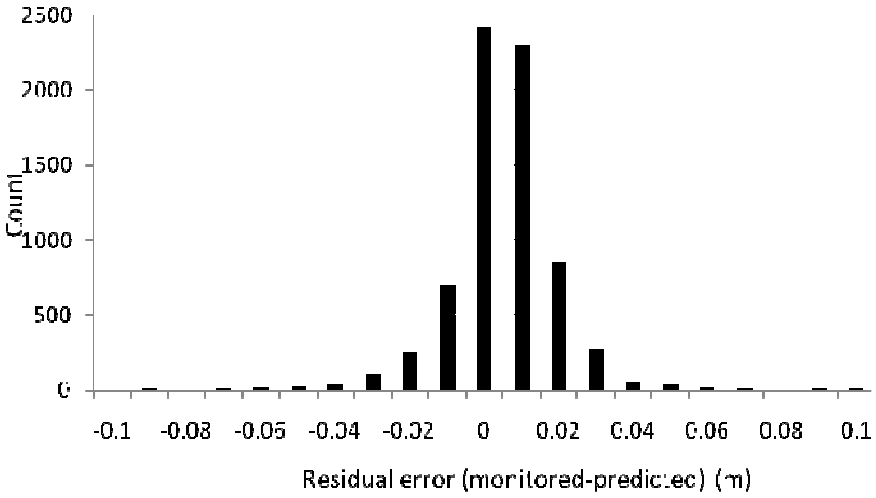

Figure 4.6 Histogram of residuals using the compound relationship.

4.3 **Sediment characteristics in the Trout Beck study reach**

The sediment in the Trout Beck study reach has been classified in terms of the spatial variations in grain-size distribution and the extent of sediment cover through the reach. The distributions of grain-size at 41 sites through the study reach have been discussed in section 3.2.3, and it is concluded from Figure 3.4 that there is little spatial variation in distribution of sediment size. However, from observations in the field and the morphological surveying undertaken, there is spatial variation in the amount of sediment stored in the channel. In order to quantify this, the percentage cover across the channel width has been calculated. This was done by mapping the sediment cover in the channel and then by dividing the width of sediment cover, by the width of the active channel, every 0.5 m downstream. As a result the channel type has been characterised. The quantity of sediment storage in the channel has been assessed in conjunction with the geometry of the river channel and zones of sediment transport identified.

4.3.1 **Sediment storage in the channel**

The sediment cover in the study reach varies markedly. Between the top of the reach (0 m downstream) and 170 m downstream the channel is predominantly bedrock with minor patches of alluvium (Figure 4.7). Downstream from this point the sediment cover increases but fluctuates significantly. Between 170 m and 330 m there is a distinct zone of sedimentation peaking at c.240 m (72% cover). Following a short bedrock section, from 330 m downstream sediment cover increases rapidly and by 350 m has a greater than 90% cover over the rest of the reach.

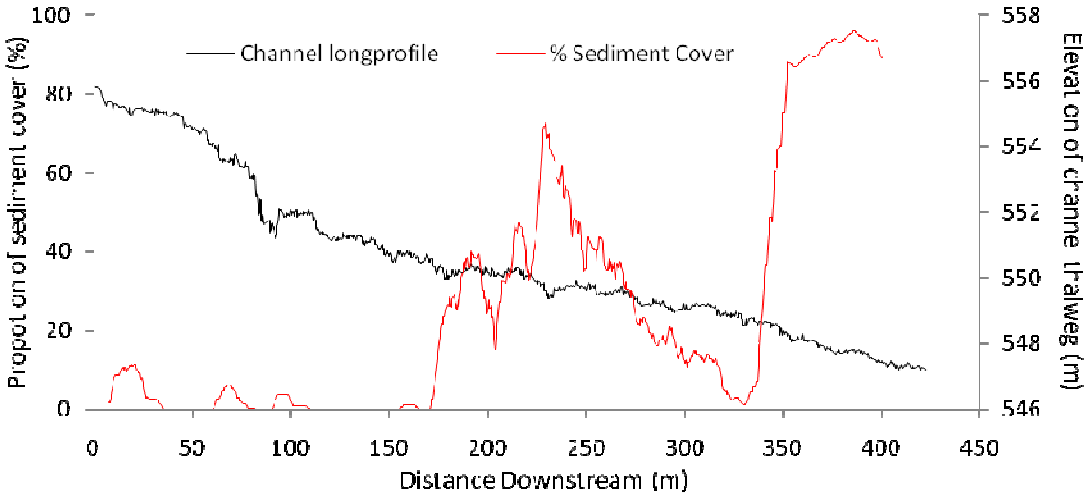

Figure 4.7 Graph showing the percentage of channel sediment cover and the long profile of the channel thalweg through the study reach.

The nature of the channel sediment cover, local channel slope and channel width have been analysed to determine whether sediment cover is dependent on either of these variables (Figure 4.8a and Figure 4.99). Channel slope appears not to be a major controlling influence on the proportion of sediment in the channel (Figure 4.8b). An explanation for this is that sediment is not stored in the thalweg of the study reach, which was surveyed to calculate the channel slope. There are, however, two locations where a reduction in slope is followed by an increase in sediment cover (at 170 m and 320 m). However at each of these locations the peak in sediment cover is 60 m downstream of the lowest gradient. This lag distance is too long for it to be directly related to local channel slope.

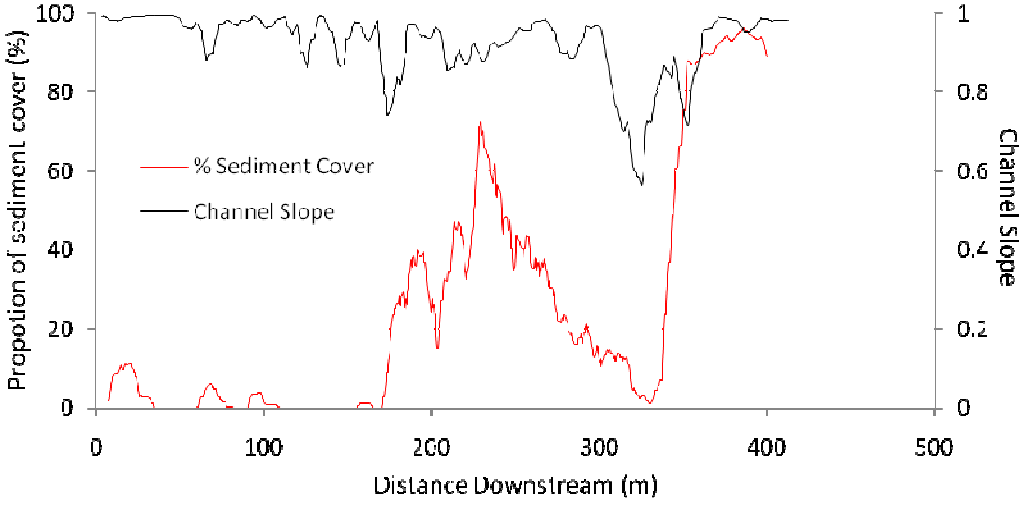

Figure 4.8a The percentage of sediment cover in the channel and the local slope.

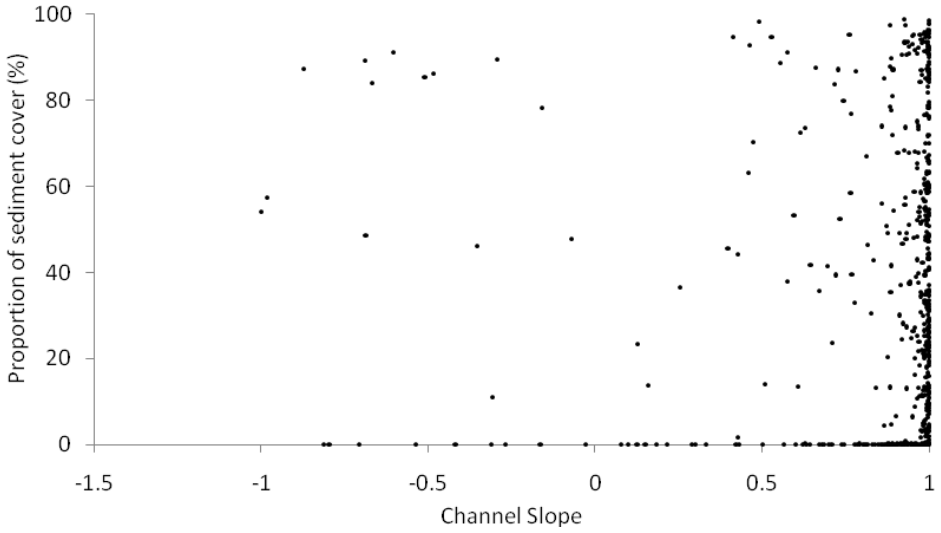

Figure 4.8b Relationship between the proportion of sediment in the channel and the channel slope.

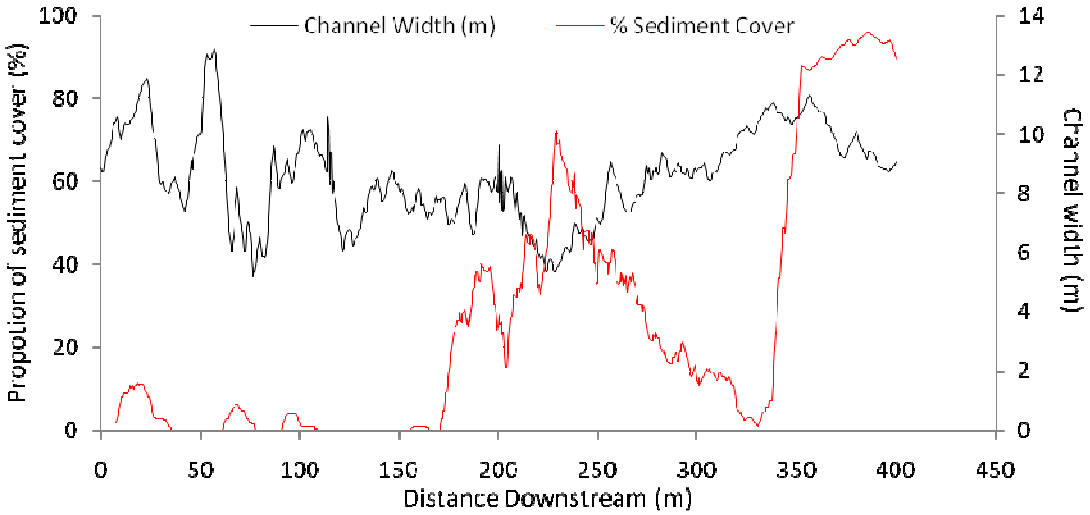

Figure 4.9 The percentage of sediment cover in the channel and channel width.

Generally channel width has some correlation with the proportion of sediment in the channel (Figure 4.9). Further analysis between these two variables shows that there are two separate processes occurring (Figure 4.10). Firstly there is a general inverse trend (Figure 4.10a) which shows that as channel width increases the proportion of sediment decreases or conversely the proportion of sediment increases as the channel narrows. When compared to Figure 4.9 there are: low levels of sediment at high channel widths between 0 – 35 m, 50 – 70 m, 85 – 110 m, 300 – 350 m downstream; and high levels of sediment at narrow channel widths between 200 and 225 m downstream. These two distinct patterns correlate with two processes. At the higher channel widths, stream power drops, and sediment deposition should occur. However the supply limited nature of the reach causes a limit to the sediment cover where the river channel is disconnected from an active sediment source (Church, 2006). In regions where the channel narrows, there is a choking affect caused by the channel morphology. As a result, particularly in the presence of large

boulders and bedrock structures, sediment is stalled and storage results; even though there is high stream power.

The second cluster (Figure 4.10b) indicates that at larger channel widths there is a greater proportion of channel sediment cover. This is associated with an area of active sedimentation at the distal end of the reach, where there is an abundance of deposited sediment (Figure 4.9). The processes causing these affects are determined by the channel morphology as a whole, including both intrinsic and extrinsic factors, and no single variable (slope or width) can fully explain these patterns. In this relationship these impacts are mainly controlled by the bedrock rather than feedbacks from an alluvial channel. A third processes – form interaction is also observed in Figure 4.10. This is the jump, rather than transition between clusters 'a' and 'b', indicating that stream power is competent to transport sediment, at narrowing channel widths until a threshold is surpassed for storage to be initiated.

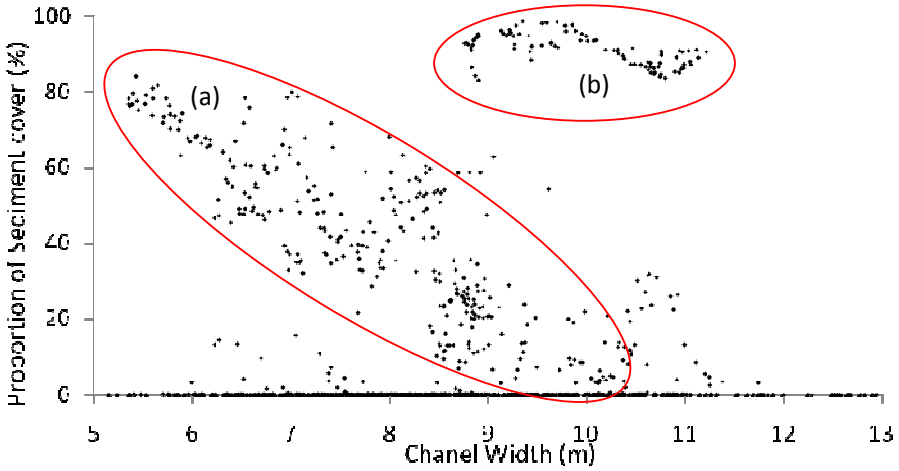

Figure 4.10 Relationship between the proportion of channel sediment cover and channel width. Cluster (a) shows an inverse relationship between sediment cover and channel width, whilst cluster (b) highlights the high storage proportion of sediment at larger channel widths.

4.3.2 **The impact of the July 17th 2009 storm on the pattern of sediment cover in the study reach**

As discussed the distribution of in channel sediment fluctuates through the study reach (section 4.5.2). This is related to the active zones in the channel where sediment is entrained, transported and deposited. In general, areas of no sediment cover indicate an active transport zone as sediment is transported through the reach and no deposition occurs. During base flow conditions the majority of the study reach is inactive and sediment storage is stable. However the peak in flow (19.57 $m^3 s^{-1}$) on the 17th of July (discharge exceedence: 0.007%, Figure 4.3) mobilised the majority of the sediment stored in the study reach. Sediment storage in the reach was mapped on two occasions: the 24th of February and then again on the 10th of August 2009 (Figure 4.11 and Figure 4.12). Results indicate that, despite high rates of sediment reworking in the study reach, there are only small changes in the position of the in channel sediment stores and the volume of sediment remains relatively constant (Figure 4.11 and Figure 4.12). Between 0 and 150 m, in the bedrock region, there is little change in the zones of sediment storage, although the volume of sediment increases slightly (Figure 4.12). Sediment is retained in bedrock cavities and local potholes. Further downstream, in the partially alluvial section of the study reach (150 – 325 m downstream) the changes in sediment storage are more evident. This is primarily due to the larger volume of sediment stored in this section of the reach, and the influence of sediment choking at channel constrictions. Finally, at the distal end of the reach the proportion of sediment

remains relatively constant between surveys. The local changes in sediment storage indicate the strong influence that bedrock structure and channel morphology have on the sediment dynamics in the study reach.

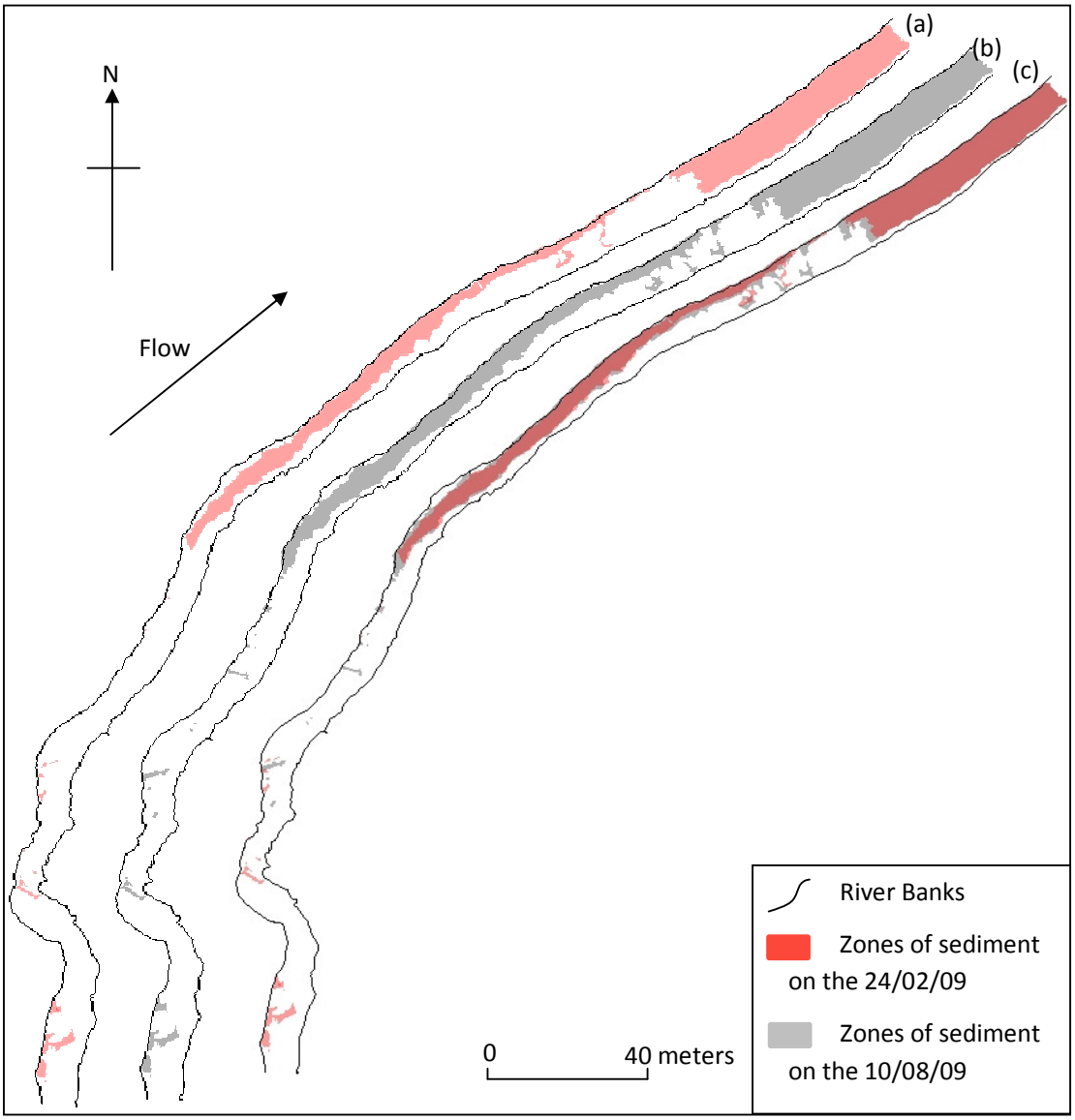

Figure 4.11 (a) map showing the regions of sedimentation on the 24th of February 2009; (b) map showing the regions of sedimentation on the 10th of August 2009; and (c) overlay of the regions of sedimentation on the 24th of February and 10th of August 2009.

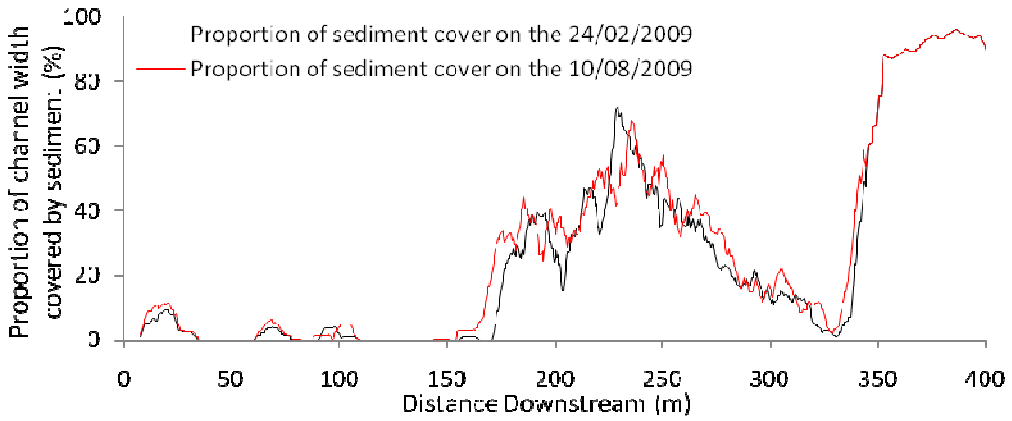

Figure 4.12 The proportion of channel width covered by sediment on the 26th of February and 10th of August 2009.

4.4 **Spatial and temporal patterns of sediment transport**

In the field, sediment transport was measured by two methods. Firstly, tracer surveys were used to measure the movement of individual tagged particles at discrete time intervals. Secondly, impact sensors were employed to continuously monitor the intensity of bedload movement at four fixed locations in the channel. The results of these two methods are analysed with respect to the flow regime of Trout Beck and the channel morphology of the study reach.

4.4.1 **Movement of sediment tracers**

The tracers, used to monitor sediment transport in the bedrock channel, were seeded 107 metres downstream from the top of the reach (Figure 4.13a). Over the course of the next six months, seven surveys were taken to monitor the movement of the tracers (Figure 4.13 and Table 4.2). Table 4.2 shows the date of the tracers surveys, the peak flow since the previous survey, the recovery rate of the tracers and the percentage of the tracers found in the bedrock and alluvial sections of the study reach. The recovery rate of the tracers in this study remains high until the tracers are more widely distributed in survey 'h' (Table 4.2). However in all surveys there are missing tracers (Table 4.2). These missing tracers can be attributed to tracer burial within sediment cluster, the high proportion of tracers in storage clusters and abrasion and braking of tracers to remove paint and dislodge magnets: making the tracers unidentifiable. Burial of tracers coupled with the high concentration of tracers in storage locations will have an impact even in the shallow sediment depth of a bedrock channel. Meanwhile the breaking up of tracers and abrasion of the paint was observed in the field during surveys.

Figure 4.13 (b) shows the initial movement of the tracers, which was characterised by deposition in sediment clusters on the left side of the channel. This initial tracer survey has been included so as to show the areas of tracer deposition, indicating areas in the channel where sediment, mobile through the reach, may be stored. Whilst the initial source location of the tracers may have been an artificial sediment store, once mobile in through the reach, natural controls on sediment transport determine the sites of deposition. From observations in the field three main locations were identified as areas of tracer deposition. Firstly, tracers were commonly found in the lee of bedrock irregularities such as potholes, cracks and scallops where flow competence was lower (e.g between 0 and 30 m downstream from the seeding site, Figure 4.13b). Secondly, tracers were deposited on the left hand bank channel margin, between 38 and 64 metres from the seeding site, on the waning limb of high flow events (Figure 4.13). Finally,

tracer deposition occurred in the areas where sediment was already present (e.g. 64 metres downstream of the tracer seeding site, Figure 4.13b). During the first three months surveying took place, 86% of the tracers which were found, had been transported through the bedrock section of the reach (0 - 64 m, Figure 4.13b - g) and stored in the partially alluvial and alluvial channel downstream (Table 4.2). However transport of tracers, in this partially alluvial section of the channel, progressively increased over time with 46% of the tracers transported between seeding and the first survey and an additional 39% of the tracers transported between the 28th of April and the 8th of May (Table 4.2). This increase corresponded to the transport of sediment from the bedrock section. The proportion of tracers found in bedrock section of the channel reduced through the course of the surveys from an initial value of 54% to 2% by the final survey. The distribution of tracers in the bedrock sections of the channel and the alluvial / partially alluvial sections show different spatial patterns. Through the bedrock sections tracers are deposited in clusters, associated with irregularities in the bedrock channel (Figure 4.13 and Figure 4.14). In the alluvial and partially alluvial sections of the channel behaviour is more typical of alluvial sediment dynamics and there is a greater selectivity of transport of sediment. As a result the tracers are more uniformly dispersed within sedimentation zones (Figure 4.14).

Survey Date	Peak Flow in period (m^3 s^{-1})	Recovery rate	% of tracers found in bedrock zones	% of tracers found in partially alluvial and alluvial zones
17/03/09 – (b)	7.84	81%	54%	46%
31/03/09 – (c)	6.55	78%	39%	61%
07/04/09 – (d)	7.30	79%	41%	59%
28/04/09 – (e)	3.41	89%	41%	59%
08/05/09 – (f)	8.69	78%	15%	85%
22/05/09 – (g)	2.06	78%	14%	86%
10/08/09 – (h)	18.35	58%	2%	98%

Table 4.2 Table showing survey periods, peak discharge between surveys, the percent of the total 800 tracers found and the percent of the tracers found in the bedrock and alluvial zones.

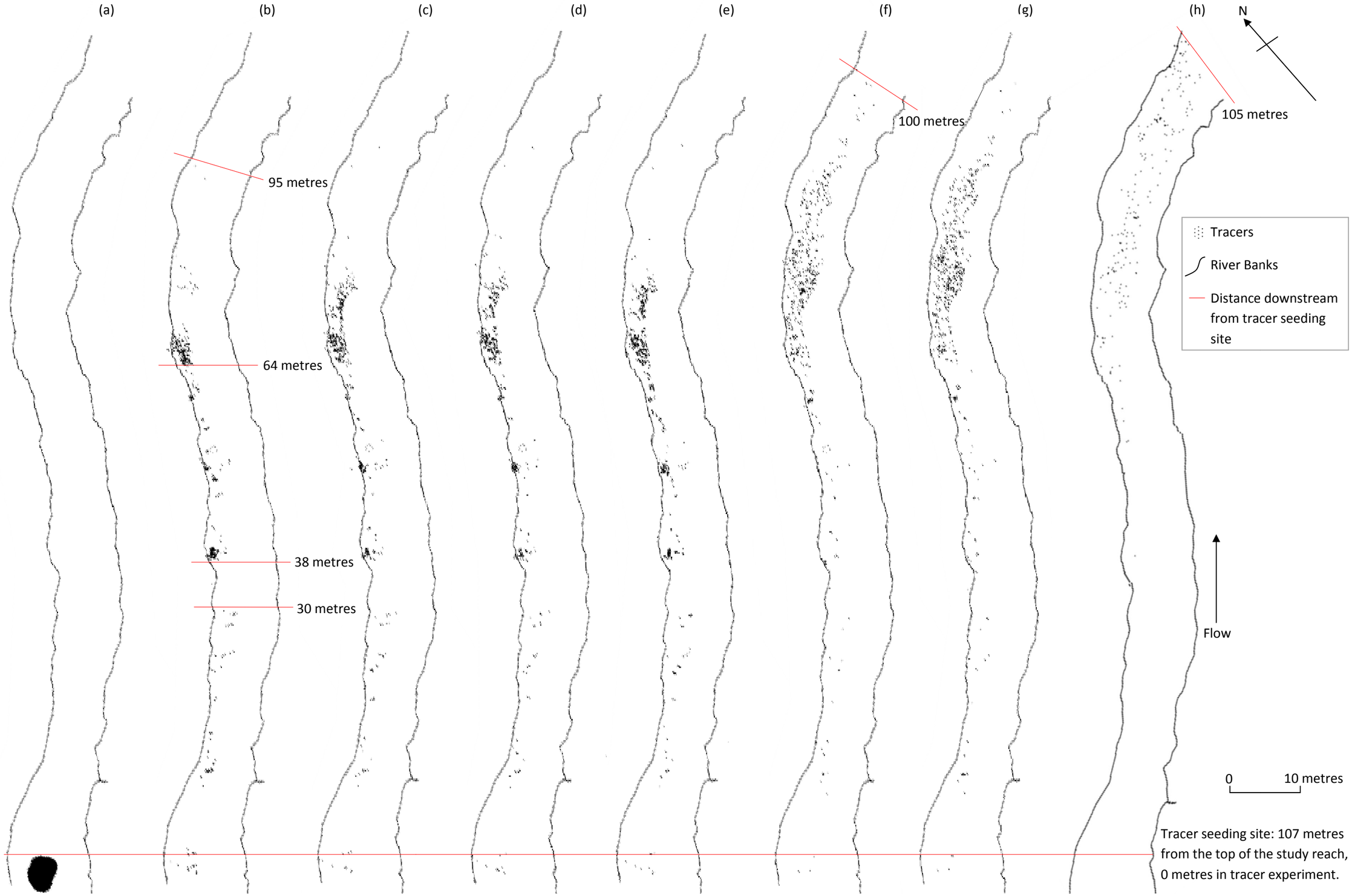

Figure 4.13 The distribution of tracers downstream from the seeding site below the large step and plunge pool, on the: (a) 26th of February, (b) 17th of March, (c) 31st of March, (d) 7th of April, (e) 28th of April, (f) 8th of May, (g) 22nd of May, (h) 10th of August 2009.

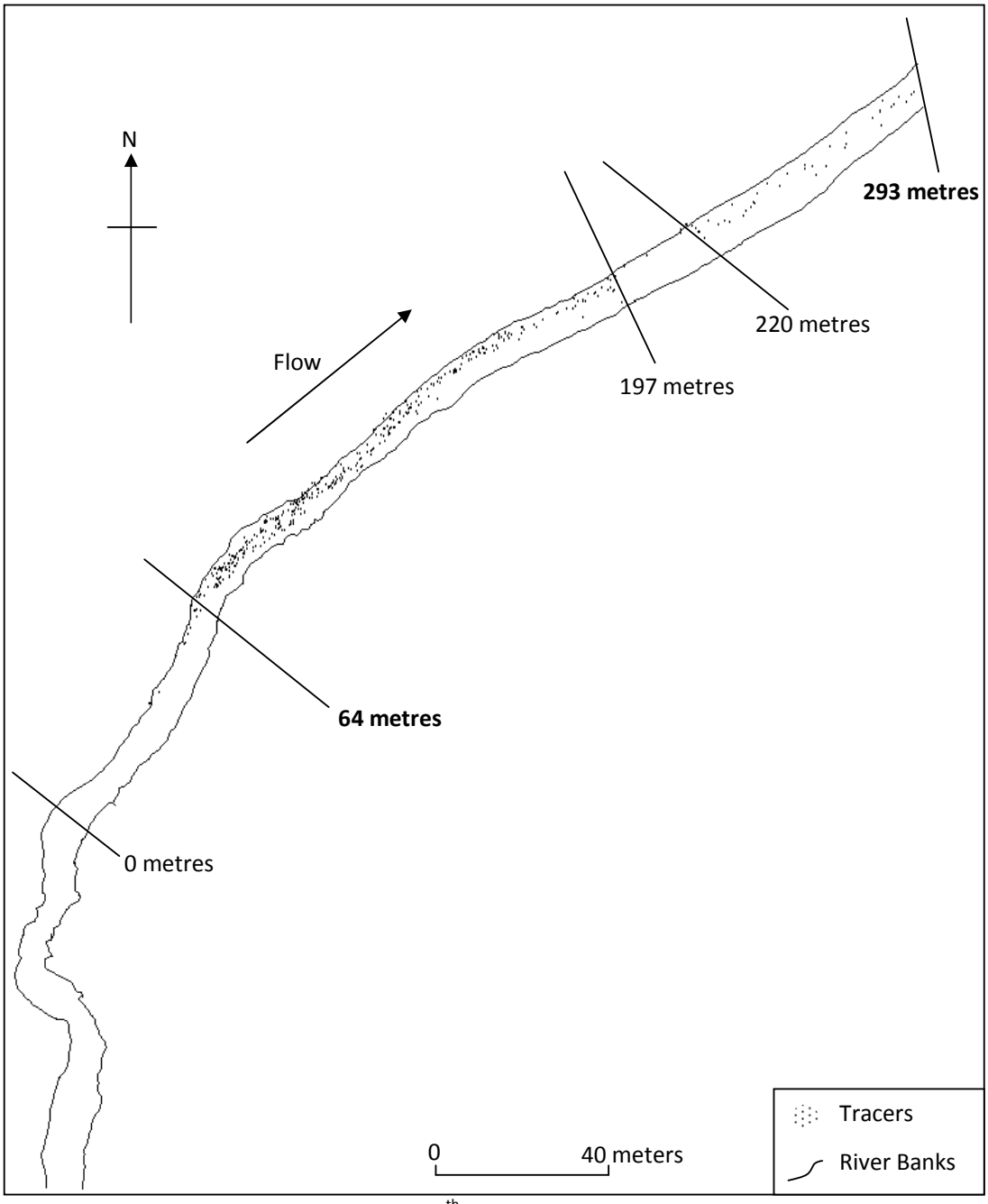

Figure 4.14 Distribution of tracers on the 10th of August 2009 and the distances downstream from the tracer seeding site.

The survey on the 28th of April showed a very similar pattern to that of the 7th of April. Because of this overall similarity and, due to the low peak discharge during the period, this was not included in the further analysis (Figure 4.13d, Figure 4.13e and Table 4.2). Considering the survey results sequentially, the movement of tracers can be seen progressing downstream and key storage points in the channel can be identified. Initially the tracers were widely distributed in both the bedrock and the (bedrock/alluvial) transitional zones of the channel. However by the last two surveys the tracers were predominately stored in the partially alluvial and alluvial section of the channel (Figure 4.19 and Figure 4.20). As the distribution of tracers changes through time, the number of tracers in storage locations fluctuates (e.g. 150, 160, 180 and 190 m downstream). This

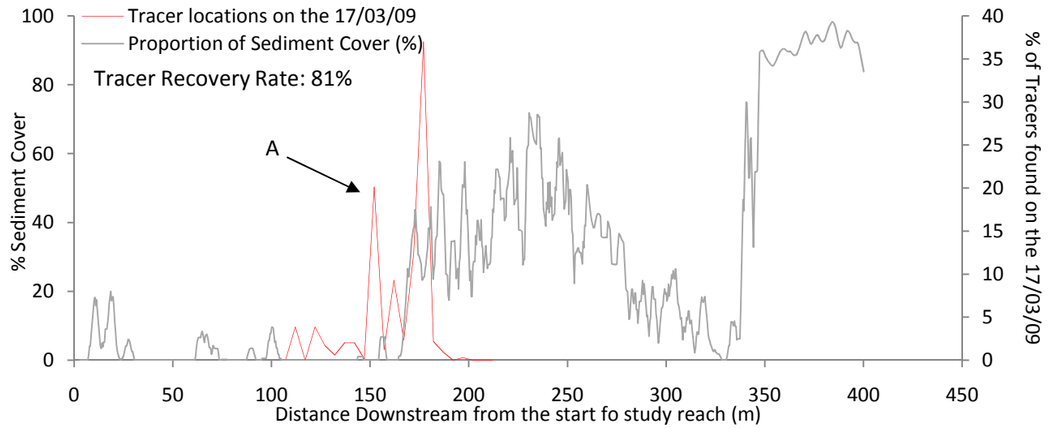

Figure 4.15 Distribution of the tracers and sediment cover from seeding site on the 17th of March 2009.

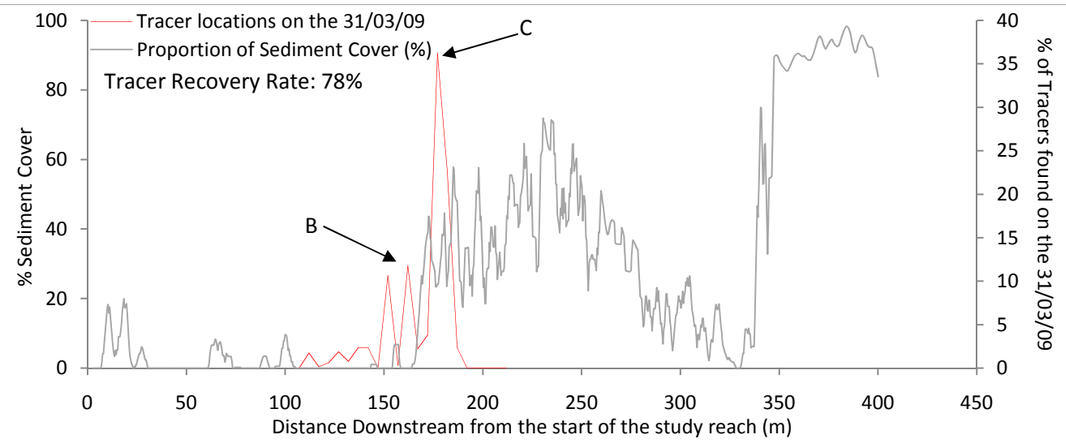

Figure 4.16 Distribution of the tracers and sediment cover from seeding site on the 31st of March 2009.

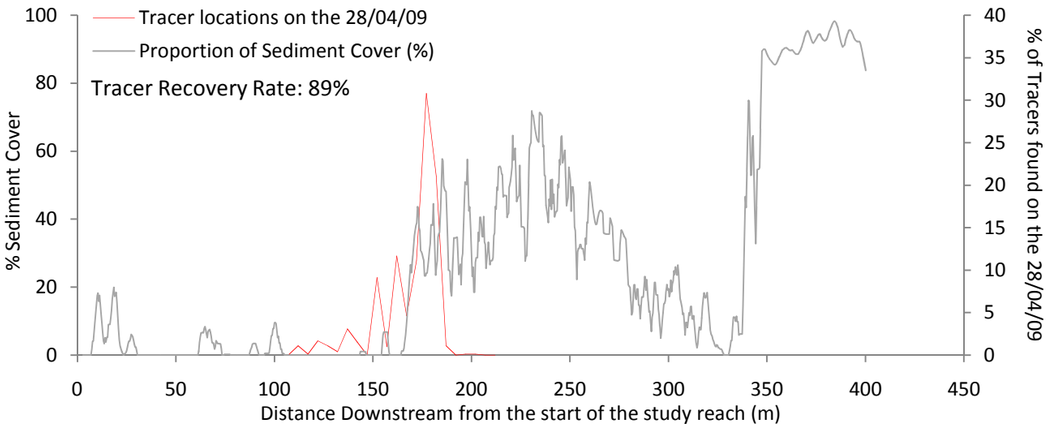

Figure 4.17 Distribution of the tracers and sediment cover from seeding site on the 28th of April 2009.

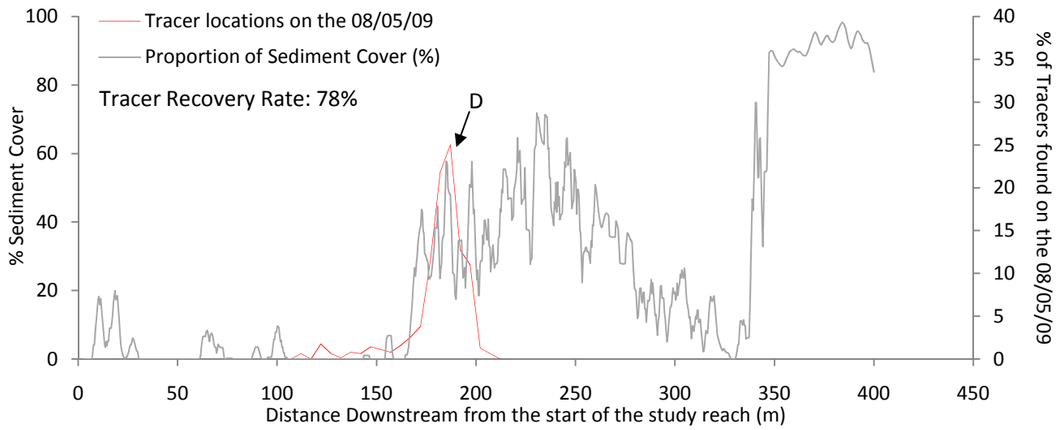

Figure 4.18 Distribution of the tracers and sediment cover from seeding site on the 8th of May 2009.

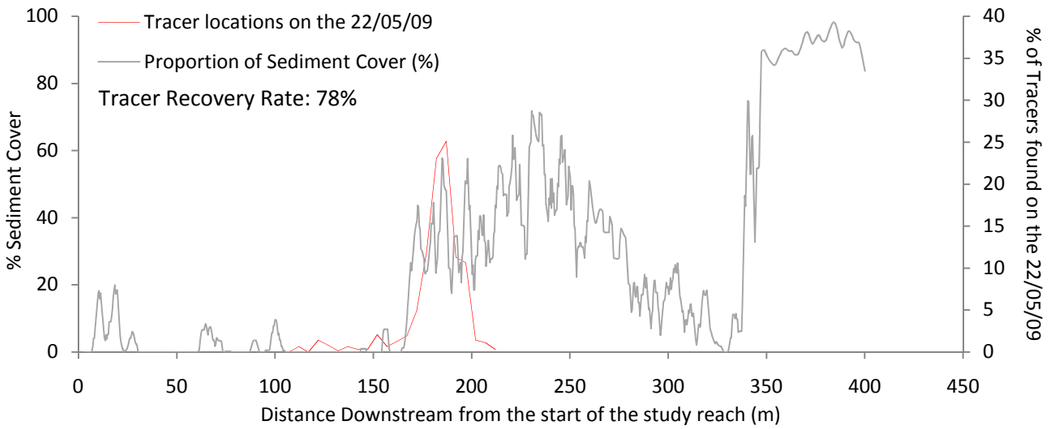

Figure 4.19 Distribution of the tracers and sediment cover from seeding site on the 22nd of May 2009.

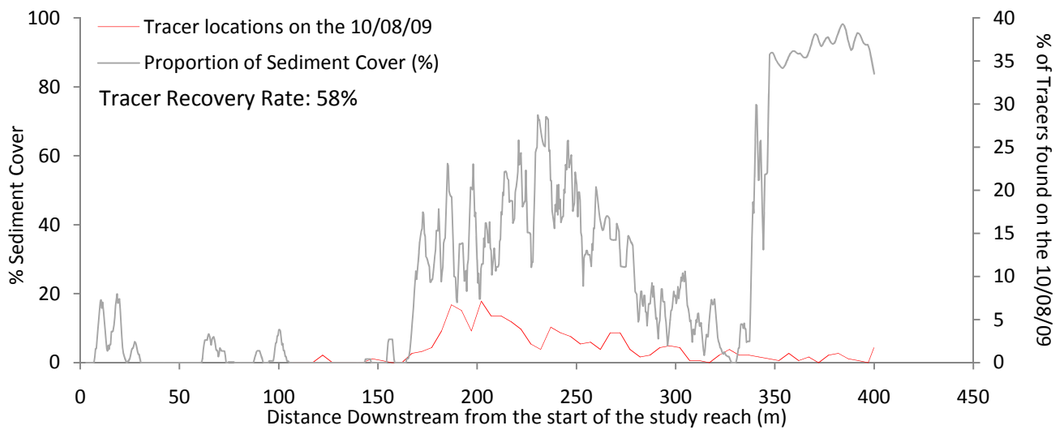

Figure 4.20 Distribution of the tracers and sediment cover from seeding site on the 10th of August 2009.

indicates that the sites of sediment deposition and sediment storage remain stationary as a result of a balance between sediment input and output, over the course of a whole event. Tracer peak 'A' (Figure 4.15) is transported and distributed between (peaks 'B' and 'C', Figure 4.16) during the flow period between the 17th to the 31st of March. This is evident in: the increased height of peak 'B' and the increased in width of peak 'C' (indicating a greater area of sediment storage); and the reduction in height of peak 'A'. The decrease in peak 'A' is less pronounced due to the continued supply of tracers from upstream. Also significant is the shift between the 28th of April and 8th of May of the tracers from peaks 'A', 'B' and 'C' to peak 'D' (Figure 4.18). The distribution of tracers between the 8th of May and 22nd of May does not vary significantly, as a result low peak discharge between the two dates (Figure 4.18, Figure 4.19 and Table 4.2). Between the 22nd of May and 10th of August the distribution of the tracers became more widespread (Figure 4.19 and Figure 4.20). This occurs as the tracers are transported through the partially alluvial section of the reach, with greater selectivity than the in the bedrock zones.

Of the three storage areas that dominated tracer deposition (sites 'A', 'B' and 'C', Figure 4.21), the furthest downstream (site 'C', Figure 4.21) is the most significant store and persists for the longest time period. These sites correspond to peaks 'A', 'C' and 'D' in Figures 4.15, 4.16 and 4.18, respectively. In the partially alluvial and alluvial sections of the channel (beyond 64 m downstream from the seeding site) there is far greater dispersal of tracers than those in the bedrock sections (Figure 4.21). The clustering of tracers, through the bedrock section, indicates a distribution dominated by local deposition sites separated by bare areas of bedrock. However, the dispersed nature of the tracers further downstream indicates more conventional sediment transport dynamics in the partially and alluvial sections of the reach (Figure 4.21). This clustering of tracers at storage sites in the bedrock section of the reach, continued from the 17th of March to the 8th of May. During this period flow peaked at 7.30 $m^3 s^{-1}$ (Figure 4.21 and Table 4.2). Later in the summer however, the storm on the 17th of July 2009 (18.35 $m^3 s^{-1}$) transported sediment beyond the bedrock/partially alluvial boundary (64 m downstream from the tracer seeding site). This suggests that at a higher discharge sediment is entrained from stationary storage sites and that there is some difference in entrainment threshold for the transport of sediment through partially alluvial and alluvial zones.

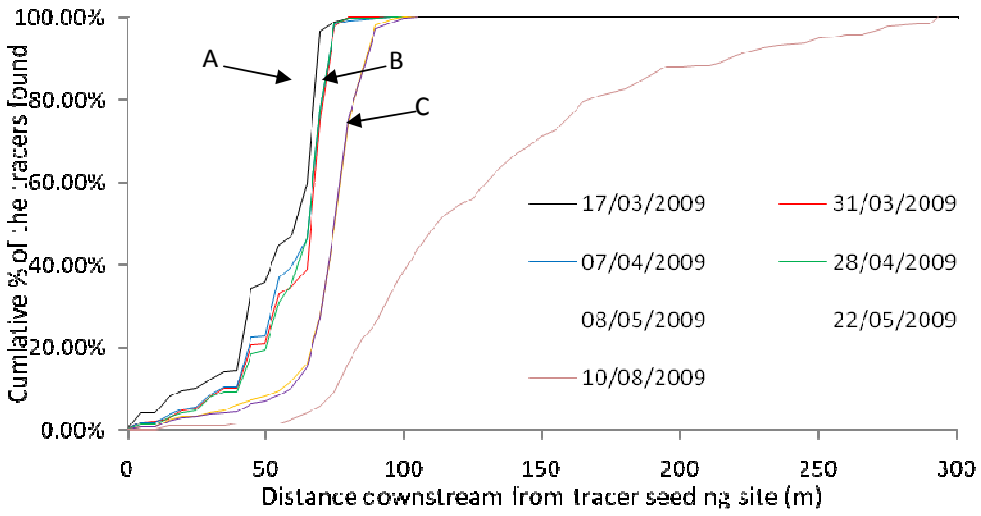

Figure 4.21 Cumulative histogram showing the proportion of tracers stored in the study reach downstream from the tracer seeding site.

The differential transport of sediment tracers in alluvial river experiments has been defined by the different characteristics of sediment clasts (e.g. Warburton and Demir, 2000). However in this study the degradation of tracer surfaces and the time constraints on surveying periods meant that sediment identification became difficult. Also the transport of the sediment in waves, with complete areas of sediment mobile between survey periods through the study reach, lead to the conclusion that sediment transport occurred primarily due to the position of the tracers in the channel. Thus that channel morphology and flow competence had the primary control over sediment entrainment potential through the bedrock reach. The critical shear stress for coarse grain sizes, between 16 mm and 256 mm are further discussed in section 5.4.

4.4.2 **Predicting sediment transport using a critical discharge approach**

Predicting the onset of sediment transport in steep mountain and upland rivers is often done using the Schoklitsch equation (Bathurst, 1987; Warburton, 1990). The equation uses an empirical relationship between flow and sediment properties to approximate the critical flow conditions when sediment will be transported (Eq. 4.3). The Schoklitsch equation is one of a number of such formulae which can be used to predict the critical conditions for sediment entrainment. However, due to its development for steep mountain channels with coarse sediment loads, it is well-suited to the current study (Bathurst et al., 1985 and Warburton, 1990). The critical discharge for the Trout Beck at the pressure transducer was calculated to be 5.59 $m^3 s^{-1}$. This value (calculated using Eq. 4.3) was compared to the complete flow series measured at the EA gauging station, from 1992 to March 2009, in order to assess the period of time which the flow was greater than the threshold for sediment transport to occur (Table 4.3). For the period which the tracer experiment was undertaken the flow exceeded this threshold for only 0.6% of the time. This threshold is now considered in relationship to the transport of tracers through the study reach.

$$Q_{cr} = 0.26 \times \left(\frac{\rho_s}{\rho} - 1\right)^{\frac{5}{3}} \times \frac{D_{40}^{\frac{3}{2}}}{S^{\frac{7}{6}}}$$

Eq. 4.3

Where, ρ_s the density of sediment (2611 kg m^{-3}); ρ the density of water (1000 kg m^{-3}); D_{40} the 40th percentile in the grain size distribution of the tracers used in the tracer experiment (60.9 mm); and S the local channel gradient (0.0039).

Critical Discharge ($m^3 s^{-1}$)	% of time which the flow exceeded the critical discharge (1992 – March 2009)	Time (Hours)	Time (Days)
5.59	1.216	1589	66.208

Table 4.3 The critical discharge for the mobility of the tracers at the study site.

The threshold for sediment transport (as predicted by the Schoklitsch equation) has been considered in relation to the tracer surveys, using the local stage in study reach (Figure 4.22). Peaks 'A' – 'D' (Figure 4.22) represent the flow events which peaked over 0.79 m (5.59 $m^3 s^{-1}$) between the 26th of February and the 10th of August 2009. These flow events correspond well with the significant changes in the distribution of tracers within the study reach, between the: 26th of February – 17th of March (peak 'A'); 17th of March – 31st of March (peak 'B'); 28th of April – 8th of May (peak 'C'); and 22nd of May – 10th of August (peak 'D'). Alternatively to this there is little change in the distribution of the tracers through the study reach between surveys which do not

have a flow peak above 0.79 m (Figure 4.21). It is conclude therefore that the transport of the tracers, through the bedrock section of the study reach, can be approximated by the threshold for sediment transport as predicted by the Schoklitsch equation; but whether this holds true for all bedload transport through the study reach, must be further investigated. In order to do this the *in situ* impact sensors have been analysed to determine the spatial differences in the discharge threshold at which sediment transport begins.

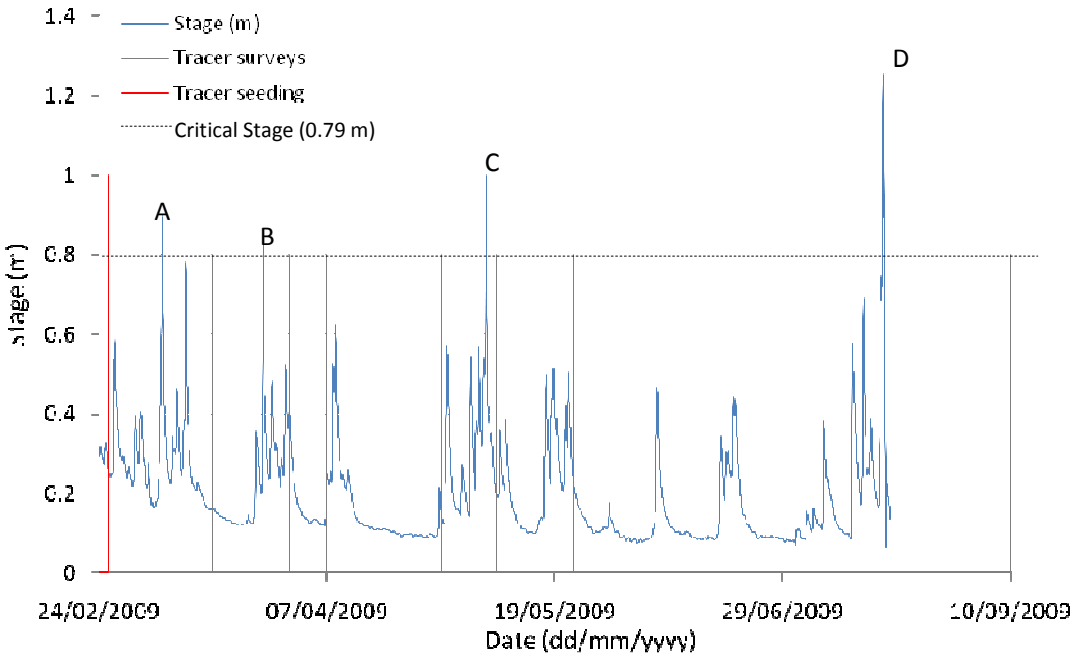

Figure 4.22 Stage hydrograph for the study period, indicating the times when tracer surveys were undertaken and the critical threshold for bedload transport. Stage recordings finish on the 18th of July 2009 as the pressure transducer was dislodged.

4.4.3 **Monitoring bedload transport using impact sensors**

The use of impact sensors at four locations in the study reach provided a continuous spatially distributed record of bedload transport. Impact sensor records have been analysed to assess the influence of the flow on sediment transport: by calculating the distribution of impact intensities for discharges between 0.01 $m^3 s^{-1}$ and 12 $m^3 s^{-1}$, at intervals of 0.25 $m^3 s^{-1}$. Sensors 1, 2 and 4 show similar patterns in sediment transport (Figure 4.23, Figure 4.24 and Figure 4.26), whilst sensor 3 appears to experience less activity (Figure 4.25). The inter-quartile ranges of impacts remain low until a takeoff of sediment transport (indicated by increased impacts) at sensor 1, 2 and 4 (Figure 4.23, Figure 4.24 and Figure 4.26). For sensors 1 and 2 this threshold is between 5.75 and 6.25 $m^3 s^{-1}$, whilst at sensor 4 it occurs at 5.25 $m^3 s^{-1}$. Sensor 3 shows very low numbers of impacts before an increase in activity at 9 $m^3 s^{-1}$. It is likely this occurs because the sensor is positioned slightly to the side of the main thalweg and thus sediment only hits the sensor plate sometime after transport has been first initiated. Another similarity observed between sensors 1, 2 and 4, is the saturation (255 impacts) at around 8 $m^3 s^{-1}$ when presumably most of the bed is actively transporting material. These estimates of the onset of sediment transport (at sites 1, 2 and 4), agree remarkably well with prediction for critical discharge made using the Schoklitsch equation (5.59 $m^3 s^{-1}$), as is further explored in Table 4.4.

The percentage time that: impacts have been detected; no impacts have been detected; and which there is saturation of impact intensity (255 impacts in a 15 minute interval), have been

calculated for discharge over 5.59 $m^3 s^{-1}$ at each of the impact sensors (Table 4.4). This value represents the critical threshold for sediment transport (as calculated by the Schoklitsch equation) and is below the thresholds observed in Figures 4.23 – 4.26, for each of the sensors. The results for sensors 1, 2 and 4 demonstrate that there is sediment transport occurring between 96% and 98% of the time (above the 5.59 $m^3 s^{-1}$) compared with a saturation frequency of less than 2% (Table 4.4). The lower frequency of recorded movement at sensor 3 can once again be attributed to the location of the sensor to the margin of the channel.

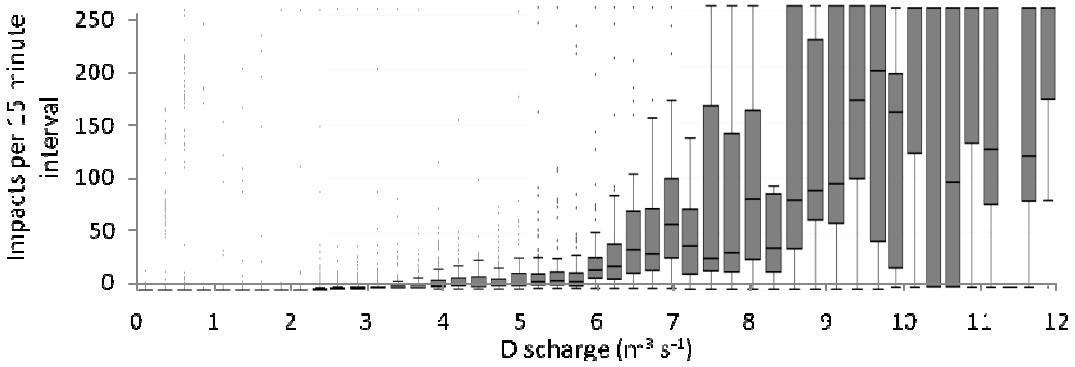

Figure 4.23 The relationship between discharge and bedload impact intensity: impact sensor 1.

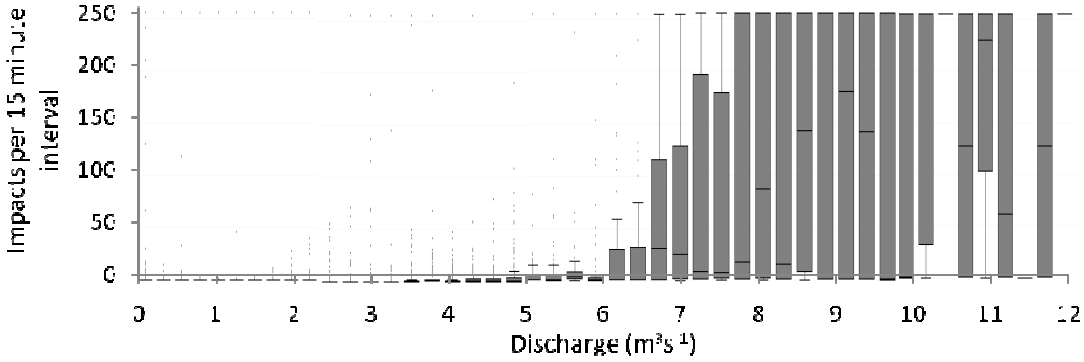

Figure 4.24 The relationship between discharge and bedload impact intensity: impact sensor 2.

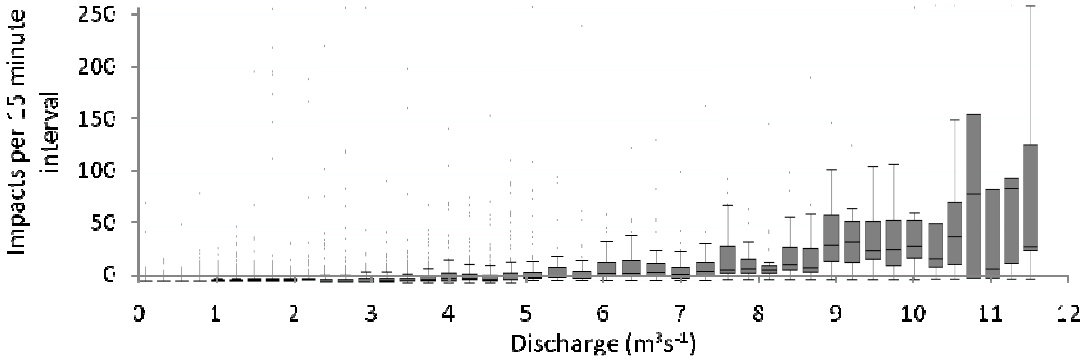

Figure 4.25 The relationship between discharge and bedload impact intensity: impact sensor 3.

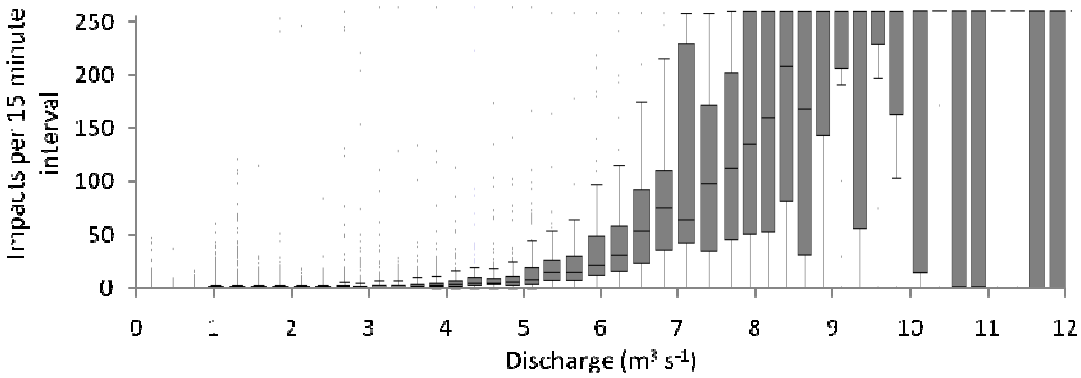

Figure 4.26 The relationship between discharge and bedload impact intensity: impact sensor 4.

Sensor	% of the time where impacts are detected	% of the time where there are no impacts detected	% of the time where the sensors reach saturation
1	96.80	1.23	1.97
2	96.38	2.16	1.47
3	56.50	37.24	6.26
4	98.29	0.31	1.39

Table 4.4 The percentage of time which: impacts are detected; there is no movement; and the sensors become saturated, for flows over 5.59 $m^3 s^{-1}$.

Cross correlation between 15 minute discharge values and 15 minute impact logger hit frequency was undertaken for all flow events which exceeded 5.59 $m^3 s^{-1}$ (the threshold for sediment transported predicted by the Schoklitsch equation) for the period 17th of July 2007 to the 8th of March 2009. The result was 40 flow events which had a peak above the critical threshold for sediment movement. Cross correlation between the discharge and impact intensity (recorded by the impact sensors 2, 3 and 4) showed a maximum correlation at a lag of between -1 and 1 for all of the sensors, during the model flow event on the 7th and 8th of March

2009

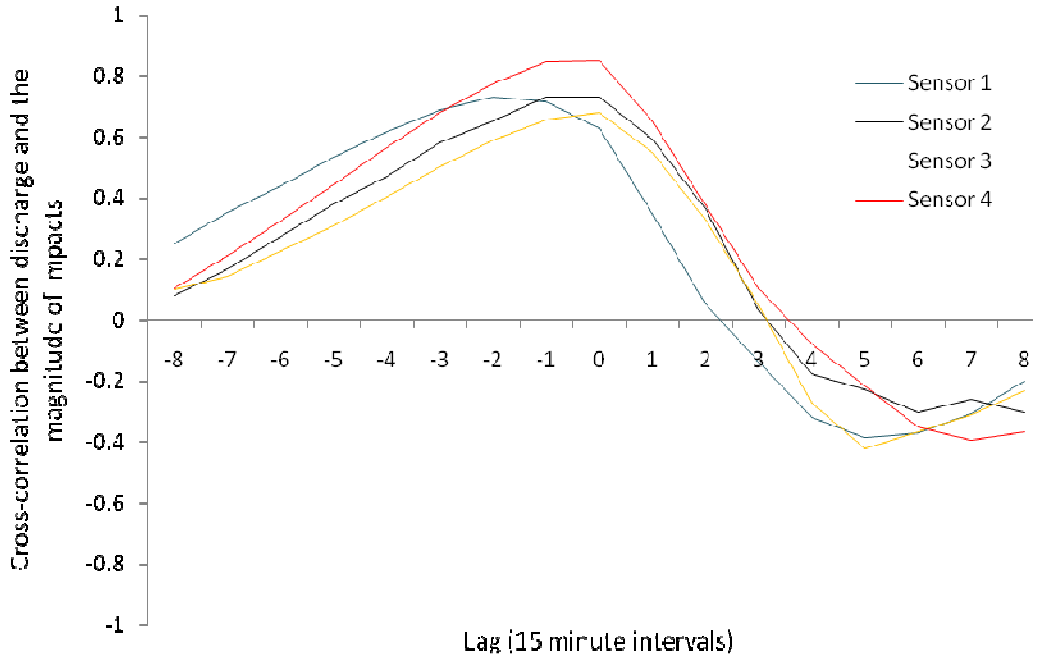

(

Figure 4.27). Sensor 1 however, shows that the sediment transport intensity correlates most closely with discharge at a lag of -2; indicating that sediment transport intensity is most closely predicted by the flow which occurred 30 minutes previously. This is somewhat counter-intuitive but may relate to either sediment supply limitations in the proximal part of the study reach or may reflect the unusual location of the sensor immediately below a large step and plunge pool. There is a limitation to this analysis, as it included periods in the flow series when the sensors recorded saturation and the impact intensity may have continued to rise. However, this only represents a limited period (between 1.39 and 6.26% of the time, Table 4.4) and is observed at sensors 1,2 and 4 to occur above 8 $m^3 s^{-1}$ (with an exceedence frequency of 1% between 1992 and March 2009, Figure 4.3 and Figures 4.23 – 4.26).

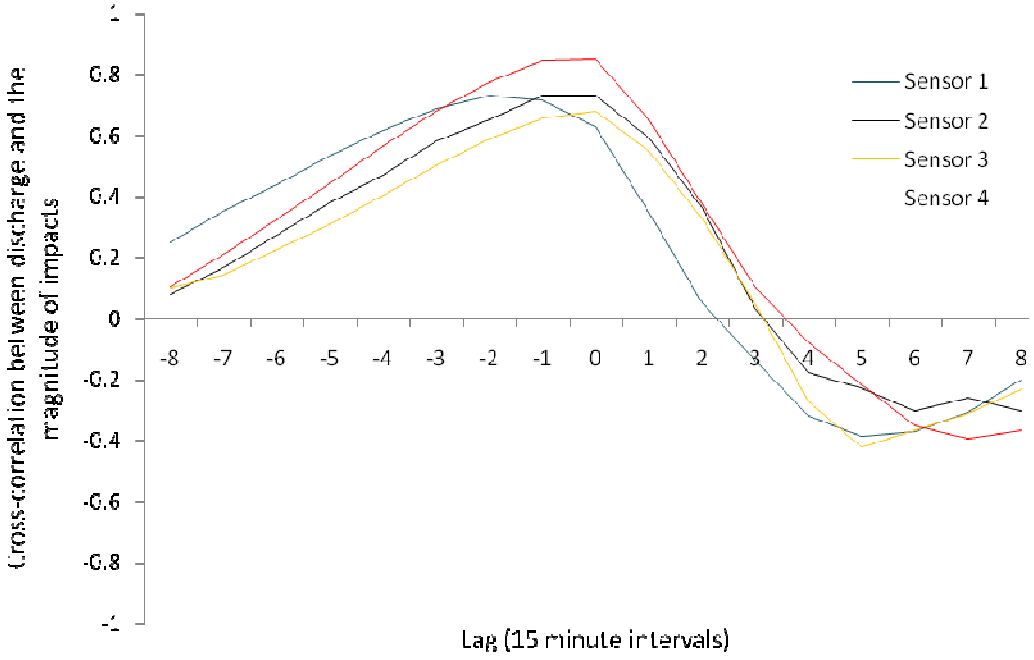

Figure 4.27 Cross correlation, representative of the model flow event (7th – 8th of March 2009), at each of the impact sensors in the study reach.

4.5 **Conclusions from field monitoring**

The framework for field monitoring was designed around the 'fluvial trinity' so that analysis of the interactions between channel morphology, flow and sediment cover, which cause sediment transport, could be undertaken. The characteristics of the channel morphology show less changes in elevation in the smooth bedrock regions of the study reach, than in the partially alluvial and alluvial sections of the reach where there is greater differences in elevation over smaller areas. Also the narrow, incised channel in the bedrock changes downstream to a wider shallower channel in the alluvial zones.

The nature of flow at Trout Beck has been monitored both over a long period downstream at the EA gauging station and since the 24th of February 2009 locally in the study reach. The study reach stage record showed three main characteristics. Firstly base flow, which had a declining trend throughout the recorded period. Secondly, the short term flow events which rise above the base flow briefly. Thirdly, more sustained periods of flow occur where the stage was distinctly higher than base level.

The size distribution of sediment in the channel is spatially consistent, however the amount of sediment stored through the reach varies. It has been observed that the variation in sediment cover is related to changes in channel width through the study reach. As the channel widens there is a decrease in stream power which results in sediment deposition (consistent with observations in alluvial channels). However two processes have been observed which influence this trend. Firstly, where there is a lack of sediment supply to the bedrock channel: the channel remains sediment free. Secondly in regions of the channel where constrictions occur there is a choking of sediment. The result is that sediment storage is not only controlled by the local width of the channel, but by the nature of sediment supply to the channel and the local hydraulics in the channel.

The transport of sediment through the study reach has been monitored using tracers and the *in situ* impact sensors. The tracers demonstrated that sediment storage occurred at stationary locations through the bedrock section of the reach (i.e. pothole, cracks in the bedrock reach and at the bedrock/alluvial transition zone), and the importance of flow events over critical discharge (5.59 $m^3 s^{-1}$, predicted by the Schoklitsch equation) in causing transport. The affect of a critical threshold for sediment transport was subsequently observed in the impact sensor record, which also highlighted the correlation between sediment transport and flow at the same instant. At impact sensor sites 1, 2 and 4 there is a close correlation between the monitored threshold of sediment transport in the channel and critical threshold predicted by the Schoklitsch equation, whilst site 3 suffered from its location at the margin of the channel. Overall it is concluded from monitoring sediment transport in the field that: the critical discharge needed for sediment transport in bedrock section of the reach is consistent with that predicted by the Schoklitsch equation (5.59 $m^3 s^{-1}$), whilst the critical discharge for saturation of impacts sensors (indicating sediment transport in the partially alluvial and alluvial section of the reach) is 8 $m^3 s^{-1}$. However the saturation of impact sensors 1, 2 and 4, limits the upper threshold for sediment transport monitoring by these sensors. In order to determine whether there is a threshold for which all sediment in the channel is mobile: further analysis of sensor 3 at higher discharges could be carried out; or the sensors could be recalibrated to record shorter time intervals and to record the occurrence of 255 impacts in a 15 minute interval. This second method would reduce the resolution of sediment entrainment at lower impact rates, but may demonstrate that there is an upper threshold to which sediment entrainment does increase, indicating complete mobility in the channel.

The influence of flow on sediment transport has been monitored in the field, whilst the influence of channel morphology and flow interactions in causing sediment transport through the study reach, is considered further in Chapter 5. The role of channel shape and roughness have on controlling the transport potential (approximated by shear stress) is discussed and the spatial variation of shear stress through the course of storm events is analysed. From this, further conclusions are reached with regard the controls over different sediment transport dynamics in the bedrock and partially alluvial sections of the study reach.

Chapter 5:

Applying a 1D model to bedrock channel sediment dynamics

5.1 **Introduction**

The HEC-RAS one dimensional model has been applied to investigate the interaction between the channel geometry and the hydraulic conditions in the mixed bedrock/alluvial study reach. A stable model was constructed then verified and validated. This included an assessment of three components of the energy loss term ($h_{L_{1-2}}$): the expansion and contraction coefficients and the Manning's roughness term (as discussed in section 3.3). Once an optimal parameter set was identified the model was used to calculate the local shear stress at the 21 cross sections through the reach.

5.2 **Setting the initial model conditions: morphology and flow input**

The boundary conditions used in the HEC-RAS model are the geometry of the channel, an input discharge at the inlet and the flow conditions at the downstream end of the reach. The 21 channel cross sections (identified in section 4.1.1) have been used to define the channel geometry. These 21 cross sections were taken at breaks in channel slope through the reach to capture the same study reach as used in the tracer experiment. This method of defining the channel was chosen as HEC-RAS required 1D cross-sections of the river and by incorporating changes in the channel slope, the variations in channel morphology were included. The cross section, furthest upstream, was below the large step and plunge pool, but upstream of the seeding location the tracers and distal cross sections was 400.16 m downstream, beyond any bedrock in the channel. The cross sections were taken perpendicularly to the flow (Figure 5.1 and Figure 5.2). The cross sectional spacing varies depending upon the breaks in channel slope, however interpolation within HEC-RAS has been used to interpolate cross sections within the model (increasing the number of cross sections to 58) to ensure mass conservation. The flow hydrograph used as the input condition for unsteady flow analysis was taken from a storm event on the 7th and 8th of March 2009 and its selection has been justified in section 3.3.3 (Figure 3.8). Model sensitivity analysis was undertaken at cross section 16 located 12.9 metres down the study reach. This section was identified because the local stage was monitored at this point enabling validation of the model and it was far enough away from either the inlet or outlet not to be affected by the boundary conditions (Horritt, 2000).

5.3 **Calibrating the HEC-RAS model using sensitivity analysis**

The construction of a numerical model which represents the physical environment raises a complex set of questions of how natural processes are empirically represented. In all models there is a need to reduce the complexity of the system. As the adopted approach becomes more simplistic there is a greater reliance on the use of parameters to represent the processes that are not captured by the governing equations (Lane et al., 1994). The result is that parameters are used to represent a combination of processes (e.g. roughness, Chow, 1959) and the value of these parameters needs to be investigated. In order to determine the value of each parameter sensitivity analysis has been undertaken by considering:

1. the best parameter value to represent the forms and processes occurring in the river (Beven and Binley, 1992); and
2. the influence each parameter has on the stability of the model and how this may affect the definition of other parameters used in the model (Beven and Binley, 1992; Tayefi, 2005).

In section 3.3 the energy loss term ($h_{L_{1-2}}$) was introduced. This is a product of the contraction coefficient, expansion coefficient and the Manning's roughness parameters. The

contraction and expansion coefficient represents the degree to which the channel cross sectional area changes between sections, whilst the Manning's term represents roughness which can also be considered as the topography which is not captured in the model's spatial discretisation. In the bedrock channel, with the relatively smooth channel sides (see section 4.4.2), it is suggested that the contraction and expansion coefficients will have a greater influence than the Manning's roughness value for validating the hydraulic scheme. This differs from traditional applications of HEC-RAS to alluvial channels (Horritt and Bates, 2002) but as discussed (in section 1.2 and 3.3.1), the bedrock sections of the channel act more like a conduit rather than a classical alluvial channel and therefore the traditional approach of parameterising a one dimensional hydraulic model for river applications may not be directly applicable in the study of bedrock channels. Furthermore, the downstream boundary condition (discussed in section 3.3.3) determines the initial energy gradient between cross sections and due to the steep nature of the channel the normal depth boundary condition is also investigated.

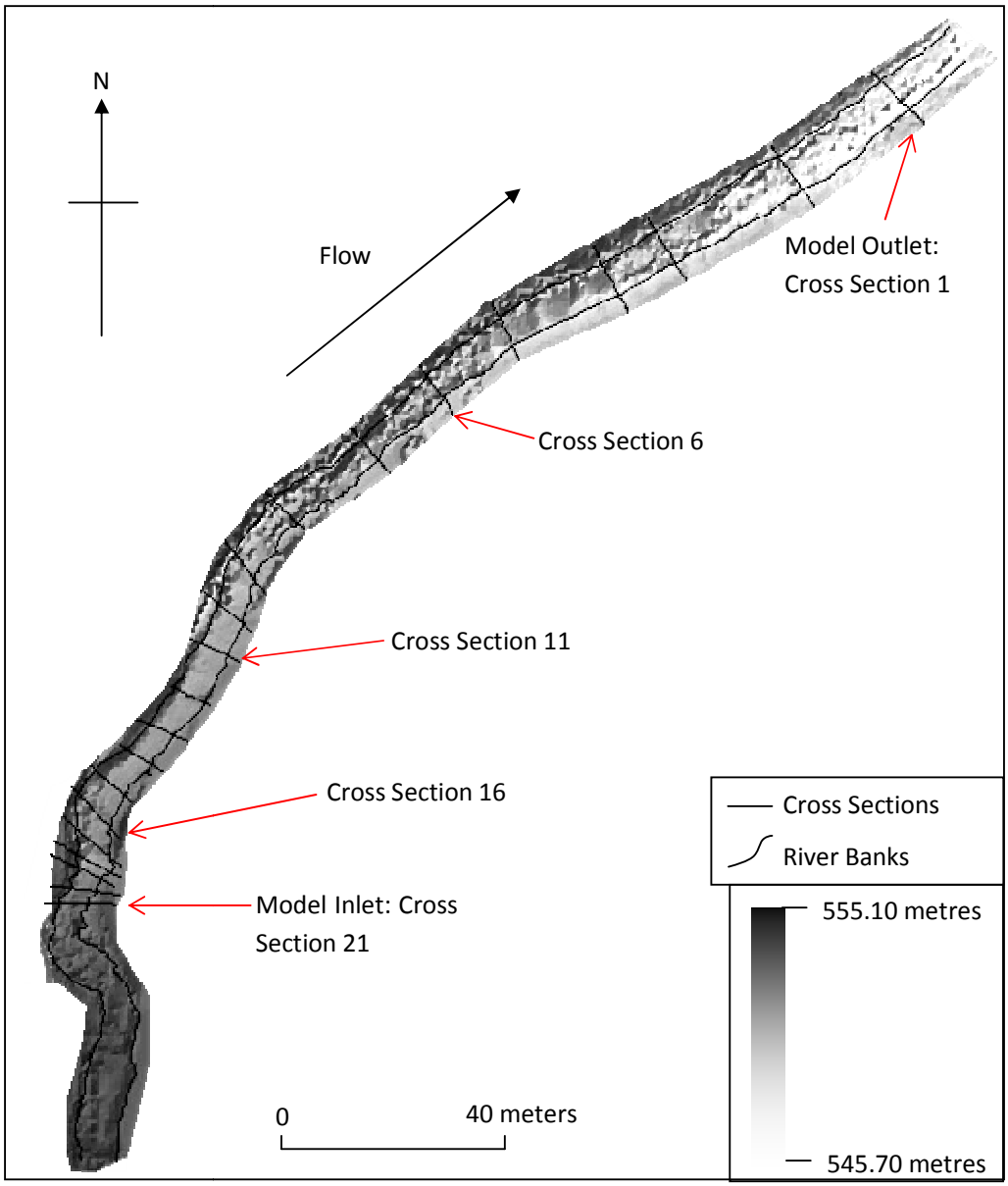

Figure 5.1 The location of the 21 cross sections used to define the morphology of the study reach in the HEC-RAS model within the DEM developed from morphological surveying. The cross

sections are situated perpendicular to the flow and cross section 16 (local stage monitoring site) is located 12.9 m downstream from the model input.

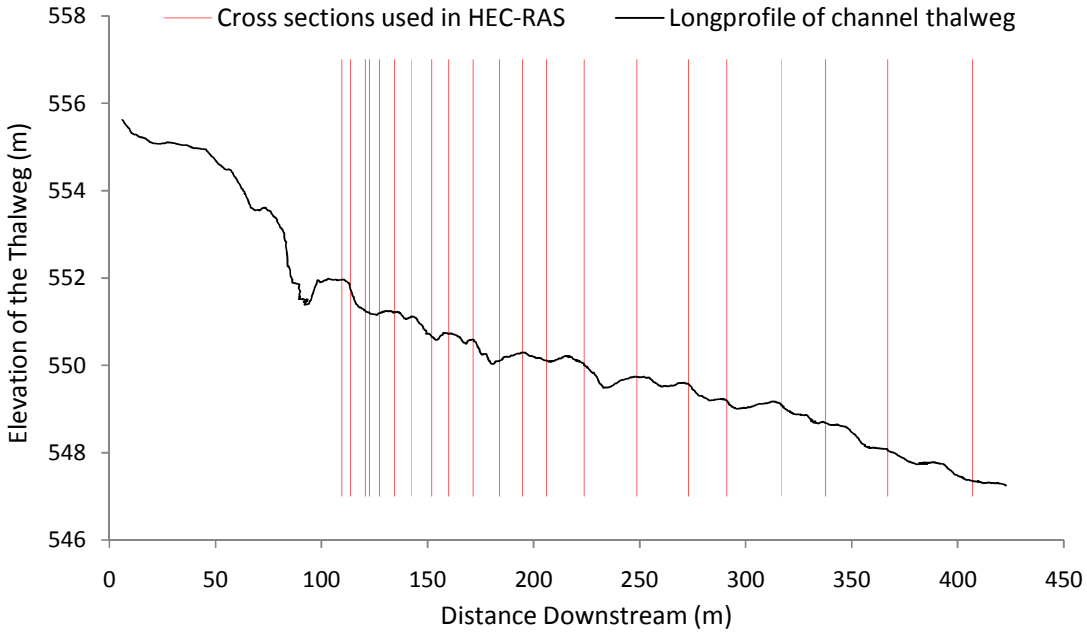

Figure 5.2 The long profile of study reach with the location of the 21 cross sections used to define the morphology in the one dimensional model.

5.3.1 **Sensitivity analysis of the contraction and expansion coefficients, with the downstream normal depth**

The initial sensitivity analysis considered the coefficients of contraction and expansion along with the downstream boundary condition (normal depth). The contraction and expansion coefficients are numerical representations of the influence of contracting and expanding river morphology on the flow properties in the river (Hunt and Brunner, 1995). In a prismatic channel with a uniform cross section at every location downstream, the contraction and expansion coefficients would have a value of 0. However, if the channel contracts and expands in an abrupt nature (e.g. between cross sections 15 and 14, Figure 4.2), the coefficient would typically have a value of 0.8 (Haestad et al., 2003). In natural rivers, the channel's cross sections are rarely regular and nor do they vary in a uniform manner. Therefore, the contraction and expansion parameter space must cover all the range of situations which occur in the reach. A sensitivity analysis was performed for values between 0 and 0.8.

In conjunction with the expansion and contraction coefficient, the normal depth at the downstream flow boundary was considered. This condition is the flow stage for which flow is uniform (Haestad et al., 2003). It is calculated, initially, using the Manning's equation from the input flow, channel form and user defined energy gradient and Manning's coefficient (Equation 5.1, Brunner, 2009, p.2-4). The energy gradient is usually approximated from the average channel slope, however due to the steep nature of channel and abrupt changes in channel slope a range of energy gradient values between 0.001 and 0.05, (in increments of 0.001) were tested in the calculation of the initial downstream normal depth.

$$Q = \frac{k}{n} A R^{\frac{2}{3}} s_0^{\frac{1}{2}}$$

Eq. 5.1

Where, Q is the initial discharge ($m^3 s^{-1}$), k is a constant (1.486), n is the Manning's coefficient (-), R is the hydraulic radius ($m^2 m^{-1}$) and s_o is the energy gradient (-).

In total 3850 model runs were undertaken using the HEC-RAS model for different combinations of contraction, expansion and normal depth values. Of these runs 810 (21%) ran to completion and were classified as stable whilst the other 79% were unable to be verified within twenty iterations (the maximum number of iterations defined within the HEC-RAS model, Brunner, 2008) to solve the St. Venant equations and were therefore classified as unstable.

The modelled stage and river stage measured in the field were compared at cross section 16, to assess the validity of each of the stable parameter sets with the conditions in the bedrock channel. This was completed using the model efficiency approach proposed by Nash-Sutcliffe (1970) to determine the goodness of fit between the observed and modelled data (Equation 5.2 - Nash and Sutcliffe, 1970; Bevan, 2002; Beven, 2002). If the model efficiency is 1 then the modelled and monitored stage are in perfect agreement, if the efficiency has a value of 0 then the model is no better than predicting the mean value for the stage at any time step. If the efficiency is negative then the model is classified as non-behavioural where the model demonstrates no relationship to the monitored cases (Bevan, 2002) and the model represents the natural conditions no better than if the model was calibrated taking a random set of parameters from within the parameter space (Bevan, 2002).

$$E = \left[1 - \frac{\sigma_\varepsilon^2}{\sigma_o^2}\right]$$

Eq. 5.2

Where, E is the model efficiency, with a value between 1 and -1, σ_ε^2s the error variance between the modelled and observed data and σ_o^2 is the variance in the observed data.

Of the 810 stable parameter sets, 7% showed a behavioural relationship between the modelled and monitored stage at cross section 16. The distribution of efficiency values for the behavioural models is discretely spread with values being either high or low, with none in-between (Figure 5.3). This pattern indicates that there are few parameter sets which reproduce the observed processes in the reach and those that do either have high or low model efficiency. Further analysis of the model efficiency and the values of individual parameters (contraction, expansion and energy gradient) shows that there is a uniform distribution in discrete intervals of either highly efficient (>0.8), inefficient (<0.2 but >0) and non-behavioural (<0) model runs (Figure 5.4, Figure 5.5 and Figure 5.6). As a result of this scatter, it is suggested that none of these three variables have a greater weighting on the model efficiency and that the parameter set used should represent the most efficient combination of all three.

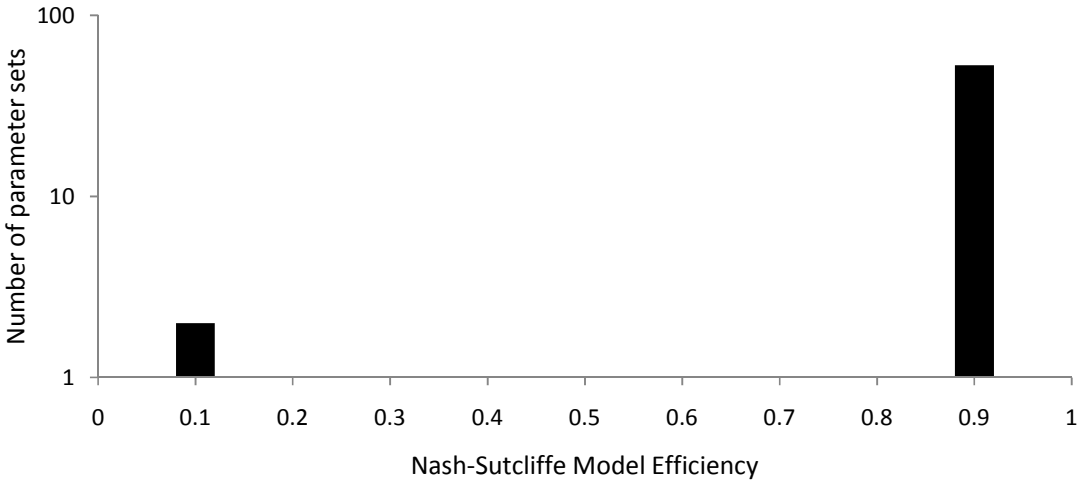

Figure 5.3 The distribution of model efficiency values as calculated from the Nash-Sutcliffe (1970) approach for the behavioural models.

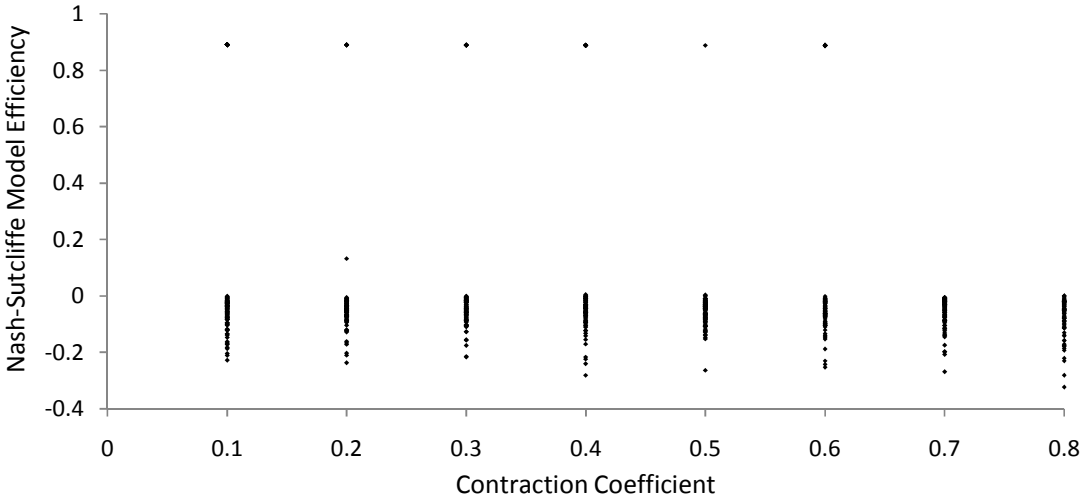

Figure 5.4 Distribution of Nash-Sutcliffe efficiency values for all the contraction coefficient values used in the sensitivity analysis.

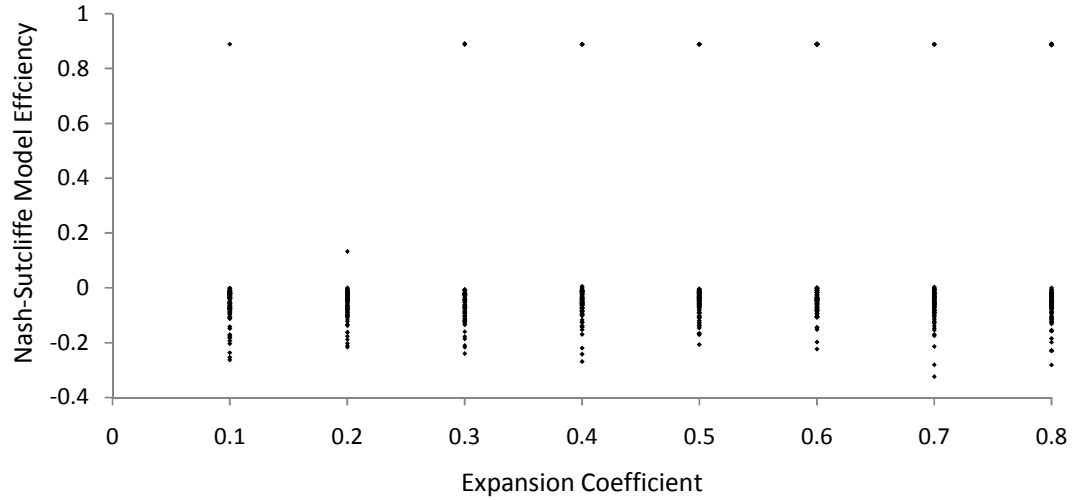

Figure 5.5 Distribution of Nash-Sutcliffe efficiency values for all the expansion coefficient values used in the sensitivity analysis.

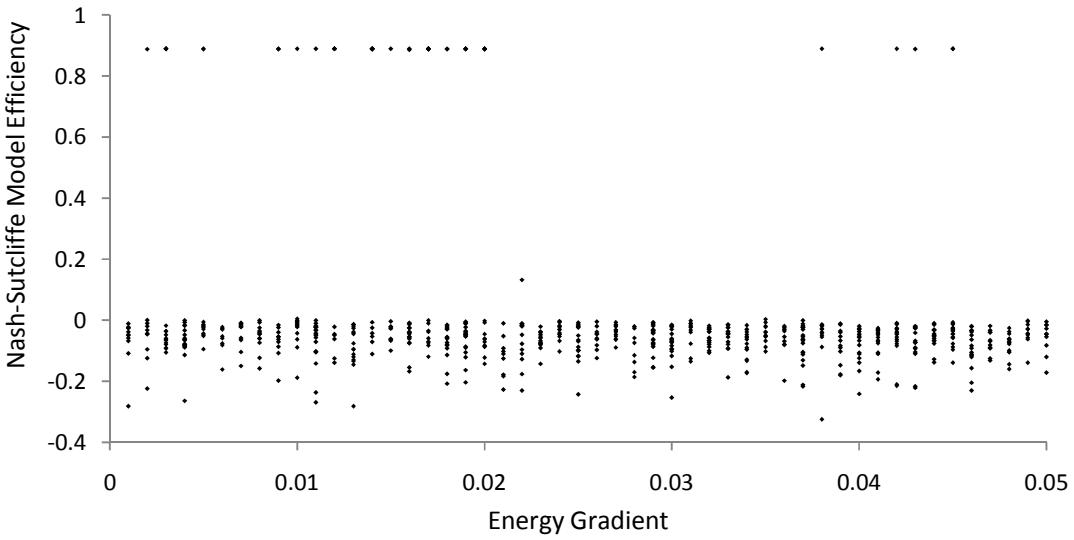

Figure 5.6 Distribution of Nash-Sutcliffe efficiency values for all the energy gradient values used in the calculation of the downstream normal depth boundary condition, and assessed in the sensitivity analysis.

The parameter sets with high model efficiencies have been analysed to assess whether a single value for each of the tested variables, is statistically more likely to produce a verified model which also can be validated. Initially the contraction and expansion coefficients were tested with the energy gradient for parameter sets which had a model efficiency of greater than 0.88 (identified as the lower boundary for the most efficient sensitivity runs) (Figure 5.7 and Figure 5.8). Contraction values of 0.1 and expansion values of 0.6 captured 34% and 32% of the high model efficiency runs, respectively (as indicated by the ovals in Figure 5.7 and Figure 5.8). The distribution of stable runs for these contraction and expansion values are similar. The values cluster between 0.01 and 0.02 with outliers around 0.04. This pattern suggests that there is a relationship between the two values in the river channel and that they represent the different fluctuations in the form of the bedrock channel. A contraction value of 0.1 represents a gradually contracting channel, identified in the field due to the constrictive nature of the bedrock channel as it narrows gradually downstream and then widens suddenly (section 4.2.2). The higher expansion value of 0.6 represents this abrupt expansion through the river reach. This occurs due to sudden expansion of the bedrock river channel in areas where the channel banks are unconsolidated or there are weaknesses in the bedrock and as a result lateral erosion has occurred.

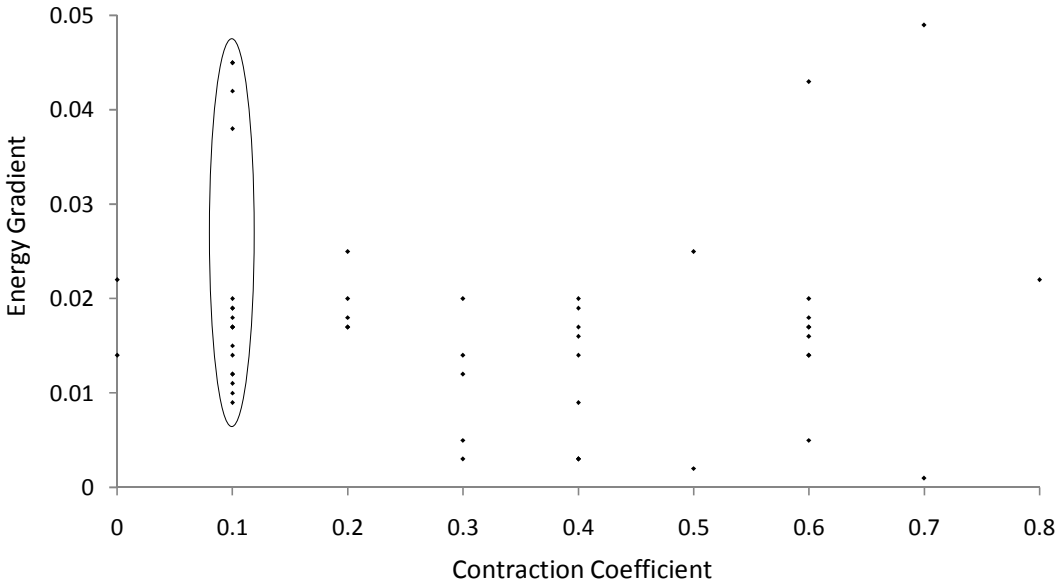

Figure 5.7 Distribution of contraction coefficient values for the range of energy gradient values which contribute to the parameter set and produce a stable model, with an efficiency of between 0.88 and 0.9. The oval highlights the 34% of the stable runs with a contraction value of 0.1.

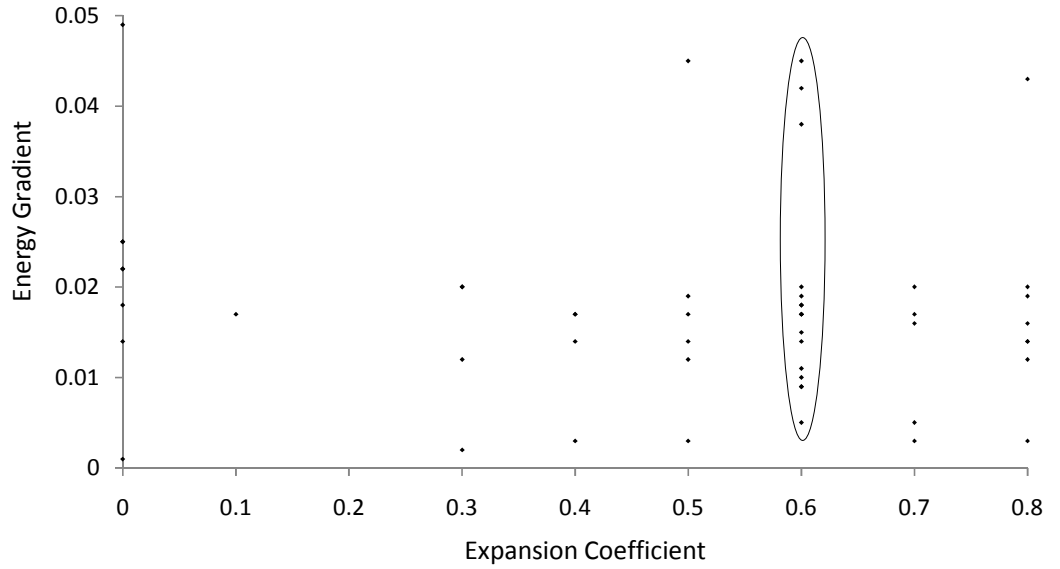

Figure 5.8 Distribution of expansion coefficient values for the range of energy gradient values which contribute to the parameter set and produce a stable model, with an efficiency of between 0.88 and 0.9. The oval highlights the 32% of the stable runs with an expansion value of 0.6.

The distribution of energy gradient values tested in the sensitivity analysis is shown in Figure 5.9. A wide range of values between the minimum (0) and maximum (0.05) were tested but no identifiable clustering occurred at high model efficiency. However, when the values of 0.1 and 0.6 (the most common contraction and expansion values, Figure 5.7 and Figure 5.8) are set, the range of energy gradient values which provide a stable, efficient model are reduced. Figure 5.9 show the percentage frequency with which each of the energy gradient values produces a parameter set that corresponds to a stable model. Of these 0.017 produces the most stable model runs and is used in the optimum parameter sets in subsequent simulations.

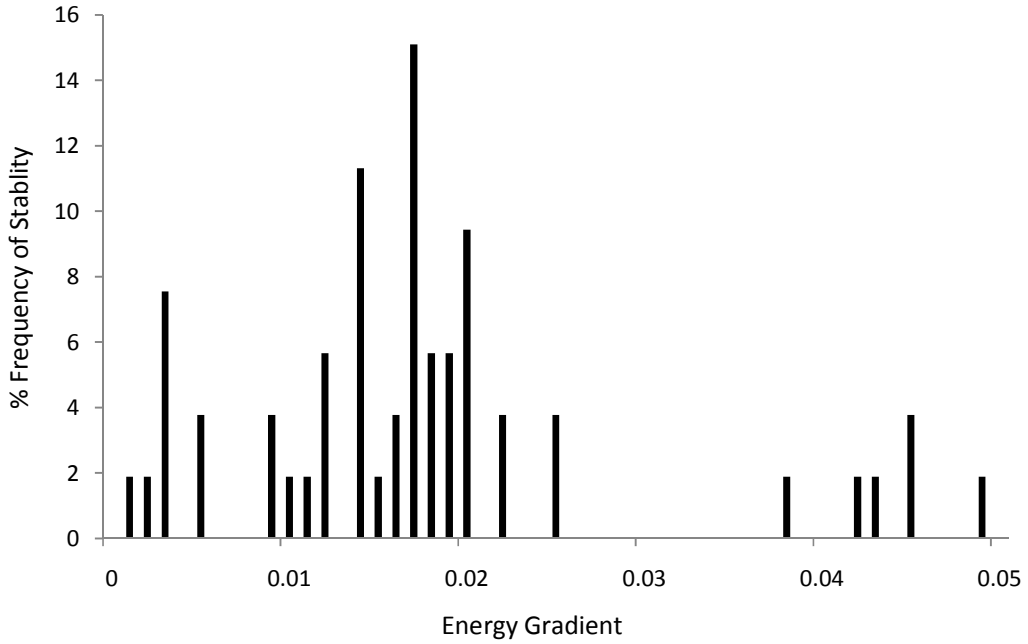

Figure 5.9 The frequency of energy gradient values which contributing to the parameter set and produce a stable model, with an efficiency of between 0.88 and 0.9.

5.3.2 **Sensitivity analysis of the Manning's roughness coefficient**

The Manning's roughness coefficient is used to represent roughness in HEC-RAS. In hydraulic models of alluvial rivers the roughness parameter is used to represent the resistance at the bed-flow interface. These processes are operating at the sub-grid scale in the model of a bedrock channel and include micro-scale resistance, friction at the bed and variations in the flow profile associated with dispersion and turbulence (Lane, 2005). The channel boundaries are defined by shape and the slope between them, whilst roughness is parameterised to represent the interactions between flow and the channel boundaries. The value used to represent roughness in this model was identified from observations in the field. A value of 0.025 was chosen as the optimal for representing the study reach (Chow, 1959). This value of Manning's coefficient represents '*a clean straight channel with no rifles or pools at bankfull discharge (if natural) or the maximum value for a man made channel made of concrete, but with a natural roughness on the bottom*' (Chow, 1959).

Sensitivity analysis was performed on a range of ±20% of the Manning's values and uses the chosen value (from observations and the literature) as the mean as defined in previous studies (e.g. Pappenberger et al., 2005). The sensitivity analysis used the optimal parameter set for the contraction, expansion and normal depth coefficients. Of the 101 runs made using these values 34.7% (35 runs) were stable. These 35 runs were tested to determine their efficiency of modelling the stage at cross section 16, using the Nash-Sutcliffe approach. Of those simulations, 37.1% of the stable models returned model efficiency values greater than 1, indicating that the model had a behavioural relationship with the monitored conditions in the field (Figure 5.10). The other 62.9% of the runs were non-behavioural and had efficiency values of less than 0 (Figure 5.10). Once again the efficiency values are clustered close to 0.9, however there is a negative linear relationship in the efficiency value, as the Manning's value increases form 0.025. As a result 0.025 is taken to be the optimum for use in the parameter including contraction, expansion and normal depth coefficients.

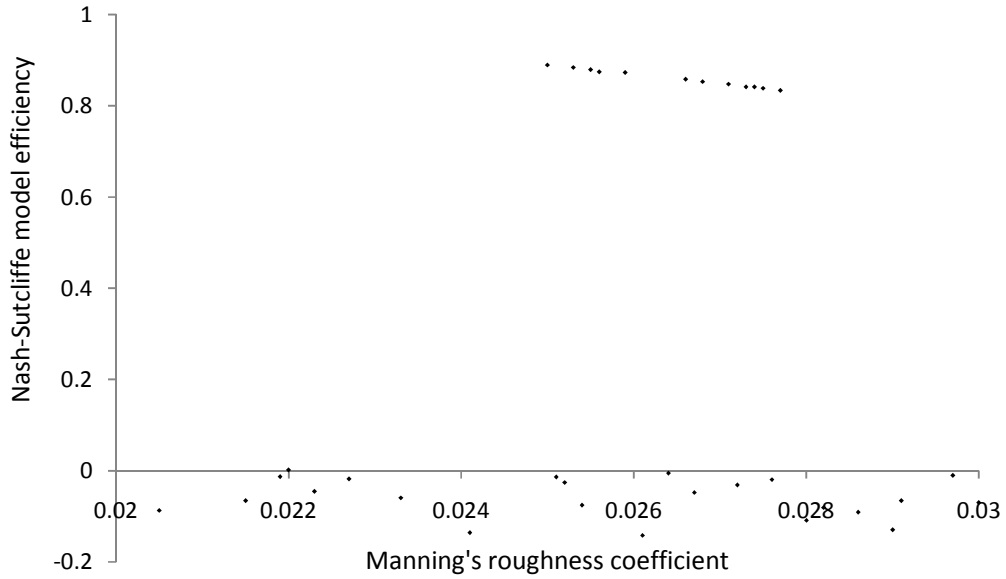

Figure 5.10 Distribution of Manning's coefficient values tested and returned Nash-Sutcliffe model efficiency for stable parameters.

The use of a single Manning's coefficient for the entire river reach, contradicts the idea that bedrock and alluvial sections of the river channel have different bed roughness. However due to the limited sensitivity of the model; the fact that the Manning's coefficient is not calculated from the empirical roughness of a surface; and that HEC-RAS does not modify the channel roughness with flow depth, means that a single value was chosen for this study.

5.3.3 **Calibrating HEC-RAS using the optimal parameter set**

The optimal parameter set used to calibrate the HEC-RAS model for the study reach was defined from the sensitivity analysis performed on four variables, as part of the verification and validation of the models. The values chosen were: 0.1 and 0.6 for the contraction and expansion coefficients respectively; 0.017 for the normal depth value; and 0.025 for the Manning's roughness coefficient. The chosen values are generally representative of the natural conditions and show high efficiency in representing the local stage measured in the field conditions. The overall model efficiency for the storm hydrograph of March 7th and 8th 2009 was 0.89, with a close fit for the flow at stage values above 0.65 metres (Figure 5.11). The closeness of fit to the monitored stage above 0.65 metres is useful in analysis of sediment transport. It is lower than the critical stage of 0.79 m, as predicted by the Schoklitsch equation (and monitored in the field by the impact sensors, sections 4.5.2 and 4.5.3). It is therefore suggested that a validated hydraulic model has been developed and this can now be used to asses shear stress distribution through the reach to infer sediment dynamics.

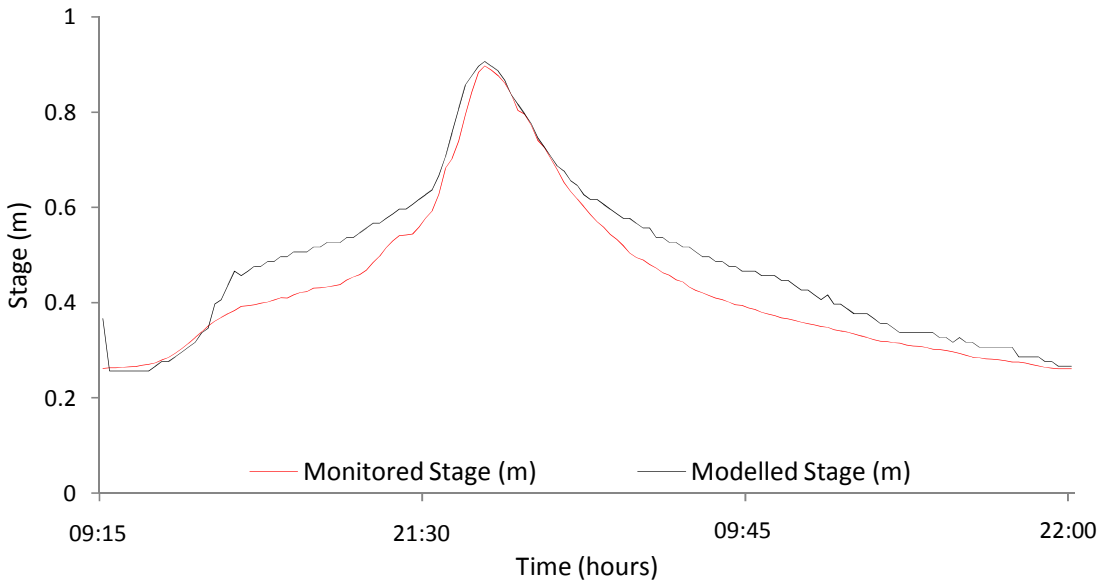

Figure 5.11 Monitored and modelled distribution of stage through the stage hydrograph, at cross section 16 on the 7th of March 2009.

5.4 **Assessing the distribution of shear stress through the study reach**

The spatial distribution of the local shear stress at each of the cross sections through the modelled reach has been assessed for a single storm event (7th of March 2009) and at the peak discharge of high flows on the 7th March, 26th March and 17th July 2009. This analysis allows an insight into the temporal and spatial distribution of shear stress through the reach and acts as a proxy for the potential transport capacity of the flow. However, the actual volume of sediment transported depends on the properties of the sediment available for transport. As a result, the transport potential for the nine grain-size classes (section 3.2.3) has been estimated using critical shear stress (Figure 5.12). The critical shear stress has been calculated using the Shield's equation for a well mixed grain-size distribution (Eq. 5.3, from Knighton, 1984) and an approximation of the dimensionless critical shear stress (Eq. 5.4) from Andrews (1983). Where, τ_{ci} is the dimensionless critical shear stress (-); g is the acceleration due to gravity (9.81 m s^{-2}), ρ_s the density of sediment (2611 kg m^{-3}); ρ the density of water (1000 kg m^{-3}); and D_i is the grain-size of interest (mm); D_i is the grain-size of interest (mm); and D_{50} is the 50th percentile in the grain size distribution of the tracers used in the tracer experiment (0.0663 m).

$$\tau_{cr} = \tau_{ci}\, g\, (\rho_s - \rho) D_i \qquad \text{(Eq. 5.3)}$$

$$\tau_{ci} = 0.0834 \left(\frac{D_i}{D_{50}}\right)^{-0.872} \qquad \text{(Eq. 5.4)}$$

Thus for grains of up to 16 mm (b-axis) the critical shear stress is 73.4 N m^{-2} and for grains of up to 256 mm (b-axis) it is 104.4 N m^{-2}. These thresholds are now considered in relation to the distribution of shear stress, through individual flow events, and spatially, through the study reach.

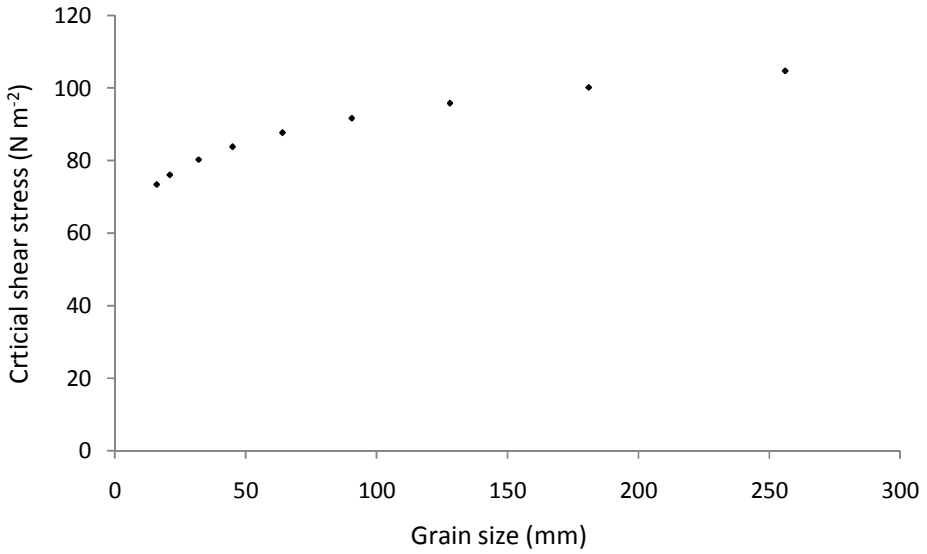

Figure 5.12 The distribution of critical shear stress for the 9 grain size classes used to define the grain-size distribution of sediment in the channel (section 3.2.3).

5.4.1 **The spatial distribution of shear stress**

The distribution of shear stress through the storm event, spanning the 7th and 8th of March 2009, has been calculated in HEC-RAS at 13 cross sections through the modelled reach and is shown in relation to the critical shear stress thresholds for grain with 'b-axis' of 16 mm and 256 mm (Figure 5.13). The 13 cross sections examined are those identified as 6 to 18 in Figure 5.2 and Figure 4.2. These cross sections, incorporating both bedrock and partially alluvial sections of the reach, were the only ones examined as those with closer proximity to the distal ends of the model, potentially have boundary condition effects. There is also some boundary errors observed at the start and end of the storm hydrograph (Figure 5.11) and this is accepted in hydraulic modelling as a product of instabilities caused by stationary boundary conditions (Horritt, 2000). The distribution of shear stress at each of the cross sections has a distinct pattern, representing the strong influence of the morphology on the flow. The distribution of shear stress through time, at all sites, mirrors the flow hydrograph as you would expect, (Figure 5.13) as it rises then falls as the flood wave moves through the reach. However, when investigated spatially, the magnitude of the shear stress reflects the local channel morphology. Furthermore, it is possible to observe that there is a marked spatial contrast in the magnitude of shear stress downstream. That is, the shear stress for cross sections in the partially alluvial zone, are much lower than that in the bedrock zone (Figure 5.13). This occurs due to the lower slopes in the partially alluvial zone, and causes sediment storage which further reduces the channel slope. Sediment storage will also cause a greater roughness, that is not varied in the model parameterisation, in the alluvial zones of the channel and therefore the modelled shear stresses may be an over prediction of the value in reality.

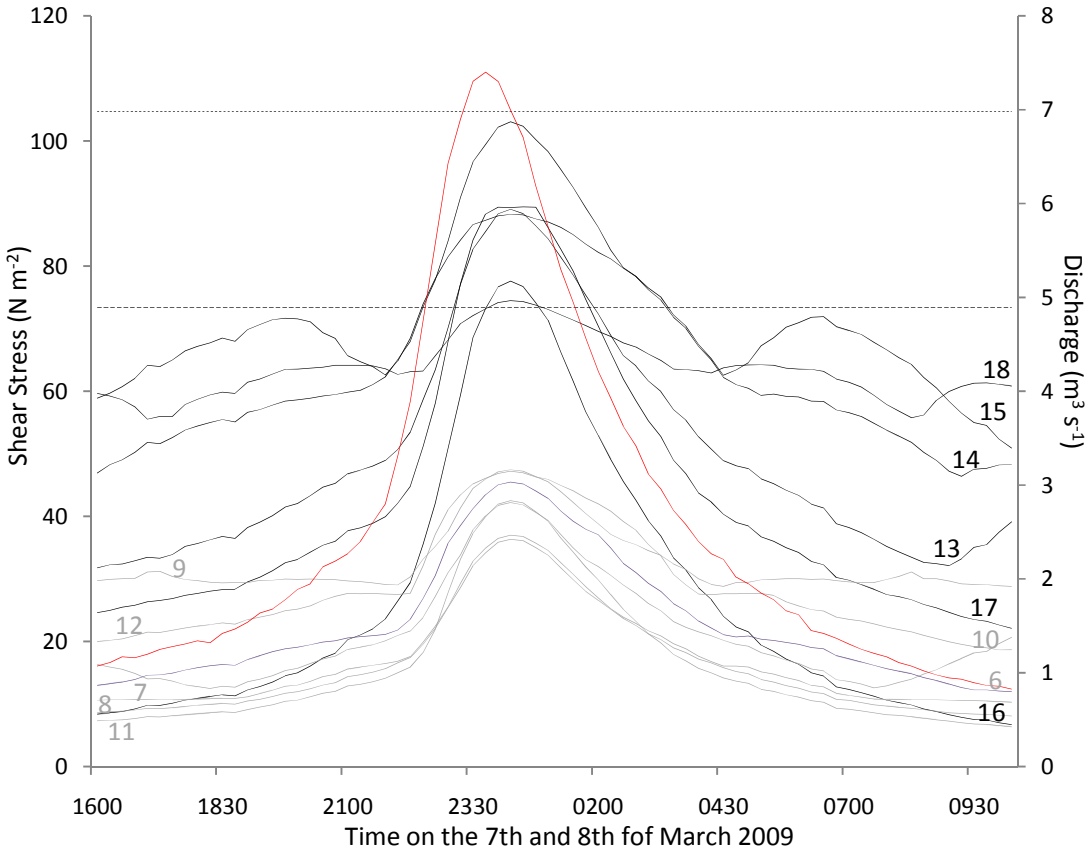

Figure 5.13 The distribution of shear stress at 13 modelled cross sections, over the course of the storm event on the 7th and 8th of March 2009 and the critical shear stress need to entrain the maximum and minimum grain size classes.

A second pattern which is evident, between the shear stress distributions in the bedrock and partially alluvial sections of the reach, is that the shear stress distributions in the partially alluvial zone have a more gradual profile that those in the bedrock zone. This is because of the difference in the geometric shape between the two types of cross sections. The bedrock cross sections exhibit discrete changes in the width at stationary intervals in depth, as a result of their step like form (identified in Figure 1.5, section 1.2.2 and section 4.2.2), whilst the partially alluvial cross sections have more gradual channel boundaries and a steady width – height ratio. It is concluded that the flow controls the timing of the shear stress peak, whilst the morphology controls the local magnitude. This is further examined by considering the distribution of peak shear stress at peak discharge for the flow events on the 7th of March, 26th of March 2009 and 17th of July. The shear stress corresponding to peak discharge has been examined as this will cause the highest shear stress and causes greatest sediment transport (as observed in Figure 5.13 and the cross-correlation results for the intensity of sediment transport over time, recorded by the impact sensors: section 4.5.3).

Another condition presented on this graph is the different shear stress thresholds for the range of grain-sizes present in the study reach. The peak modelled shear stress at all bedrock cross sections is above the critical shear stress threshold for transport of sediment with 'b-axis' of 16 mm (Figure 5.13). However, the modelled shear stress at all the cross sections never reaches or exceeds the critical threshold for transport of sediment with a 'b-axis' of up to 256 mm (Figure

5.13). This implies that the largest class of sediment is not fully mobile at these cross sections through the bedrock reach according to the model. However the full class range may be transported if there are regions of the channel with higher shear stress, not modelled by these discrete cross sections or the model is under predicting the time averaged shear stress. At the alluvial cross sections the shear stress is typically much lower and as a result at no point during this flow event was the critical threshold for coarse sediment transport surpassed (Figure 5.13). These observations agree with the field observations of sediment transport as a result of this flow event. The tracers were transported as a wave through the bedrock section of the reach and then deposited at the bedrock/alluvial transition (Figure 4.21).

5.4.2 **The magnitude of shear stress**

The flow hydrograph from the 7th of March is now considered against hydrographs from storms on the 26th March and 17th July 2009. All three hydrographs have flows which rise from base flow to a peak value, above the critical discharge for sediment transport calculated from the Schoklitsch equation (Figure 5.14, Figure **5.15** and Figure **5.16**). These three storms occurred during the period when tracer transport was monitored (26th of February to the 10th of August 2009). Whilst the hydrograph from the 7th of March is single peaked, rising from base to peak and back to base flow; the others have multiple peaks, all of which are above the critical threshold. These additional hydrographs represent more complex storm regimes (Figure 5.15 and Figure **5.16**). By examining the peak shear stress of these three storms, the spatial variation in sediment transport potential in the study reach can be considered.

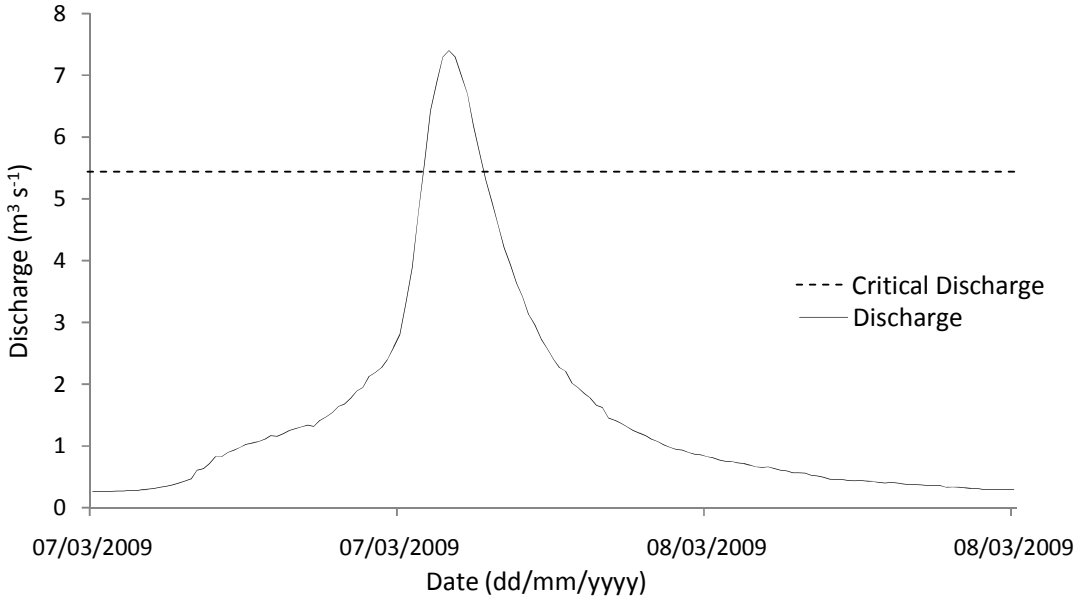

Figure 5.14 Storm hydrograph for event 1, from 00:00 on the 7th of March 2009, with a peak discharge of 7.41 $m^3 s^{-1}$.

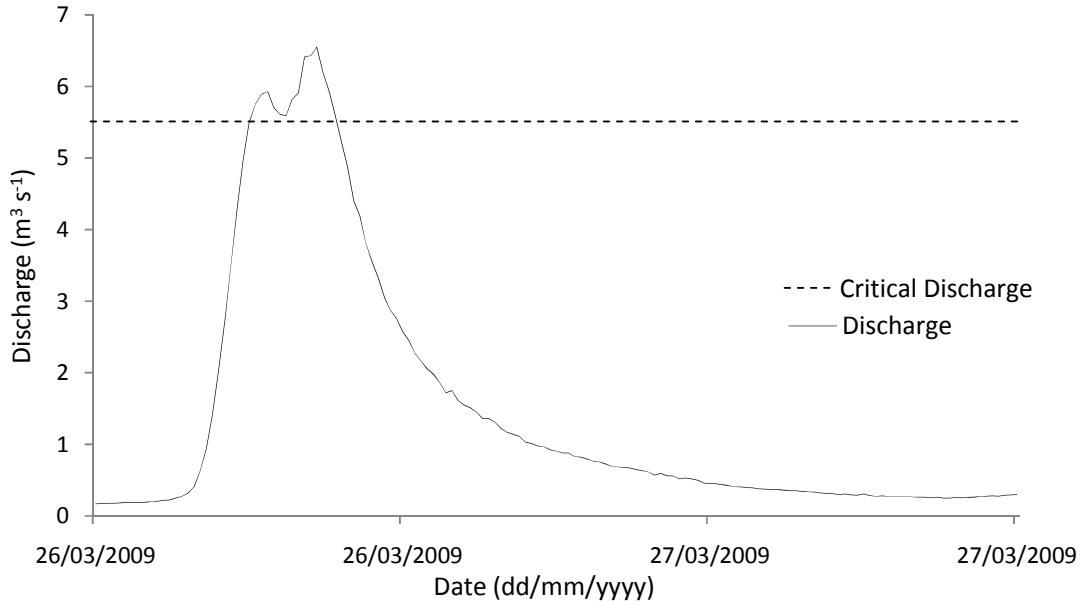

Figure 5.15 Storm hydrograph for event 2, from 00:00 on the 26th of March 2009, with a peak discharge of 6.55 $m^3 s^{-1}$.

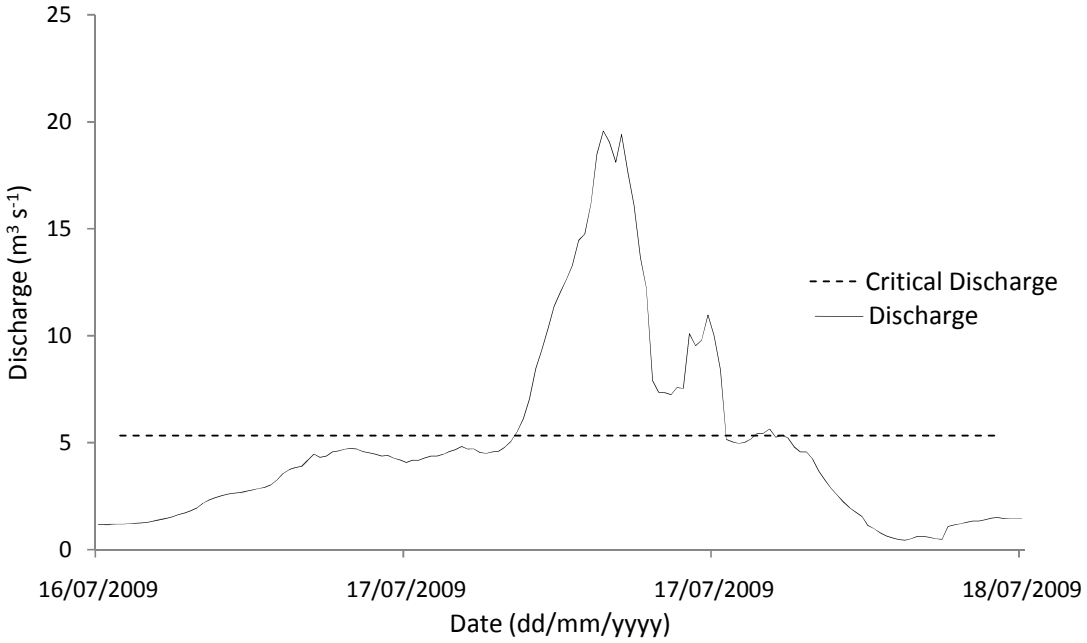

Figure 5.16 Storm hydrograph for event 2, from 22:00 on the 16th of July 2009, with a peak discharge of 19.57 $m^3 s^{-1}$.

The shear stress at the peak flow for the three storm events through the modelled reach is shown in Figure 5.17. The shear stress distribution is consistent at each of the flow peaks, highlighting the 'fixed' control which the shape of the channel has on the shear stress (Figure 5.17). This suggests that within the channel there are zones that always have high transport sediment potential and zones which have lower sediment transport potential. However, whilst the pattern of shear stress remains constant, the magnitude of shear stress varies through the reach. These results suggest that the different flow events are competent to transport different grain-sizes at different locations in the reach. This is evident in Figure 5.18, where the peak flow of the 17th July hydrograph is capable of transporting grains up to 16 mm over 90% of the modelled reach, whilst the peak flow in the two smaller events is only capable of transporting the 16 mm

grain-size class in 18 – 25% of the reach. Similar differences, of differing magnitude, are observed for other grain-sizes up to 256 mm (Figure 5.18). For example at the peak flow on the 17th of July 25% of the channel is capable of transporting all sediment. Within the study reach the highest shear stresses are found in the bedrock section (107 – 171 m, Figure 5.17) and this is the consistent 20% of the channel where sediment transport potential is always high. It is therefore suggested here that zones of sediment storage during small and medium flow events become zones of sediment transport during larger flow events.

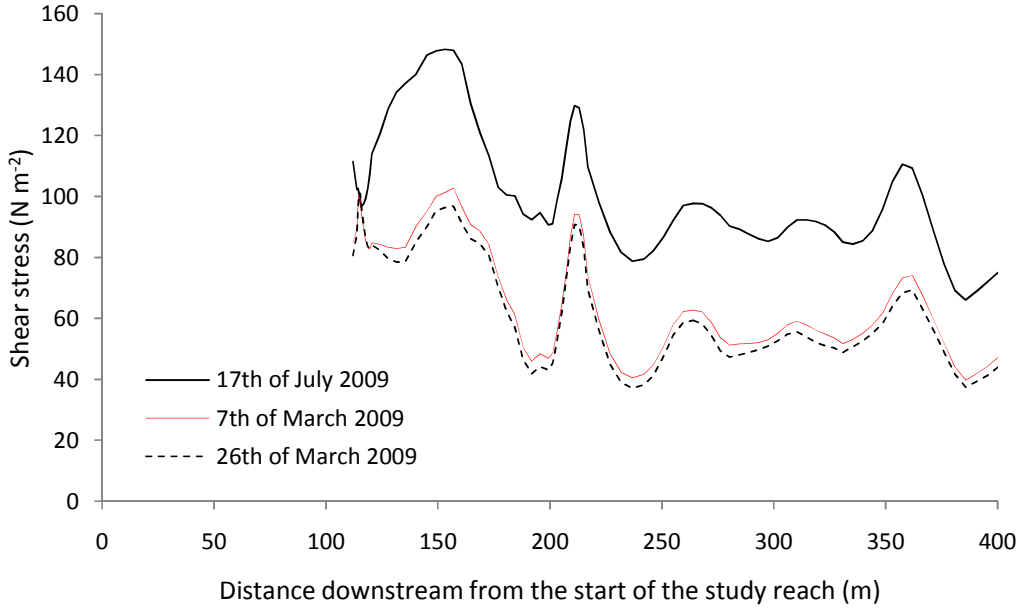

Figure 5.17 The spatial distribution of shear stress, downstream through the modelled reach, during storm events on the 7th of March, 26th of March and 17th of July 2009.

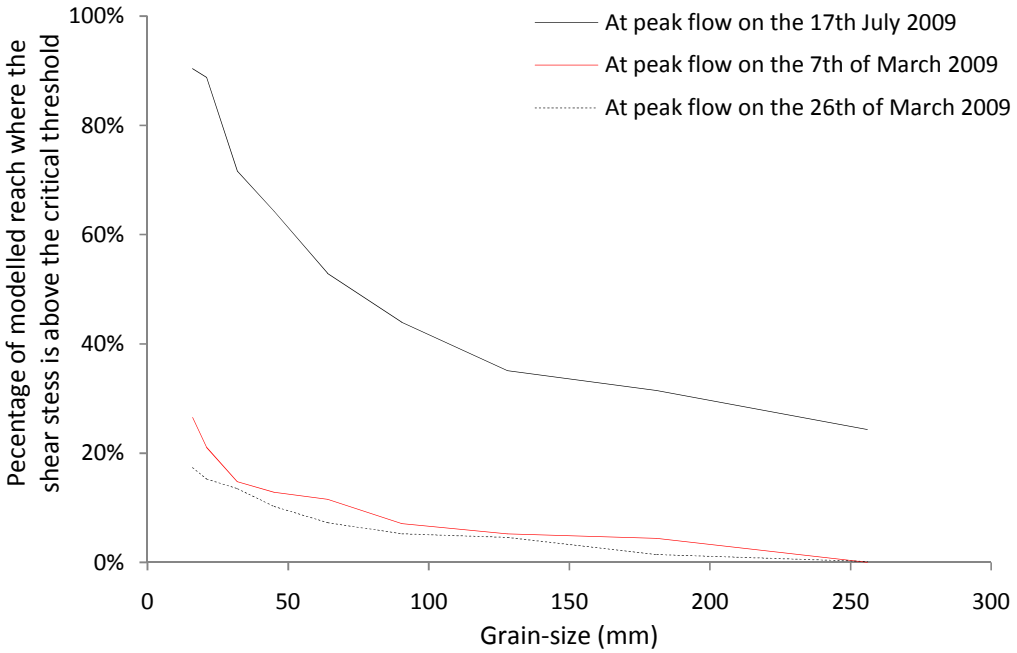

Figure 5.18 The percentage of the modelled bedrock channel for shear stress above the critical threshold for each grain-size classes.

5.4.3 **The spatial correlation of shear stress and sediment storage**

The correlation between storage locations of tracers and the shear stress modelled through the bedrock channel have been assessed for the storm events on the 7th of March, 26th of March and 17th of July 2009 and the surveys undertaken on the 17th of March, 31st of March and 10th of August 2009. The results shows that the largest proportion of tracers are stored downstream of a high shear stress region at the bedrock/alluvial boundary (180 m downstream, Figure 5.19, Figure 5.20 and Figure 5.21). This storage location occurs after the zone of shear stress competent to transport the majority of the in-channel sediment (through the bedrock reach: 107 – 180 m, Figure 5.19 and Figure 5.20) and is followed by a zone of low shear stress through the partially alluvial section of the reach (180+ m). However, the tracers stored further upstream (during the first two surveys), in the bedrock section of the channel are not found in the modelled zone of low shear stress (Figure 5.19 and Figure 5.20). It is suggested that the storage of sediment (peaks 'A' and 'B', Figure 5.19 and Figure 5.20) occurs due the deposition of sediment in zones of hydraulic lows (e.g. potholes), which HEC-RAS is unable to predict. The distribution of modelled shear stress and the spatial pattern of tracers (surveyed 10th of August), as a result of the storm on the 17th of July, highlight the significance of this large flow event. The greatest proportion of tracers are stored in the bedrock/alluvial transitional zone (peak 'A', Figure 5.21), however the amount of sediment is much lower and there has been an increase through the partially alluvial zone (Figure 5.21). The percentage of tracers represented in Figure 5.19, Figure 5.20 and Figure 5.21, does not therefore correspond to the proportion of channel width occupied by stored sediment (section 4.4.1). Thus the relationship between the proportion of channel sediment cover and shear stress is also assessed.

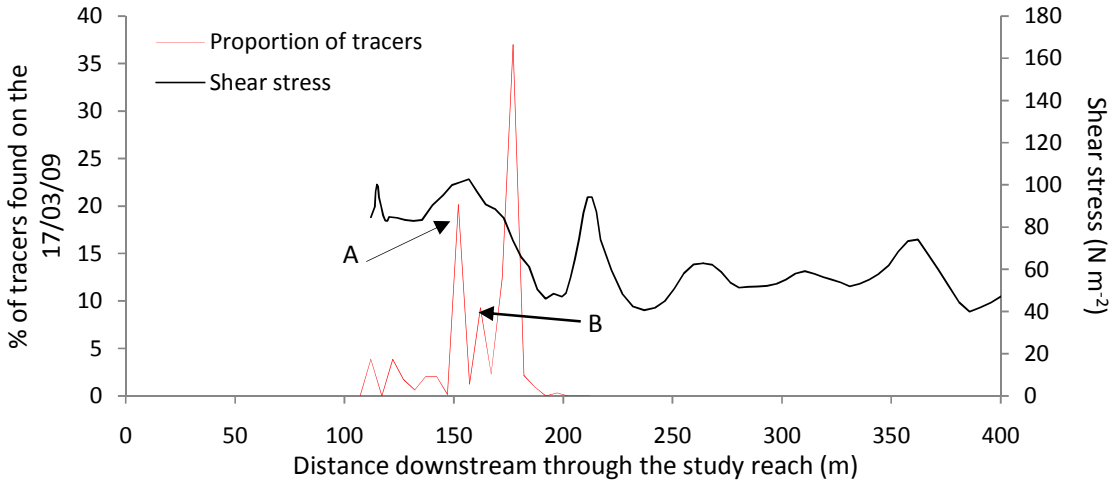

Figure 5.19 The distribution of shear stress from the storm event on the 7th of March and the proportion of tracers from the survey on the 17th of March.

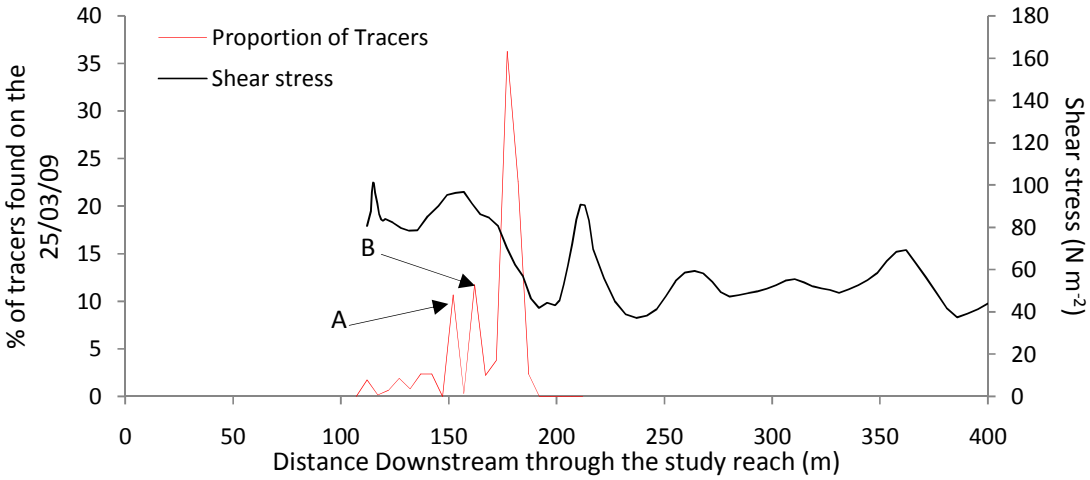

Figure 5.20 The distribution of shear stress from the storm event on the 25th of March and the proportion of tracers from the tracer survey on the 31st of March.

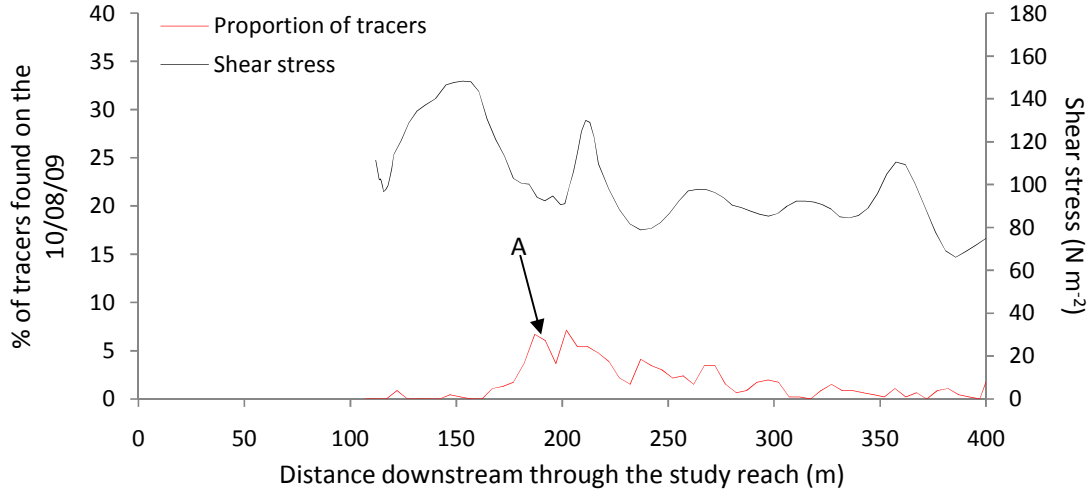

Figure 5.21 The distribution of shear stress from the storm event on the 17th of July and the proportion of tracers from the tracer survey on the 10th of August.

The downstream variability in shear stress through the modelled reach is spatially consistent over a range of flow magnitudes (Figure 5.17). Thus a single representative shear stress profile is now considered in relation to the proportion of sediment in the channel. The peaks in sediment storage, in the partially alluvial zone, occur at points 'A' and 'B' in Figure 5.22. These peaks correspond to a trough in the shear stress at 190 and 240 m downstream. However these are not the only peaks in sediment storage in the channel. At point 'C' there is a small peak in the sediment storage which corresponds to an increase in shear stress (Figure 5.22). However this increase in sediment storage occurs as a result of sediment choking at a narrowing of the channel. Furthermore, there is also a drop in proportion of sediment storage at 330 m, corresponding to the short bedrock section identified in Figure 4.1. This section occurs after peak 'B' in sediment storage, which has a low shear stress and acts a sediment sink (Figure 5.22). Further downstream, beyond 340 m, the increased proportion of sediment stored in the channel, occurs as the channel form becomes fully alluvial, the result of lower shear stress controlled by the increased channel width (Figure 5.22).

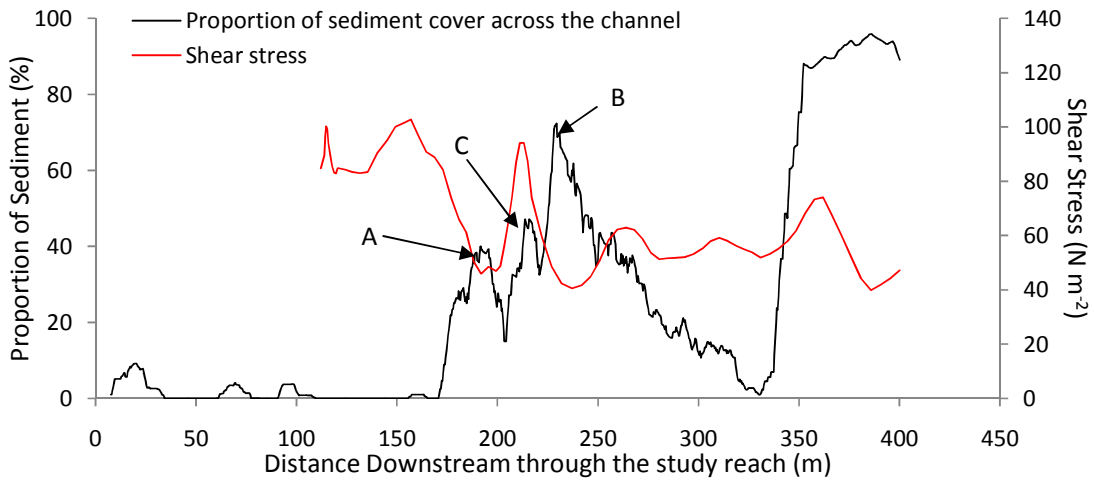

Figure 5.22 The distribution of in channel sediment and shear stress (at peak flow on the 7th of March 2009) through the study reach. The proportion of sediment is taken from the survey undertaken on the 24th of February 2009 and is considered stationary (section 4.4.2).

Overall the distribution of shear stress through the study reach generally controls the transport of sediment through the bedrock reach of the river, by conveying available sediment through regions of high shear stress and depositing it downstream as shear stress drops. The spatial profile of shear stress through the reach is morphologically controlled and, as a result of the structured bedrock channel boundaries, areas of low shear stress tend to persist at the same locations in the channel. The result is that areas of sediment storage are static. During the flow events on the 7th and 26th of March 2009 sediment transport was only active in the bedrock section of the channel. However, for the larger flow event on the 17th of July a greater proportion of the channel exceeded the critical shear stress for a greater range of grain-sizes. It is concluded that during small storms, when discharge only exceeds the critical threshold for sediment transport, locally sediment moves through the bedrock section and is stored in the partially alluvial sections. However, at higher discharges active transport occurs throughout all of the study reach and sediment is transferred through all channel types.

5.5 **Summary of model development and results**

This application of the HEC-RAS one dimensional numerical model for the study reach has explored the influence of the contraction and expansion coefficient, normal depth downstream boundary condition and the Manning's roughness coefficient when applying this hydraulic model to a bedrock channel reach. A sensitivity analysis has been undertaken to determine the extent to which these parameters influence the predictive ability of HEC-RAS for this a mixed bedrock, partially alluvial and alluvial river. The morphology of the bedrock channel causes the contraction and expansion coefficients to control the energy loss term. This is due to the reduced roughness of the channel boundaries in bedrock channels and the nature of channel contraction (as a result of bedrock resistance to erosion), coupled with abrupt expansion of the channel (at weaknesses in the lateral boundaries). Once the optimal parameter set had been identified (with an efficiency of 0.89), the model was used to analyse the distribution of shear stress both temporally and spatially through the study reach. Throughout the modelled reach, the shear stress is primarily controlled by the morphology of the channel. The peak discharge for any hydrograph defines the magnitude of shear stress, but the relative spatial pattern through the reach remains constant through the reach. This is control is identified as particularly important in controlling the higher efficiency of sediment transfer through the bedrock sections of the channel.

Chapter 6:

Discussion and Conclusions

6.1 **The scope of this research**

The purpose of this thesis was to further our understanding of coarse sediment transfer in upland bedrock channels. This has been achieved through addressing the five research objectives. The objectives were to: identify the nature of sediment storage; monitor the temporal patterns of sediment transport; monitor the movement of sediment tracers; model the temporal and spatial hydraulics; and define different rates of sediment transport through contrasting sections of the study reach. This chapter reviews the research findings of each of these objectives and presents the main conclusions from this research.

6.1.1 **Identifying the nature of sediment storage through the study reach**

The storage of sediment through the study reach is defined by the dominant processes occurring locally in the bedrock, partially alluvial and alluvial channel sections of the channel. Through the bedrock sections there is little sediment storage due to the high transport capacity of the flow which conveys sediment downstream. The few local storage zones are usually associated within hydraulically sheltered areas of the channel. These areas include features such as potholes in the centre of the channel and sheltered zones at the margins of the channel. Sediment mapping on the 24th of February and 10th of August 2009 showed that the areas of sediment storage, in the bedrock section of the channel, remained relatively stable over the course of this period (section 4.4.2). As a result the transport of sediment through the channel relies on the supply of sediment from external sources.

In the transitional zone, between bedrock and alluvial sections of the channel, partially alluvial channel has developed. In these sections sediment storage is more variable, in space and time, as a result of process feedbacks from the channel boundaries. During low flow conditions, when sediment transport is low and the sediment covers the bedrock channel boundaries, the shape of the channel is defined by sediment stored in the channel. At high flows however, the shape of the bedrock channel boundaries are more dominant in defining the channel cross section. In the partially alluvial sections of the channel these ephemeral connections between channel form and sediment transport are accentuated.

In alluvial sections of the reach there is a much greater amount of sediment storage. Over the course of single events the alluvial areas of the channel remain fairly static, although there may be degradation and aggradation during the course of high flow events, as sediment becomes available from within the channel (Church, 2006). Overall the reliance on sediment supply: defines the shape of the river channel; controls the amount of sediment storage; and by identifying the forms and processes, defines whether bedrock, partially alluvial or alluvial processes and forms are dominant at any location in the channel.

6.1.2 **Monitoring temporal patterns of sediment transport**

The timing of sediment transport is determined by the occurrence of conditions which are able to cause the initiation (Coleman and Nikora, 2008), transport and deposition of individual sediment clasts in the channel. In this study bedload entrainment has been predicted using the Schoklitsch equation to calculate the critical flow conditions (discharge: 5.59 $m^3 s^{-1}$ or stage: 0.79 m). This threshold for sediment movement was surpassed on four occasions between the 24th of February and 10th of August 2009 (A – D, Figure 4.22**Error! Reference source not found.**) and events of similar magnitude represent only 1.2% of the long-term flow record (1992 to 2009). From cross correlation analysis it is evident that peak flow conditions are most significant in determining the amount of sediment transport which is occurring through the study reach. These

fluctuating patterns, of sediment transport potential and the importance of peak flow are manifest in the different patterns of tracer movement (Figure 4.21).

6.1.3 **Monitoring the spatial movement of sediment tracers through the bedrock channel**

Sediment transport through bedrock channels is determined by the supply of sediment and the competence of flow to keep it entrained. The importance of differences in the availability of sediment for transport has been discussed with regard to different channel types (section 6.1.1). Through the bedrock section of the reach there are no available sources of sediment; whilst in the alluvial and partially alluvial sections of the reach there is always sediment available for transport. This distinction is observed in the field. In the bedrock section of the channel there is little sediment storage and only by directly seeding the tracers in this zone were they available for transport. Once sediment is present within the bedrock section of the reach, it is transported as a single pulse (Figure 4.21). This pattern of transport is reliant on the competence of flow to entrain and transport the sediment. Through the smooth boundaries of the bedrock channel, the hydraulic roughness is low and flow competence is high. However when the tracer pulse reaches the partially alluvial zone (64 m downstream from the tracer seeding site) the hydraulic roughness increases and the transport capacity of the flow drops. This pattern is evident as the transport of sediment to the transitional boundary occurs before the 31st of March and following this, only short steps in tracer movement are observed until the higher magnitude flow event on the 17th of July. This high flow had a stage which was over 0.3 m higher than any other flow recorded during the tracer experiment. As a result the flow was competent to transport the tracers through the partially alluvial and alluvial reaches where previous (lower) flows had failed (Figure 4.21). The higher threshold for sediment transport in the alluvial section of the channel is a result of the interactions between the tracer clasts and the bed sediment stored in the channel (Carling and Tinkler, 1998 and Carling et al., 2002).

Overall, the different rates of sediment transport in the bedrock, partially alluvial and alluvial reaches are the result of different local hydraulic conditions. In the bedrock zones, sediment is transported as a pulse, with full mobility of all sediment through the reach when the flow is competent. In the alluvial zones the threshold of entrainment is higher and sediment will be more selectively transported. As a result the local hydraulic conditions needed for entrainment must be considered at all locations in the channel in order to predict sediment transfer through river systems (Ferguson et al., 2002).

6.1.4 **Modelling of the temporal and spatial hydraulics of the study reach**

The temporal and spatial hydraulics of the study reach vary as a result of the flow regime of the river system and the local shape of the channel. The sediment transport potential in the channel is controlled by the competence of the flow, defined by the local shear stress. In general, the shear stress increase is proportional to the flow magnitude. However, through the reach there are spatial variations in shear stress and as a result the sediment transport potential fluctuates through the reach (Figure 5.17). These fluctuations have been defined using empirical relationships primarily defined for alluvial channels. However the definition of a bedrock channel presented in chapter 1 characterises any channel as bedrock if it is cut into the bedrock or has a wetted perimeter of greater than fifty percent bedrock (Ferguson, 1981; Howard, 1987; Tinkler and Wohl, 1998; Wohl and Merritt, 2001; Carling, 2006). This means that there will be some sediment stored within bedrock channels and as this sediment is supplied from external sources, away from the immediate channel boundaries, it will have been sorted through processes of sediment transport upstream. As a result equations such the Shield's and Andrew's will hold true

for predicting sediment transport in areas of the study reach were sediment is present. When related to areas of the channel which are competent to transport sediment, the range in critical shear stress values are rapidly surpassed through the course of the any single event which peaks above 5.59 m^3s^{-1} and therefore there is little differentiation in the entrainment of sediment sizes (Figure 5.12 and 5.13).

Through the bedrock section of the river, the geometry of the channel is constant at any given location over the time-scale of years. At the longer time-scale there may be changes in the shape of the channel, as a result of incision into the bedrock. The actions which cause this have been much debated (e.g. Douglas et al., 1996; Jansen, 2006; Finnegan et al., 2007), but have ultimately been defined as the product of the bedrock resistance and the rate of uplift verses fluvial incision. Through the alluvial sections of the reach the channel morphology changes at a short a time-scale and the feedbacks control sediment transport (section 6.1.1 and 6.1.3). The hydraulics through the study reach are therefore relatively stable through the bedrock section, but considerably more variable through the alluvial and partially alluvial zones. The distribution, of shear stress through the study reach at the peak flow, is higher in the bedrock zone and lower in the partially alluvial and alluvial zones (Figure 5.22). This distinction is a result of the channel type, but also feedbacks (in the channel) between sediment transport and storage at the local scale.

The long-term evolution of bedrock channels is primarily defined by the processes outline above. There are however short-term impacts of sediment dynamics which may accumulate over time to influence the rate of degradation or sedimentation within the channel. Hodge and Hoey (2009) have suggested that sediment may act as an agent for channel degradation by erosive processes (e.g. abrasion) or as a shielding tool, sheltering the channel from erosion where sediment is stored. Jansen (2006) also proclaimed that partially-alluvial sediment cover may optimise or impede the rate of bedrock incision, influencing the evolution of the channel. As a result of this dyadic of possibilities the outcome of sediment transport through the bedrock reach is unknown. The dynamics of sediment transport, investigated in this project, will only affect the short-term changes in the channel. In order for longer term evolutionary predictions to by made, wider investigations as to the nature of sediment production and catchment geometry are needed.

6.1.5 **Defining different rates of sediment transport through contrasting sections of the channel**

The rate of sediment transport through the study reach is controlled by the sediment balance of each the different types of channel. In the bedrock channels, the transport of sediment is dependent on the rate of supply from external sources. This is evident due to the low levels of sediment storage in the bedrock channel, essentially resulting in zero storage. If there is high connectivity between the bedrock channel and sediment sources higher in the sediment cascade then the rate of sediment transport will be high (i.e situation 2, Hooke, 2003). This situation arises as bedrock channels have a fixed geometry, with few local sediment stores, resulting in a consistent hydraulic regime. In addition, the smooth bedrock boundaries of low flow resistance result in higher shear stress. In Chapter 1, the continuum of fluvial trinities was developed to represent the interactions between channel morphology, flow and sediment transport in river channels with different forms (Figure 1.4). The increasing detachment between sediment transport and channel morphology, as the channel becomes more bedrock dominated and sediment storage becomes negligible, is clearly demonstrated in this study. In partially alluvial and alluvial channels the rate of sediment transport is more variable as a result of greater sediment

availability and feedbacks with channel form. The role of sediment storage – channel form linkage dictates the hydraulic nature of partially alluvial and alluvial channels. Bedrock channels have a more fixed morphology and consistent hydraulic regime through space and time.

6.2 **Links with other studies into sediment dynamics in other bedrock channels**

Bedrock river studies have, in the main, focused on the process pertaining to incision occurring as a result of floods with a periodicity of multiple years or over the time scale of many floods (e.g. Palmer, 2001; Sklar and Dietrich, 2001). This has occurred as a result of the view that bedrock channels are fixed and act as rigid conduits during single and frequent flow events (Carling, 2006). However bedrock river channels do not occur in isolation and are commonly just individual reaches within the whole river system (Hooke, 2003). In bedrock channels whilst the morphology of the channel boundaries may be fixed, the sediment transport occurring through them is dynamic over short-time scales. In order to address this, this study has investigated the dynamics of sediment transport through a mixed bedrock and alluvial river reach.

There are some other studies which have examined shorter time scale sediment dynamics in bedrock river channels. Dogwiler and Wicks (2004) found that in two mixed river systems (of bedrock cave reaches and surface alluvial systems) in Missouri and Kentucky, USA, the transport capacity at bankfull discharge transporting sediment up to d_{85}. However this work focused primarily on bankfull discharge and thus only fleeting comments were made as to the threshold, at lower stages, needed for sediment transport. The threshold for sediment transport in Trout Beck was calculated to be 5.59 m^3s^{-1}: well below the bankfull discharge. However the definite threshold identified in each of these studies suggests some limiting factor in determining the timing of sediment transport. Hodge and Hoey (2009) are also investigating sediment transport, through a bedrock river on the River Calder, Scotland. They have found that for coarse sediment tracers (with b-axis between 22 and 90 mm) the transport occurs periodically with high mobility during flows competent to entrain the sediment and low mobility during weaker flow periods. This agrees with the results obtained in Trout Beck for coarse sediment transport in a bedrock river channel.

6.3 **Limitations within the research**

This research, into sediment dynamics of the bedrock reach on Trout Beck, is a short-term investigation using intense field monitoring and the development of a numerical model. This has made it possible to monitor the nature of sediment transport, flow and channel morphology and model the flow conditions for the same short period. However the length of the study has caused drawbacks for both field and modelling aspects of the research. The field monitoring methods, whilst well developed, only captured a limited number of flow events. The tracer experiment was only installed halfway through the investigation, as a result of bad weather conditions and limited access to the field site. Meanwhile as a result of the desire to monitor all conditions in unison over as many events as possible, there was little scope for recalibration of field equipment to monitor events at different magnitudes (e.g. impact sensors).

The development of a numerical model for the bedrock river reach was done by using the field data to calibrate the existing 1D HEC-RAS model. As a result the modelling had to fit within the parameter demands of the model. As it was a 1D model only a series of 1D cross-sections could be used to define the morphology of the channel. In conjunction with this the interface of the model did not lend itself to quick uploading of many cross-sections. As a result only 21 cross-sections were used to define the 400 m study reach within the model. Coupled with output of

results (i.e. shear stress) was confined to the originally defined cross-sections by the user. To combat these restrictions, time was taken over selecting the survey locations of the cross-sections used to define the channel boundary.

6.4 **Future research at Trout Beck and for other bedrock channels.**

In order to further the research undertaken in this project several extensions to the work are suggested. Firstly alterations to the methodology used will allow for further conclusions to be made as to the sediment dynamics within the study reach; secondly wider studies into sediment dynamics in other reaches; and finally further investigations into the influence of sediment transport action on longer term evolution of bedrock study reaches is needed.

The methodology alterations would extend the temporal and spatial resolution of field monitoring, whilst altering the parameters in the river model. Repeat tracer experiments over different timescales and by seeding the tracers at different locations within the river, will allow for sediment transport within a wider variety of flow conditions to be monitored. Also by extending the length of the tracer study, the travel steps of individual tracers could be better monitored as there will be more time to develop efficient surveying techniques. This would enable analysis of individual clast sizes to be made and conclusions as to the role of size selectivity, in determining the rate of sediment transport through bedrock channels, to be made. The second methodological enhancement would be to investigate how the impact sensors could be utilised to determine not only the rate low end rates of sediment transport, but also higher rates over varying time intervals.

Secondly, as was identified in chapter 1 and again in the discussion, there is a lack of research into the role of bedrock channels in determining sediment transport through the river system and little work into the implications of these controls on long-term channel evolution. By replicating this study in other rivers, with mixed bedrock and alluvial reaches, further conclusions will be possible as to the links between sediment transport, flow and morphology in bedrock channels.

The development of the bedrock river model using the HEC-RAS 1D model has shown that through the bedrock study reach there are spatial differences in the sediment transport potential. However due to the draw backs in defining the channel boundaries within the model, future research might investigate methods of integrating higher spatial resolution surveys of the channel, into the river model. This would allow for better parameterisation of the channel shape and may enable further, higher resolution, investigations into the sensitivity of the roughness parameter for mixed bedrock and alluvial channels.

Finally, there is a gap in bedrock river studies, concerning the long-term impact of sediment dynamics on channel evolution. By coupling field monitoring and numerical modelling it might be possible to determine the role of sediment transport in shaping bedrock river channels. This however will need to couple higher resolution field monitoring, at different study locations, through a greater variety of flow regimes, in order to better develop a bedrock river model which is able to predict sediment transport.

6.5 **Conclusions**

- The rate of sediment transport through a river system is spatially defined by the local channel characteristics. In this project differences between channel types have been conceptualised using the continuum of the ‘fluvial trinities’. This model demonstrates that the

interaction of sediment and channel morphology is partly disconnected in bedrock channels. Conversely, in partially alluvial and alluvial channels there are important feedbacks between sediment stored locally in the channel, channel form and sediment transport.

- Sediment storage defines the partially alluvial and alluvial sections of the channel, with very little sediment storage in bedrock reaches. Where this does occur it is in hydraulically sheltered sites. This pattern of sediment storage indicates that there are different rates of sediment transport (and corresponding deposition) occurring through different sections of the channel reach.
- There are significant differences in the critical threshold of shear stress for sediment transport down reach. Sediment which is transported through the bedrock reach will be deposited and stored in the partially alluvial and alluvial sections of the reach at the same flow conditions. As the flow magnitude increases above the critical threshold, the sediment transport potential increases throughout the whole channel until sediment transport potential is surpassed throughout the whole reach. However, the sediment transport potential in the bedrock channels is always higher than in the partially alluvial and alluvial channels.
- More efficient sediment transfer through the bedrock channels is the result of the local hydraulics. The low resistance to flow and stable channel boundaries cause little sediment storage and a downstream conveyance of the full grain-size distribution during periods when flow is competent and sediment is supplied from external sources.
- The combined methodology of detailed field investigations and 1D modelling used in this project provides a useful tool for analysing process form relationships in mixed bedrock – alluvial channel systems.

Chapter 7:

References

ANDREWS, E. D. (1983) Entrainment of gravel from naturally sorted riverbed material. *Geological Society of America Bulletin,* 94**:** 1225-1231.

ARCHER, D. & STEWART, D. (1995) The installation and use of a snow pillow to monitor snow water equivalent. *Journal of Chartered Institute of Water & Environmental Management,* 9**:** 221-230.

ASHWORTH, P. J. & FERGUSON, R. I. (1986) Interrelationships of channel processes, changes and sediments in a proglacial braided river. *Geografiska Annaler. Series A, Physical Geography,* 68**:** 361-371.

AUGUSTIN, N. H., BEEVERS, L. & SLOAN, W. T. (2008) Predicting river flows for future climates using an autoregressive multinomial logit model. *Water Resources Research,* 44**:** WR005127.

BAGNOLD, R. A. (1941) *The physics of blown sand and dessert dunes,* London, Methuen.

BAGNOLD, R. A. (1977) Bed load transport by natural rivers. *Water Resources Research,* 13**:** 303-312.

BAKER, D. B., RICHARDS, R. P., LOFTUS, T. T. & KRAMER, J. W. (2004) A new flashiness index: characteristics and applications to Midwestern river and streams. *Journal of the American Water Resources Association,* 40**:** 503-522.

BATHURST, J. C. (1987) Measuring and modelling bedload transport in channels with coarse-bed materials. IN RICHARDS, K. S. (Ed.) *River Channels: Environment and Process.* Oxford, Basil Blackwell. 272-294.

BEST, J. L. (1986) The morphology of river channel confluences. *Progress in Physical Geography,* 10**:** 157-174.

BEVEN, K. & BINLEY, A. M. (1992) The future of Distributed Models: Model Calibration and Uncertainty Prediction. *Hydrological Processes,* 6**:** 279-298.

BEVEN, K. J. (2002) *Rainfall-runoff modelling: the primer.* Chichester, John Wiley and Sons Ltd.

BROADHURST, L. J. & HERITAGE, G. L. (1998) Modelling stage-discharge relationships in anastomosed bedrock-influenced sections of the Sabie river system. *Earth Surface Processes and Landforms,* 23**:** 455-465.

BRUNNER, G. W. (2008) *HEC-RAS, River Analysis System User's Manual.* Davis, US Army Corps of Engineers.

BURT, T. P. (1992) The hydrology of headwater catchments. IN CALOW, P. & PETTS, G. (Eds.) *The Rivers Handbook: hydrological and ecological principles (Volume: 1).* London, Blackwell Scientific Publications. 3-29.

BURT, T. P., HOLDEN, J. & EVANS, M. (1998) The hydrology of blanket peat with special reference to the Moor House NNR. IN WARBURTON, J. (Ed.) *Geomorphological studies in the North Pennines: field studies.* Durham, British Geomorphological Research Group. 24-36.

CARLING, P. A. (1983) Particulate dynamics, dissolved and total load in tow small basins, northern Pennies, UK. *Hydrological Sciences Journal,* 28**:** 355-375.

CARLING, P. A. (1995) Flow-separation berms downstream of a hydraulic jump in a bedrock channel. *Geomorphology,* 11**:** 245-253.

CARLING, P. A. (2006) The hydrology and geomorphology of bedrock rivers. *Geomorphology,* 82**:** 1-3.

CARLING, P. A. & GRODEK, T. (1994) Indirect estimation of ungauged peak discharges in a bedrock channel with reference to design discharge selection. *Hydrological Processes,* 8**:** 497-511.

CARLING, P. A., HOFFMAN, M. & BLATTER, A. S. (2002) Initial motion of boulders in bedrock channels. IN HOUSE, P. K., WEBB, R. H., BAKER, V. R. & LEVISH, D. R. (Eds.) *Ancient floods, modern hazards; principles and applications of paleoflood hydrology.* Washington, D.C., American Geophysical Union. 147-160.

CARLING, P. A., KELSEY, A. & GLAISTER, M. S. (1992) Effect of bed roughness, particle shape and orientation on initial motion criteria. IN BILLI, P., HEY, R. D., THORNE, C. R. & TACCONI, P. (Eds.) *Dynamics of Gravel-bed Rivers.* Chichester, John Wiley and sons. 23-39.

CARLING, P. A. & TINKLER, K. J. (1998) Conditions for the entrainment of cubiod boulders in bedrock streams; an historical review of literature with respect to recent investigations. IN TINKLER, K. J. & WOHL, E. E. (Eds.) *Rivers over rock: fluvial processes in bedrock channels.* Washington, D.C., American Geophysical Union. 19-34.

CHALOV, R. S. (2004) Morphological expression of river sediment transport and their role in channel processes. IN GOLOSOV, V., BELYAEV, V. & WALLING, D. E. (Eds.) *Sediment transfer through the fluvial system.* Wallingford, IAHS. 288:205-210.

CHATANANTAVET, P. & PARKER, G. (2008) Experimental study of bedrock channel alluviation under varied sediment supply and hydraulic conditions. *Water Resources Research,* 44: W12446.

CHOW, V. T. (1959) *Open Channel Hydraulics,* New York, McGraw-Hill Book Company.

CHURCH, M. (2006) Bed material transport and the morphology of alluvial river channels. *Annual Review of Earth and Planetry Sciences,* 34**:** 325-354.

CLARK, J. M., CHAPMAN, P. J., ADAMSON, J. & LANE, S. N. (2005) Influence of drought-induced acidification on the mobility of dissolved organic in peat soils. *Global Change Biology,* 11**:** 791-809.

COLEMAN, S. E. & NIKORA, V. I. (2008) A unifying framework for particle entrainment. *Water Resources Research,* 44**:** W04415.

CONWAY, V. M. & MILLAR, A. (1960) The hydrology of some small peat-covered catchments in the Northern Pennines. *Journal of the Institute of Water Engineers,* 14**:** 415-425.

CUNDILL, A. P., CHAPMAN, P. J. & ADAMSON, J. K. (2007) Spatial variation in concentrations of dissolved nitrogen species in an upland blanket peat catchment. *Science of The Total Environment,* 373**:** 166-177.

DEMIR, T. (2000) The influence of particle shape on bedload transport in coarse-bed river channels. *Department of Geography.* Durham, Durham University.

DOGWILER, T. and WICKS, C.M. (2004) Sediment entrainment and transport in fluviokrast systems. Journal of Hydrology, 295: 163-172.

DOUGLAS, W., BURBANK, D. W., LELAND, J., FIELDING, E., ANDERSON, R. S., BROZONVIC, N., REID, M. R. & DUNCAN, C. (1996) Bedrock incision, rock uplift and threshold hillslopes in the northwestern Himalayas. *Nature,* 379**:** 505-510.

EVANS, M. G., BURT, T. P., HOLDEN, J. & ADAMSON, J. K. (1999) Runoff generation and water table fluctuations in blanket peat: evidence from the UK spanning the dry summer of 1995. *Journal of Hydrology,* 221**:** 141-160.

FERGUSON, R. (1981) Channel form and channel changes. IN LEWIN, J. (Ed.) *British Rivers.* London, Allen & Unwin. 90-125.

FERGUSON, R. (1994) Critical discharge for entrainment of poorly sorted gravel. *Earth Surface Processes and Landforms,* 19**:** 179-186.

FERGUSON, R. I., BLOOMER, D. J., HOEY, T. B. & WERRITTY, A. (2002) Mobility of tracer pebbles over different timescales. *Water Resources Research,* 38**:** 1045.

FINNEGAN, N. J., SKLAR, L. S. & FULLER, T. K. (2007) Interplay of sediment supply, river incision and channel morphology revealed by the transient evolution of an experimental bedrock channel. *Journal of Geophysical Research,* 122**:** FO3S11.

FRIPP, J. B. & DIPLAS, P. (1993) Surface sampling in gravel streams. *Journal of Hydraulic Engineering-ASCE,* 119**:** 473-490.

GARDE, R. J. & RANGA RAJU, K. G. (1977) *Mechanics of sediment transport and alluvial stream problems.* Delhi, Wiley Eastern Ltd.

GREEN, J. C. (2003) The precision of sampling grain-size percentiles using Wolman method. *Earth Surface Processes and Landforms,* 28**:** 979-991.

GUSTARD, A. (1996) Analysis of river regime. IN PETTS, G. & CALOW, P. (Eds.) *River flows and channel forms.* Oxford, Blackwell Science Ltd. 32-51.

HAESTAD, M., DRYHOUSE, G., HATCHETT, J. & BENN, J. (2003) *Floodplain Modelling using HEC-RAS,* Waterbury, CT USA, Haestad Press.

HARDY, R. J. (2006) Fluvial geomorphology. *Progress in Physical Geography,* 30**:** 553-567.

HERITAGE, G. L., BROADHURST, L. J. & BIRKHEAD, A. L. (2001) The influence of contemporary flow regime on the geomorphology of the Sabie River, South Africa. *Geomorphology,* 38**:** 197-211.

HERSCHY, R. W. (1999) *Hydrometry: Principles and Practices,* New York, Wiley.

HIGGITT, D., WARBURTON, J. & EVANS, M. G. (2001) Sediment transfer in upland environments. IN HIGGITT, D. & LEE, E. M. (Eds.) *Geomorphological processes and landscape change: Britain in the last 1000 years.* Oxford, Blackwell Publishers Ltd. 190-214.

HODGE, R. and HOEY, T. (2009) The action of sediment in bedrock river erosion. Geophysical Research Abstracts, 11: EGU2009-7380.

HOLDEN, J. (2001) Recent reduction of frost in the North Pennines. *Journal of Meteorology,* 26**:** 369-374.

HOLDEN, J. & ADAMSON, J. K. (2001) Gordon Manley: an upland meteorological pioneer. *Journal of Meteorology,* 26**:** 369-374.

HOLDEN, J. & ADAMSON, J. K. (2002) The Moor House long-term upland temperature record: new evidence of recent warming. *Weather,* 57**:** 119-127.

HOLLIDAY, V., HIGGITT, D., WARBURTON, J. & WHITE, S. (2003) Reconstructing upland sediment budgets in ungauaged catchments from reservoir sedimentation and rainfall records calibrated

using short-term streamflow monitoring. IN DE BOER, D., FROEHLICH, W., MIZUYAMA, T. & PIETRONIRO, A. (Eds.) *Erosion prediction in ungauged basins: integrating methods and techniques.* Wallingford, IAHS. 279:59-67.

HOOKE, J. (2003) Coarse sediment connectivity in river channel systems: a conceptual framework and methodology. *Geomorphology,* 56**:** 79-94.

HORRITT, M. (2000) Calibration of a two-dimensional finite element flood flow model using satellite radar imagery. *Water Resources Research,* 36**:** 3279 - 3291.

HORRITT, M. & BATES, P. D. (2002) Evaluation of 1D and 2D numerical models for predicting flood inundation. *Journal of Hydrology,* 268**:** 87-99.

HOWARD, A. D. (1987) Modelling fluvial systems: rock-, gravel-, and sand-bed channels. IN RICHARDS, K. S. (Ed.) *River channels: environment and process.* Special publication / Institute of British Geographers. Oxford, Blackwell. 69-94.

HUDSON-EDWARDS, K., MACKLIN, M. & TAYLOR, M. (1997) Historic metal mining inputs to Tees River sediment. *Science of the Total Environment,* 194-195**:** 437-445.

HUNT, J. H. & BRUNNER, G. W. (1995) *Flow transition in bridge backwater analysis,* Davis, CA: US Army Corps of Engineers.

JANSEN, J. D. (2006) Flood magnitude-frequency and lithologic control on bedrock river incision in post-orogenic terrain. *Geomorphology,* 82**:** 39-57.

JOHNSON, G. A. L. & DUNHAM, K. C. (1963) *The geology of Moor House,* London, Her Majesty's Stationary Office.

JOHNSON, J. P. & WHIPPLE, K. X. (2007) Feedbacks between erosion and sediment transport in experimental bedrock channels. *Earth Surface Processes and Landforms,* 32**:** 1048-1062.

KNIGHTON, D. (1984) *Fluvial forms and processes,* London, Arnold.

KOMAR, P. D. & REIMERS, C. E. (1978) Grain shape effects on settling rates. *Journal of Geology,* 86**:** 193-209.

LANE, S. N. (2005) Roughness - time for a re-evaluation? *Earth Surface Processes and Landforms,* 30**:** 251-253.

LANE, S. N., CHANDLER, J. H. & RICHARDS, K. S. (1994) Development in monitoring and modelling small-scale river bed topography. *Earth Surface Processes and Landforms,* 19**:** 349-368.

LANE, S. N. & RICHARDS, K. S. (1997) Linking river channel form and process: time, space and causality revisited. *Earth Surface Processes and Landforms,* 22**:** 249-260.

LANE, S. N., RICHARDS, K. S. & CHANDLER, J. H. (1994) Application of distributed sensitivity analysis to a model of turbulent open channel flow in a natural river channel. *Proceedings of the Royal Society London, Series A,* 447**:** 49-63.

LEMMON, T. & BIDDISCOMBE, P. (2005) *Trimble 3D scanning for surveyors,* Dayton, USA: Trimble Navigation Limited.

LITCHTI, D.D., GORDIN, S.J. and TOPDECHO, T. (2005) Error models and propagation in directly georeferenced terrestrial laser scanner networks. Journal of Surveying Engineering, 131(4): 135-142.

MACKLIN, M. G. (1997) Fluvial Geomorphology of North-East England. IN GREGORY, K. J. (Ed.) *Fluvial Geomorphology of Great Britain.* London, Conservation Reviews Series, Chapman & Hall. 203-238.

MACKLIN, M. G. & ROSE, J. (1986) *Quaternary river landforms and sediment in the Northern Pennines, England: Field Guide.* London, British Geomorphological Research Group / Quaternary Research Association.

MANLEY, G. (1941) The Durham meteorological record. *Quarterly Journal of the Royal Meteorological Society,* 67**:** 363-380.

MARCUS, W. A., LADD, S. C. & STROUGHTON, J. A. (1995) Pebble counts and the role of user-dependent bias in documenting sediment size distributions. *Water Resources Research,* 31**:** 2625-2631.

MET OFFICE (2009) *Climate Averages: long-term averages*. [12/02/2009]**:** http://www.metoffice.gov.uk/climate/uk/averages/19712000/index.html.

MEYER-PETER, E. & MÜLLER, R. (1948) Formulas for bed-load transport. *Proc. 3rd Meeting of IAHR, Stockholm.*

MONTGOMERY, D. R. & BUFFINGTON, J. M. (1997) Channel-reach morphology in mountain drainage basins. *Geological Society of America Bulletin,* 109**:** 596-611.

NASH, J. E. & SUTCLIFFE, J. V. (1970) River flow forecasting through conceptual models part I -- A discussion of principles. *Journal of Hydrology,* 10**:** 282-290.

NELSON, P. A., VENDITTI, J. G., DIETRICH, W. E., KIRCHNER, J. W., IKEDA, H., ISEYA, F. & SKLAR, L. S. (2009) Response of bed surface patchiness to reductions in sediment supply. *Journal of Geophysical Research - Earth Surface,* 114**:** F02005.

ORDNANCE SURVEY (2009) "© Crown Copyright/database right 2009. An Ordnance Survey/(Datacentre) supplied service". [22/05/2009]**:** http://edina.ac.uk/digimap/.

PALMER, A.N. (2001) Dynamics of cave development by allogenic water. Acta Carsologica, 30(2): 14-32.

PAPPENBERGER, F., BEVEN, K., HORRITT, M. & BLAZKOVA, S. (2005) Uncertainty in the calibration of effective roughness parameters in HEC-RAS using inundation and downstream level observations. *Journal of Hydrology,* 302**:** 46-69.

PELLETIER, J. (2008) *Quantitative modelling of earth surface processes.* Cambridge, Cambridge University Press.

PICKUP, G. & RIEGER, W. A. (1979) A conceptual model of the relationship between channel characteristics and discharge. *Earth Surface Processes and Landforms,* 4**:** 37-42.

POUNDER, E. (1989) *Classic landforms of the northern Dales,* Sheffield, Geographical Association in conjunction with the British Geomorphological Research Group.

RAVEN, E. K., LANE, S. N., FERGUSON, R. I. & BRAKEN, L. J. (2009) The spatial and temporal patterns of aggradation in a temperate, upland, gravel-bed river. *Earth Surface Processes and Landforms,* 24**:** 1181-1197.

REID, L. M. & DUNNE, T. (1996) *Rapid evaluation of sediment budgets,* Reiskirchen, Catena Verlag.

REID, S. C., LANE, S. N., BERNEY, J. M. & HOLDEN, J. (2007) The timing and magnitude of coarse sediment transport events within an upland, temperate gravel-bed river. *Geomorphology,* 83**:** 152-182.

RICE, S. & CHURCH, M. (1996) Sampling surficial fluvial gravels; the precision of size distribution percentile sediments. *Journal of Sedimentary Research,* 66**:** 654-665.

RICHARDS, K. S. (1982) *River: form and process in alluvial channels.* London, Methuen.

RICHARDSON, K., BENSON, I. & CARLING, P. (2003) An instrument to record sediment movement in bedrock channels. IN BOGEN, J., FERGUS, T. & WALLING, D. E. (Eds.) *Erosion and sediment movement in rivers: technological and methodological advances.* Oslo, IAHS. 283:228-235.

RICHARDSON, K. & CARLING, P. A. (2006) The hydraulics of a straight bedrock channel: Insights from solute dispersion studies. *Geomorphology,* 82**:** 98-125.

REUSSER L.J., BIERMAN, P.R., PAYICH, M.J., ZEN, E-an., LARSEN, J. and FINKEL, R. (2004) Rapid Late Pleistoncene incision of Atlantic passive-margin gorger. Science, 305: 499-502.

SCHICK, A. P., HASSAN, M. A. & LEKACH, J. (1988) A vertical exchange model for coarse bedload movement - numerical considerations. *Catena Supplement,* 10**:** 73-83.

SEDIMETRICS ® DIGITAL GRAVELOMETER (2006) *Sedimetrics: technical information*. [11/12/2008]**:** http://www.sedimetrics.com/documentation/technical_information.html.

SIVAPRAGASAM, C. & MUTTIL, N. (2005) Discharge rating curve extension - A new approach. *Water Resources Management,* 19**:** 505-520.

SKLAR, L. S. & DIETRICH, W. E. (1998) River longitudinal profiles and bedrock incision models: stream power and the influence of sediment supply. IN TINKLER, K. J. & WOHL, E. E. (Eds.) *Rivers over rock: fluvial processes in bedrock channels.* Wahsington, D.C., American Geophysical Union. 237-260.

SKLAR, L. S. & DIETRICH, W. E. (2001) Sediment and rock strength controls on river incision into bedrock. *Geology,* 29**:** 1087-1090.

SKLAR, L. S. & DIETRICH, W. E. (2004) A mechanistic model for river incision into bedrock by saltating bedload. *Water Resources Research,* 40**:** WR0002496.

SMITH, H. M. (2004) Significance of bedrock channel morphology and sediment dynamics in a UK upland river. *Department of Geography.* Durham, Durham University.

SYKES, J. M. & LANE, A. M. J. (1996) *The United Kingdom Environmental Change Network: protocols for standard measurements at terrestrial sites,* London, The Stationary Office.

TAYEFI, V. (2005) One- and two- dimensional modelling of upland floodplain flows in response to different channel configuration. *School of Geography.* Leeds, University of Leeds.

THE MATHS WORKS (2007) *MATLAB Function Reference: griddata*. [03/02/2009]**:** http://www.mathworks.com/access/helpdesk/help/techdoc/index.html?/access/helpdesk/help/techdoc/ref/griddata.html&http://www.google.co.uk/search?hl=en&q=matlab+help+griddata&btnG=Google+Search&meta=&aq=f&oq=.

THOMPSON, C. & CROKE, J. (2008) Channel flow competence and sediment transport in upland streams in southeast Australia. *Earth Surface Processes and Landforms,* 33**:** 329-352.

TINKLER, K. J. & WOHL, E. E. (1998) A primer on bedrock channels. IN TINKLER, K. J. & WOHL, E. E. (Eds.) *Rivers over rock: fluvial processes in bedrock channels.* Washington, D.C., American Geophysical Union. 1-18.

TINKLER, K. J. & WOHL, E. E. (1998) A primer on bedrock channels. IN TINKLER, K. J. & WOHL, E. E. (Eds.) *Rivers over rock: fluvial processes in bedrock channels.* Washington, D.C., American Geophysical Union. 1-18.

TRIMBLE NAVIGATION LIMITED (2007) *Datasheet: Trimble GX 3D scanner,* Dayton: Trimble Navigation Limited.

TUROWSKI, J. M., HOVIUS, N., WILSON, A. & HORNG, M.-J. (2008) Hydraulic geometry, river sediment and the definition of bedrock channels. *Geomorphology,* 99**:** 26-38.

WARBURTON, J. (1990) Comparison of bed load yield estimates for a glacial melt water stream. *Hydrology in Mountains Regions. I - Hydrological Measurments; the Water Cycle.* Proceedings of two Lausanne Symposia, August 1990, IAHS. 193:315-323.

WARBUTON, J. & DEMIR, T. (2000) Influence of bed material shape on sediment transport in gravel-bed rivers: a field experiment. IN FOSTER, I. D. L. (Ed.) *Tracers in geomorphology.* Chichester, John Wiley. 401-410.

WARBUTON, J. & SMITH, H. M. (2005) Observations of gravel re-sedimentation in an upland bedrock channel following a major flood. *6th Gravel Bed Rivers Conference.*

WHIPPLE, K. X. (2004) Bedrock rivers and the geomorphology of active orogens. *Annual Review of Earth Planetary Sciences,* 32**:** 151-185.

WHITE, C. M. (1940) The equilibrium of grains on the bed of a stream. *Proceedings of the Royal Society London, Series A,* 174**:** 332-338.

WIBERG, P. L. & SMITH, J. D. (1987) Initial motion of coarse sediment in streams of high gradient. IN BESCHTA, R. L., BLINN, T., GRANT, G. E., ICE, G. G. & SWANSON, F. J. (Eds.) *Erosion and Sedimentation in the Pacific Rim`.* Wallingford, IAHS. 165:299 - 308.

WOHL, E. E., GREENBAUM, N., SCHICK, A. P. & BAKER, V. R. (1994) Controls on bedrock channel incision along Nahal Paran, Israel. *Earth Surface Processes and Landforms,* 19**:** 1-13.

WOHL, E. E. & MERRITT, D. M. (2001) Bedrock channel morphology. *Geological Society of America Bulletin,* 113**:** 1205-1212.

WOLMAN, M. G. (1954) A method of sampling coarse river-bed material. *American Geophysical Union, Transactions,* 35**:** 951-956.

WOODHOUSE, R. (1991) *The River Tees: A North Country River,* Lavenham, Suffolk, Terrence Dalton Limited.

WORRALL, F., BURT, T. P. & ADAMSON, J. (2006) Long-term changes in hydrological pathways in an upland peat catchment--recovery from severe drought? *Journal of Hydrology,* 321**:** 5-20.

WORRALL, F., BURT, T. P. & ADAMSON, J. (2006) The rate of and controls upon DOC loss in a peat catchment. *Journal of Hydrology,* 321**:** 311-325.

YOUNG, W. J., OLLEY, J. M. & PROSSER, I. P. (2001) Relative changes in sediment supply and sediment transport capacity in a bedrock-controlled river. *Water Resources Research,* 37**:** 3307-3320.